Final response for the following manuscript:

Luo, X., Li, H.-Y., Leung, L. R., Tesfa, T. K., Getirana, A., Papa, F., and Hess, L. L.: Modeling surface water dynamics in the Amazon Basin using MOSART-Inundation-v1.0: Impacts of geomorphological parameters and river flow representation, Geosci. Model Dev. Discuss., doi:10.5194/gmd-2016-210, in review, 2016.

December 21, 2016

Dr. Jeffrey Neal

Topical Editor of Geoscientific Model Development
School of Geographical Sciences
University of Bristol

Dear Dr. Neal,

We would like to submit the final response and the revised manuscript.

Both referees provided very constructive comments. We have addressed all the comments and made the corresponding changes in the revised manuscript. The major modifications are summarized as follows:

1. As suggested by the referees, we clarified the main contribution of our study as incorporating an inundation scheme in the MOSART model, which is used in Earth System Models. To document our effort, we conducted a new simulation called "NoInund" (with the inundation scheme turned off) and compared its results with those of the control simulation "CTL" (where the inundation scheme was turned on). This comparison revealed the effects of the inundation scheme on modeled surface hydrology, and was presented in a new subsection (Section 4.1 Representing floodplain inundation).

2. We included more discussions to compare our study with previous studies, which provided the foundation for the approaches we have taken. Although some of our results agree with those of former studies, we have also provided some new insights in terms of methodologies, model results and analyses. The manuscript was revised to be clearer on this point.

3. We also addressed the other comments of the referees to make the manuscript clearer, more precise, or more complete than before.

4. As a result of the above revisions, five of the 13 figures and two of the four tables were updated in the revised manuscript.

We appreciate your time and effort for this manuscript.

Sincerely,

L. Ruby Leung Ph.D.
Laboratory Fellow
Atmospheric Sciences and Global Change Division
Pacific Northwest National Laboratory
Richland, Washington State, USA

Response to Referee #1

We appreciate the time and effort of the reviewer and thank the reviewer for the constructive comments. We provided replies to all the comments, and made the corresponding changes in the revised manuscript.

In the following text, we use blue color for the reviewer comments, black color for the replies, and italics for the revisions in the manuscript.

**Comments**

[C1-1]

This manuscript describes the development of the MOSART river transport model to include a flood inundation scheme which was then tested across the Amazon basin. Excellent detail is given as to the setup of the model including the processing of the DEM and channel geometry parameters. The model is run for a time period longer than 20 years and evaluated against in-situ streamflow observations and remotely sensed satellite data of river stage and flood extent. Results from the evaluation showed good agreement in each of these aspects. A sensitivity analysis was then conducted to assess the impact of the DEM and channel geometry corrections, setting a uniform Manning's n and using a kinematic channel flow equation. Sensitivities were found in each variable due to the influence they have upon the floodplain elevation, channel capacity and flow velocity.

The manuscript's contribution to model development is the inclusion of an inundation scheme to the MOSART model, however this is not explicitly stated until page 6 therefore leaving the reader unclear about the paper's contribution for most of the introductory sections. The authors should revise the abstract to state much more clearly that this is one major contribution of the manuscript.

Reply: We thank the reviewer for the positive evaluation and suggestion. In the Abstract and Introduction of the revised manuscript, we more clearly stated the goal of our study as mainly to incorporate and document an inundation scheme in the MOSART model, which is used in Earth System Models.

[C1-2]

One aim of the manuscript is to investigate the importance of geomorphic parameters and river flow representation when modelling the Amazon basin. This is done through the results of the sensitivity analysis, however these mostly back up results from previous papers which also describe the parameterisation of large scale river models in the Amazon basin. Therefore the novel contribution from this aspect is minimised, the greatest contribution from this paper is in describing the model development of the MOSART model.

Reply: In the initial manuscript, the comparisons between our study and previous studies were not clear. We added more discussions to compare the results of our study with those of former studies. On one hand, our work was based on the important foundation of previous studies; on the other hand, our study had some new points in terms of methodologies, model results and sensitivity analyses.

While our modeling approach and improvements do not differ conceptually from those already explored in previous studies, we attempted to generalize various methods for application over the entire Amazon Basin, which is important as MOSART is used in global Earth System Models. Our study also provided more comprehensive examination of our simulations and analysis of sensitivity of the simulations to various factors, which yielded some findings that have not been discussed in former studies, or are different from those of former studies.

[C1-3]

There is no comparison between the results from the model developed in this manuscript with results from the previous version of the model without the inundation scheme. Clearly it is not possible to compare the results of inundation extent but for a model development paper there needs to be some direct comparison between the results of the developed model and those of its predecessor. In this case it should be possible to compare the results of streamflow and river stage. I believe that the model development in this manuscript is significant and merits eventual publication, however I would suggest that it is reconsidered after major revisions so that the authors can include results from a direct comparison between the two model versions.

Reply: We thank the reviewer for the suggestion and positive evaluation.

We have conducted a new simulation “NoInund” (with the inundation scheme turned off) and compared its results with those of the control simulation “CTL” (where the inundation scheme was turned on). This comparison revealed the impacts of the inundation scheme on modeled streamflow and river stages. The comparison was presented in a new subsection (Section 4.1 Representing floodplain inundation). In brief, we updated Figures 8, 9, and 10 to include the results of “NoInund” for comparison with

simulations that include the inundation scheme in different sensitivity experiments. In brief, including inundation generally improves the simulation of streamflow and river stages compared to the simulation without the inundation parameterization.

**Comments**

Additionally please find below the following minor corrections:

[C1-4]

Equation 2 define v

Reply: The definition of $v$ was added as follows (below the newly supplemented Equation (1)) :

*"... where $v$ is the flow velocity [unit: m $s^{-1}$];... "*

[C1-5]

Page 7 line 3 how was it decided to combine the neighbouring catchments?

Reply: The number of catchments is comparatively large, so to show the inundation results more concisely, the catchments were combined to a few subregions. More explanation of the combining procedure was added in this paragraph. The revised text read:

*" Twenty eight large tributary catchments were first delineated and then aggregated to nine tributary subregions. Initially, seven major catchments (i.e., Xingu, Tapajos, Madeira, Purus, Jurua, Japura and Negro) were selected as subregions or the major part of a subregion; Then the Upper-Solimoes catchments were combined as one subregion, the northeast catchments were combined as another subregion, and the remaining five large catchments were incorporated into their adjacent subregions. This way, nine tributary subregions were delineated. Lastly, all the small tributary catchments and the area draining directly to the mainstem were aggregated to be the tenth subregion (i.e., the mainstem subregion). "*

[C1-6]

Page 8 line 9 should read 'lowered to 2.5m'

Reply: The original manuscript is not clear. There should be "an amount of" added before "2.5 m". However, this sentence was removed in the revision (please see the reply to the comment below).

[C1-7]

Page 8 line 9 why was a distinction made between shrubs which were over 5m and those which were lower - why the different treatment when correcting the SRTM?

Reply: The original manuscript is not clear. Some sentences were revised.

The resolution of the vegetation height data is coarser than the resolution of the land cover data. Hence within one pixel of the vegetation height data, there may be more than one land cover class, which should not be assigned the same vegetation height. For shrubs, any vegetation height larger than 5 m should be an overestimation (according to Junk et al. 2011), so an upper limit of 5 m is imposed. After this correction, 50% of the vegetation height was deducted from the DEM pixel covered by shrubs.

The text was revised as: *"In the high resolution land cover dataset, shrubs were defined to be less than 5 m tall (Junk et al., 2011). So for DEM pixels with shrubs, the vegetation height was determined by the vegetation height data, but with an upper limit of 5 m. After this correction, the elevations were lowered by 50% of the vegetation heights for shrub DEM pixels."*

[C1-8]

Page 8 line 13 what was the uniform value that was subtracted from areas located outside the floodplain?

Reply: The original manuscript is not clear. For the fine DEM pixels within one coarse vegetation height pixel, a unique vegetation height is used, but for different vegetation height pixels, the vegetation height can be different even for the same vegetation class.

The text was revised as: *"… , a uniform vegetation height was applied for all the DEM pixels within each vegetation height pixel"*.

[C1-9]

Page 7 line 15 were the elevation profiles not defined from the vegetation corrected DEM?

Reply: Yes, the elevation profiles were generated from the vegetation corrected DEM.

In the revised manuscript, this point was clarified by the following sentence near the beginning of the second paragraph in Section 2.4 "Vegetation-caused biases in DEM" :

*" Before being used for producing elevation profiles, the void-filled HydroSHEDS DEM was processed to alleviate the biases caused by vegetation. "*

[C1-10]

Page 9 line 13 how were the gauges distributed amongst the 10 regions? Some regions might have only had a few gauges hence the significance of the RMSE value might be low, plus this might override the significance of geomorphological factors in applying this correction

Reply: The coefficients of the basin-wide channel geometry formulae were adjusted for seven of the 10 subregions (except "Xingu", "Upper-Solimoes tributaries" and "Mainstem"; shown in Table 1). Each of the seven subregions used 3 – 13 gauges.

The channel geometry is important for inundation modeling of the "Madeira" and "Negro" subregions which have evident inundation and large area. The "Madeira" and "Negro" subregions used 12 and 13 gauges, respectively.

[C1-11]

Page 10 line 16 give an example of the literature - a reference to a textbook for example

Reply: The text was revised as follows:

"*Following Getirana et al. (2012),* $n_{max}$ *and* $n_{min}$ *were set as 0.05 and 0.03, respectively. In addition, a few other studies of the Amazon Basin adopted similar values around the range of 0.03 – 0.05 for the Manning coefficient (Beighley et al., 2009; Paiva et al., 2013a; Yamazaki et al., 2011).*"

[C1-12]

Page 11 line 15 - can river flow in the upper tributaries really be evaluated using the gauge at Santo Antonio do Ica which is located much further downstream? The steeper gradients of the tributaries are likely to have different flow hydraulics to that in the mainstem, can the authors comment on this and provide further justification for using this gauge to make the evaluation?

Reply: We agree that the river flow in the tributaries could be quite different from that of the mainstem so the river flow in the tributaries cannot be represented by using results at this gauge. Our description in the original manuscript is not accurate so the sentence was revised as follows:

"*Most of this subregion is controlled by the Santo antonio do ica gauge at the upper mainstem.*"

[C1-13]

Page 11 line 22 there is a positive runoff bias in the Japura basin which goes against the overall trend of negative biases in the western portion of the basin, could the authors explain what may be causing this?

Reply: There is a negative runoff bias in the subregion "Upper-Solimoes tributaries" which is on the west side of the Japura basin (Fig. 3i). On the other hand, there is a positive runoff bias in the western part of the subregion "Negro", which is on the east side of the Japura basin (Fig. 3g). The western Negro and the Japura basin are adjacent, and both have positive runoff biases.

The runoff biases could be due to errors in precipitation inputs or errors in the land surface water fluxes calculated by the land surface model (e.g., canopy evaporation, plant transpiration, and soil evaporation).

The following sentence was added:

*"The runoff biases could be caused by errors in the precipitation forcing dataset or errors in the land surface water fluxes calculated by the land surface model (e.g., canopy evaporation, plant transpiration, and soil evaporation)."*

[C1-14]

Eq 7 This describes how the simulated river stages are converted into elevations, should this not therefore be included in section 2.5 which describes how the river channel geometry in the model was established?

Reply: Following the suggestion by the reviewer, the method for estimating the riverbed elevation was moved to Section 2.5.

[C1-15]

Page 12 line 12 how were the simulated river stages shifted to coincide with the observations?

Reply: All the simulated river stages of the same subbasin were raised or lowered by a uniform height, to facilitate comparison of the timing and magnitude between the simulated river stages and the observations. A similar method was also used in Figure 7 of Coe et al. (2002) .

The text was supplemented by *"of the same subbasin"* and *"by a uniform height"*, and now read: *"For better visual comparison, the simulated river stages of the same subbasin were shifted by a uniform height to coincide with the observations."*

[C1-16]

Page 12 line 15 should another metric be calculated alongside the correlation coefficient? In the Negro and Japura basins for example Fig 4 shows there is a very high correlation but the differences between the simulations and observations are very large. Perhaps calculating another metric might capture this?

Reply: The original manuscript was not clear. The standard deviations were calculated and used to indicate river stage fluctuations. It was discussed that the river stage fluctuations were overestimated for the subbasins of 4 gauges (i.e., Canutama[Purus], Acanaui[Japura], Serrinha[Negro] and Santo antonio do ica[Mainstem] ).

To make the text more clear, the phrase "*as well as standard deviation for simulated and observed river stages*" was replaced with "*Moreover, the standard deviations for the simulated and observed river stages were also calculated*."

[C1-17]

Page 13 line 2 should read 'lake areas'

Reply: This was corrected as suggested.

[C1-18]

Figure 6 the four plots should be replaced with two difference plots, one showing the difference between the simulated and observed during high water and the other during low water. This would better visualise the difference between the two simulations.

Reply: Fig. 6 was supplemented by two panels showing the differences during high water season (Fig. 6e) and low water season (Fig. 6f). The original four panels were kept in order to show the spatial patterns of inundation.

[C1-19]

Page 13 line 13 the statement that the GIEMS data and simulation agree reasonably well is very vague. Figure 6 appears to show that the simulation overestimates the extent in the lowland portion of the basin, especially at low water. This sentence should be expanded to include more details about where the differences occur.

Reply: We added some discussions of the similarities and differences between model results and GIEMS data in the revised manuscript (as follows).

*"Both the observations and the simulated results show evident inundation in the regions near the middle and lower mainstem. The observed inundation in the upper Madeira subregion and middle Negro subregion is partially captured by the model. The comparison also shows spatially varying differences between the modeled and observed flood extent (Figs. 6e and 6f). The modeled flood extent exceeds the observations in the lower Madeira subregion near the mainstem and around the major reaches in the middle Negro subregion. At the same time, the modeled flood extent is lower than the observations for some subbasins in the mainstem, upper Madeira, Upper-Solimoes and middle Negro subregions."*

[C1-20]

Figure 7 it could be useful to plot the data by seasons e.g AMJ, JAS, OND, JFM as this might show if the errors are concentrated in a particular season e.g. low water.

Reply: Thank you for the suggestion. Similar to Figure 7 that compares the annual averaged biases in flood extent and streamflow, we plotted the averaged monthly streamflow errors and the flood extent discrepancies (i.e., the differences between simulated flood extent and the GIEMS data) during 12 years (1995 – 2006). Please find the figure in the Appendix. This figure shows that the seasonal distribution of streamflow errors varies for different gauges. For example, for "(a) Altamira" and "(b) Itaituba", evident positive biases occur from January to April; for "(c) Fazenda vista alegre" and "(d) Guajara-mirim", positive biases are more evident from about May to October; for "(h) Acanaui", positive biases are more evident from about March to July. Except for three subregions (Negro, Cach de porteira-con, and Tabatinga), the seasonality of flood extent discrepancies follows the seasonality of streamflow errors very closely, indicating the important contribution of streamflow errors to flood extent biases on seasonal time scale.

[C1-21]

Figure 8, why does this figure refer to the average seasonal cycle from 1995-2006 whilst figures 9 and 10 refer to 2007 only? Does this explain why the results for the kinematic simulation are so different between figures 8 and 9 & 10? I would expect the kinematic simulation to be very different to the control simulation (as it appears in Figs 9 and 10), yet does this not appear to be the case for streamflow - could the authors explain why streamflow is not sensitive to the kinematic solution or replot Fig 8 for 2007 only so that it is directly comparable to Figs 9 and 10?

Reply: Figs. 8, 9 and 10 have been replotted to show the results of the same year. We did not have observed streamflow data for year 2007 so we plotted the results of another year (2005).

The three figures show that the differences in streamflow between the simulation KW (kinematic wave method) and the simulation CTL (diffusion wave method) are not as evident as those in river stages. Previous studies have yielded similar results (e.g., Fig. 5 of Yamazaki et al., 2011). The reason could be that the flow velocities in the simulation KW (which are based on riverbed slopes) are also quite different from those in the simulation CTL (which are based on friction slopes).

[C1-22]

Figure 10 is confusing with the y-axis reset for 0-1500 km for the simulations but not for the riverbed profile. These graphs should use the same y-axis for the entire river length in order to remove the confusing jump that happens at 1500 km.

Reply: Figure 10 was replotted to use the same y-axis for the entire river length. We thank the reviewer for the suggestion.

[C1-23]

Section 4.2, the greatest effect is shown in the Madeira basin, is this most likely because the multiplicative factor (0.36) has the greatest effect on changing the channel geometry relative to the other basins? This should be stated more explicitly in the second paragraph.

Reply: Yes, the reason is that the channel geometry changes in the Madeira subregion are larger than those of the other subregions.

To make the discussion more explicit, the following revisions were made in the second paragraph:

(1) "*channel geometry changes*" was replaced with "*the channel cross-sectional area is multiplied by a factor of 0.36 (Table 1)*" ;

(2) Added one sentence: *'Similar phenomenon is observed at the gauge "Cach da porteira-con" in the Northeast subregion (Fig. 8h), where the channel cross-sectional area is multiplied by a factor of 0.48.* '

(3) Added "*caused by refining channel geometry*" after "*Inundation changes*".

[C1-24]

Figure 13 needs to be redone as it is very difficult to follow the decision chain that the authors are trying to imply. For example at the second box there are four options but how is a reader meant to decide between these?

Reply: The original manuscript was not clear. In general, the phenomena before and after an arrow have the cause – effect relationship.

The figure caption was revised: "*An example of the effects of channel cross-sectional geometry on the water depth of the local channel*" was replaced with "*A diagram illustrating that decreasing the width of the local channel could bring about changes in the water depth of the local channel through various mechanisms. In general the phenomena before and after an arrow have the cause – effect relationship*" .

[C1-25]

Page 18 line 26 should read 'could have an evident effect'

Reply: "*an*" was added between "*have*" and "*evident*".

# Response to Referee #2

We appreciate the time and effort of the reviewer and thank the reviewer for the constructive comments. We addressed all the comments, and included corresponding changes in the revised manuscript.

In the following text, we use blue font for the reviewer comments, black font for our replies, and italics for the revisions in the manuscript.

## Comments

[C2-1]

The paper presents improvements on the parametrization of the MOSART surface water model. State of art methods are used to update river model and inundation parametrization. The model is evaluated in the Amazon basin and several simulations were performed to evaluate the role of the DEM, river geometry parameters, and backwater effects. The subject addressed by the paper is important. With new data available for regional/global hydrologic simulations, there are several new efforts to improve hydrological models. And the documentation of new improvements/updates of models, as the MOSART, fits the goal of GMD journal. Also, the study of impact of model errors and different parametrizations are important guide future model developments. The paper is generally clear. However, it seems that most of the conclusions from paper analyses were already provided by the past modelling studies in the Amazon (e.g. Paiva et al., 2013, Getirana et al. 2012, Yamazaki et al., 2011, Beighley et al., 2009; Baugh et al., 2013). For example, the past studies already pointed for the importance backwater effects and flooding, performed sensitivity studies on the role of river geometry errors and DEM errors on amazon simulations. So I guess that it would be better to present the paper as a documentation of the improvements of a specific model (MOSART) to move toward state of art methods. And to clarify that the analyses could reproduce similar conclusions from the past studies. So, as the documentation of model parametrizations fits the GMD journal scope, I think that the paper could be published. But it needs to be reviewed clarify the actual contributions, by addressing the comments above and below.

Reply: We thank the reviewer for the positive evaluation and suggestions. We clarified the contribution mainly as the incorporation of an inundation scheme into the MOSART model. The related revisions were added in several sections: Abstract, Introduction, Methods and data, Sensitivity study, and Summary and discussion.

Our initial manuscript was not clear in the comparisons with previous studies. Following the suggestions of the reviewers, we added more discussions on comparisons between our study and former studies.

While previous studies provided the foundation for the approaches we adopted in our study and some of our results agree with those of former studies, our study has also provided some new points in terms of methodologies, model results and analyses. These are elaborated below.

1. Methods

1.1 DEM correction

We explicitly considered the spatial variability of the vegetation-caused biases in the DEM data, which alleviated biases for hydrologic modeling in the entire Amazon Basin. The DEM correction was based on a map of spatially varying vegetation heights and a land cover dataset.

In most previous studies of hydrologic modeling for the entire Amazon Basin, the DEM was lowered by a uniform height for vegetated area (Coe et al., 2008; Paiva et al., 2013a). Although spatial variability of vegetation-caused biases in DEM was also considered in previous hydrodynamic modeling studies, they were performed only in a comparatively small area of the central Amazon region (Baugh et al., 2013; Wilson et al., 2007). We generalized the approach by using land cover data and vegetation height data that have global coverage so the method can be used in the entire Amazon Basin and other regions.

1.2 Refining channel geometry

We refined the basin-wide empirical formulae for channel cross-sectional dimensions in various subregions to improve the representation of spatial variability in channel geometry (Table 1). In many former studies, the basin-wide formulae were used (Beighley et al., 2009; Coe et al., 2008; Getirana et al., 2012; Yamazaki et al., 2011).

Paiva et al. (2013a) accounted for spatial variability of channel geometry formulae and used various coefficients in their formulae for six zones of the Amazon Basin (Table 1 of Paiva et al. 2013a). But they did not compare the results of diverse subregion formulae with those of the basin-wide formulae.

2. Sensitivity study

The sensitivity analyses of former studies primarily examined the impacts of various factors (e.g., the inundation scheme, channel geometry, Manning coefficients or backwater effects) on the total flooded area of the central Amazon region (Figs. 9 and 13 of Yamazaki et al. 2011) or the entire Amazon Basin (Fig. 10 of Paiva et al. 2013a), and streamflow and river stages of a few mainstem gauges (Figs. 13, 5a and 5b of Yamazaki et al. 2011; Fig. 10 of Paiva et al. 2013a).

In a more comprehensive manner, we examined the impacts of five factors (i.e., the inundation scheme, correcting DEM, channel geometry, Manning coefficients, and backwater effects) on modeled surface hydrology at various locations spread over the Amazon Basin, including inundation of 10 subregions

(Fig. 11), streamflow and river stages of more than 10 gauges (at both the mainstem and tributaries) (Figs. 8 and 9), and the water surface profile along the mainstem (Fig. 10).

Paiva et al. (2013a) examined the impacts of perturbing precipitation, elevation profiles or maximum soil water storage on modeled surface hydrology (Figs. 10 and 11 of Paiva et al. 2013a). We did not investigate these three factors.

Our sensitivity study yields several findings which are new or different from former studies (as follows).

2.1 Impacts of including the inundation scheme

This point was not explicitly discussed in the initial manuscript. Following the suggestions of both reviewers, in the revision this point was investigated and discussed.

Our investigation related to river stages was different from the former study. To our knowledge, only Yamazaki et al. (2011) explicitly examined the impacts of the inundation scheme on water depths at the gauge station (Fig. 5b of Yamazaki et al. 2011) and water depths along the mainstem (Fig. 7 of Yamazaki et al. 2011). They conducted three simulations: the diffusion wave simulation with the inundation scheme (FLD+Diff), the kinematic wave simulation with the inundation scheme (FLD+Kine), and the kinematic wave simulation without the inundation scheme (NoFLD). Therefore, while examining the impacts of the inundation scheme on water depths (or river stages), they used the kinematic wave river routing method, but we used the diffusion wave river routing method, which was more advanced (e.g., could represent the backwater effects) (Figs. 9 and 10).

2.2 Impacts of correcting DEM

The vegetation-caused biases in DEM were alleviated with various approaches in a few previous studies in the partial or entire Amazon Basin (Baugh et al., 2013; Coe et al., 2008; Getirana et al., 2012; Paiva et al., 2011, 2013a; Wilson et al., 2007; Yamazaki et al., 2011). To our knowledge, most of these studies did not examine and explicitly report the impacts of DEM correction on the modeled results. Only Baugh et al. (2013) showed the impacts of DEM correction on floodplain water levels and inundation in a comparatively small area in the central Amazon region (Figs. 2 and 5 of Baugh et al. 2013).

Our study examined and explicitly reported the impacts of alleviating vegetation-caused biases in DEM on modeled surface hydrology in the hydrologic modeling for the entire Amazon Basin (Figs. 8, 9, 10 and 11). These basin-wide impacts were not explicitly reported in the past.

2.3 Impacts of refining channel geometry

While examining the impacts of adjusting channel geometry on modeled surface hydrology, we used a method different from those of previous studies, where the channel widths or depths of all the channels

were perturbed by a uniform percentage (or a uniform amount) (Fig. 13 of Yamazaki et al. 2011; Fig. 10 of Paiva et al. 2013a).

We refined the basin-wide formulae of channel geometry for various subregions. The channel-geometry changes were caused by the process of refining channel cross-sections and those change ratios were different for various subregions (Table 1). We compared the results of diverse subregion formulae with those of basin-wide formulae to reveal the impacts of adjusting channel geometry on modeled surface hydrology (Figs. 8, 9, 10 and 11). Our method had more physical mechanism than the former method of perturbing channel geometry uniformly in the entire basin.

2.4 Impacts of considering backwater effects

Our model results showed the impacts of backwater effects on flood extent and river stages were more prominent than those of the previous study. To our knowledge, only Yamazaki et al. (2011) explicitly reported the impacts of backwater effects on flood extent (Fig. 9 in Yamazaki et al. 2011) and river stages (Figs. 5b and 7a in Yamazaki et al. 2011). In our study, the impacts of backwater effects on flood extent (Fig. 11) and river stages (Figs. 9 and 10) were more prominent than those of Yamazaki et al. (2011). These differences may be due to the discrepancies in channel geometry or floodplain topography between the two studies.

Our model results showed that backwater effects could advance the flood peak in the Madeira River (Fig. 8c). To our knowledge, this phenomenon has not been discussed in the previous modeling studies in the Amazon Basin.

In summary, while our modeling approach and improvements do not differ conceptually from those already explored in previous studies, we attempted to generalize various methods for application over the entire Amazon Basin, which is important as MOSART is used in global Earth System Models. We also provided more comprehensive examination of our simulations and analysis of sensitivity of the simulations to various factors, which yielded some findings that have not been discussed in former studies, or are different from those of former studies.

[C2-2]

Introduction: I feel that the main goal of this paper should be to document improvements on the MOSART model. So it is important to provide more details in the intro section.

Reply: We agree with the reviewer's assessment. We revised the Introduction to more explicitly state our objective for implementing and documenting an inundation parameterization in the MOSART model

for global application, and handling a few challenges facing the continental-scale hydrologic modeling in the Amazon Basin.

[C2-3]

Page 2. Line 25. Which of these challenges were addressed by this paper in a novel way that was not done by the past efforts?

Reply: In the initial manuscript, the comparisons between our study and previous studies were not clear. As discussed in the reply to the first comment [C2-1], on one hand, our study was based on the important foundation of previous studies; on the other hand, our work also yielded some new points in terms of methodologies, model results and sensitivity analyses.

[C2-4]

Page 3. Line 9. Vegetation errors from SRTM DEM were removed globally by F.E. O'Loughlin et al. 2016 RSE. Please review and discuss it in the paper.

Reply: We thank the reviewer for directing us to this study related to our work. The DEM correction for hydrologic modeling is discussed in this paragraph. O'Loughlin et al. (2016) did not conduct hydrologic modeling, so the discussion of their study was not added here, but in Section 2.4 "Vegetation-caused biases in DEM" of the revised manuscript (as follows).

*" O'Loughlin et al. (2016) estimated the vegetation-caused biases in the SRTM DEM data based on vegetation height data, canopy density data and the distribution of five climatic zones (i.e., Tropical, Arid, Temperate, Cold and Polar). They created the first global 'Bare-Earth' high resolution (3 arc-seconds) DEM from the SRTM DEM data. They compared their method with the static correction method (i.e., estimating the vegetation-caused bias as the product of vegetation height and a fixed percentage) used by Baugh et al. (2013) and this study, and noted that the static correction method was effective but moderately worse than their method. "*

[C2-5]

Page 3. Line 22. See also analyses from Paiva et al., 2013 WRR.

Reply: Paiva et al. (2013a, WRR) analyzed the sensitivities of streamflow, water depths and flooded area to the channel width and depth (in their Fig. 10). The citation of this reference was supplemented.

[C2-6]

Objectives. What is the new proposed contribution? If the contributions are limited to updating MOSART model with state of art methods, then I think that you should specify it in the objectives and introduce MOSART in the intro section.

Reply: As discussed in our replies to the first and second comments ([C2-1] and [C2-2]), we made our objectives more clear in the Introduction section. As a reply to a similar comment from the first reviewer, we added a new section (Section 4.1 Representing floodplain inundation) to compare the simulations with and without the inundation parameterization to document its impacts on the overall performance of MOSART. Figures 8, 9, and 10 were updated to include results for the simulation without inundation for comparison with various simulations that include the inundation parameterizations.

[C2-7]

2.1. How the model defines what is main river network and tributary subnetwork?

Reply: In the MOSART model, each computation unit (subbasin or grid cell) has a major channel (or main channel) and a tributary subnetwork which includes tributaries within the computation unit. Please see the following figure from Li et al. (2013).

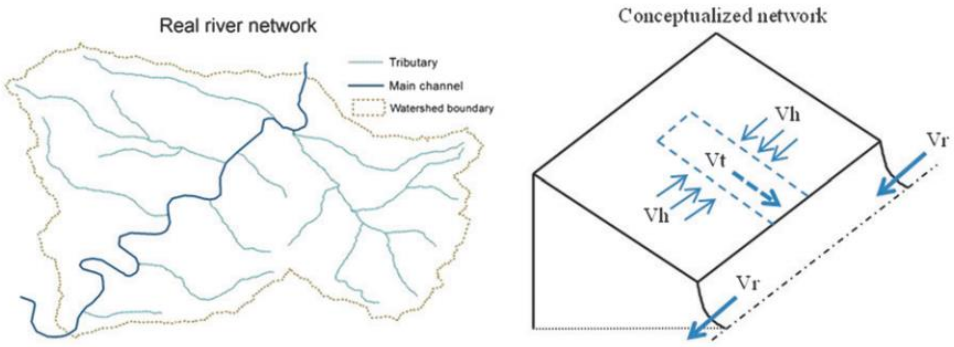


FIG. 1. Conceptualization of river network in MOSART. The runoff generated first enters the tributaries (surface runoff via hillslope routing and subsurface runoff without hillslope routing); it is then routed through the tributaries (here conceptualized as a single equivalent channel, as shown by the light blue dashed lines) and is finally discharged into the main channel. The value $V_h$ is the overland flow during hillslope routing, $V_t$ is the channel velocity within the tributaries, and $V_r$ is the channel velocity within the main channel.

The main channels of all the computation units constitute the main-channel network of the entire basin.

The following text was added in the first paragraph of Section 2.1 :

"*In the MOSART model, each computation unit (subbasin or grid cell) has a major channel (or main channel) and a tributary subnetwork that represents the combined equivalent transport capacity of all the tributaries within the computation unit.*"

[C2-8]

Eq.1. It seems g can be removed from equation.

Reply: "*g*" was deleted from this equation.

[C2-9]

Continuity equation is not shown. Please show it.

Reply: The continuity equation was added (Equation (1) in the revised manuscript).

[C2-10]

How these equations (kinematic and diffusive) are solved? Please provide details on the numerical methods. finite difference, finite volumes, implicit, explicit? Criteria for time step, spatial discretization? What is done to avoid mass errors.

Reply: The explicit finite difference method is used to solve the equations. The computation units can be grid cells or subbasins. The Courant condition is used for choosing the time step. In this Amazon application, the time step is one minute when the diffusion wave method is used. The cumulative mass error is less than 0.5 percent in these multi-year simulations.

The following text was added at the end of Section 2.1:

"*In this model, the equations are solved with the explicit finite difference method. Either square grid cells or irregular subbasins can be used as computation units. The time-step size is chosen to satisfy the Courant condition to ensure stable computation (Cunge et al., 1980).*"

[C2-11]

2.2. It is not clear how you compute river bed elevation? Is it simply the lowest DEM pixel of the catchment? How the model accounts for the fact that SRTM DEM does not see the river bed? And the fact that the river profile is not flat?

Reply: In Fig. 1b, the elevation profile and the fraction of channel area ($A_c$) can determine the elevation of the channel bank top ($E_t$). The channel bed elevation ($E_b$) is: $E_b = E_t - d$, where $d$ is the channel depth and is estimated in Section 2.5. The channel bed could be lower than the lowest DEM pixel of the catchment because the DEM does not see the channel bed.

In the elevation profile of Fig. 1b, the longitudinal profile of the channel bed is deemed to be flat, which is different from the actual condition in the real world. This assumption may bring about some error when the flooded area is estimated.

Fig. 1b was updated in the manuscript: (1) In the amended elevation profile, the channel bed elevation was lowered; (2) The bank top elevation ($E_t$) and the channel bed elevation ($E_b$) were indicated.

The following text was added in the second paragraph of Section 2.2:

"*The channel bed elevation equals the difference of the bank top elevation and the channel depth which is estimated in Sect. 2.5. The channel bed could be lower than the lowest DEM pixel of the computation unit because the DEM does not reflect the channel bed elevation.*"

[C2-12]

2.3. How the basins are defined? What is the input data? Hydrosheds? Please make it clear.

Reply: Yes, the subbasins were extracted from the HydroSHEDS DEM. The following text was revised and moved from Section 2.4 to Section 2.3.

"*The 3 arc-seconds HydroSHEDS DEM data developed by United States Geological Survey (USGS) (http://hydrosheds.cr.usgs.gov/) was used in this study. The hydrologically conditioned HydroSHEDS DEM was used to generate the digital river network and subbasins.*"

[C2-13]

Pag. 6 Line 30. What is the criteria to define river length? How time step is defined? How these choices affect model errors (model numerical stability, mass errors, numerical dispersion, … ) ? Please clarify and discuss it.

Reply: We used comparatively coarse subbasins (the average area is 1091.7 $km^2$) due to computational costs. Each subbasin has a main channel. The main channel length varies with the subbasin size.

The time step was determined based on the Courant condition and some test simulations. The time step of one minute was used so that the simulations were stable. The cumulative mass error for the entire Amazon Basin was less than 0.5 percent in the simulations.

The following text was added in the first paragraph of Section 2.3 :

"*Relatively coarse resolution subbasins were adopted as MOSART-Inundation is intended for global earth system modeling, which is constrained by computational cost. … … To ensure stable computation, the time-step size was determined based on the Courant condition and numerical tests. The time step of one minute was used for all the simulations.*"

[C2-14]

2.4. Vegetation Errors. Was the corrected DEM validated ? Please justify and compare these methods to the global SRTM DEM product free of veg errors recently developed by F.E. O'Loughlin et al. 2016 RSE.

Reply: Our method was based on that of Baugh et al. (2013). Moreover, we also used a high resolution (3 arc-seconds) land cover dataset when estimating the vegetation-caused biases in the HydroSHEDS DEM data.

The discussion on the study of O'Loughlin et al. (2016) was added in Section 2.4 "Vegetation-caused biases in DEM" (as follows).

*" O'Loughlin et al.(2016) estimated the vegetation-caused biases in the SRTM DEM data based on vegetation height data, canopy density data and the distribution of five climatic zones (i.e., Tropical, Arid, Temperate, Cold and Polar). They created the first global 'Bare-Earth' high resolution (3 arc-seconds) DEM from the SRTM DEM data. They compared their method with the static correction method (i.e., estimating the vegetation-caused bias as the product of vegetation height and a fixed percentage) used by Baugh et al. (2013) and this study, and noted that the static correction method was effective but moderately worse than their method. "*

[C2-15]

2.6. Line 16. What literature was used to define Manning at 0.03 and 0.05? I feel that the parametrization of Manning needs more justification (past studies or calibration). How these choices will impact model results?

Reply: Previous studies were cited to justify our choice of the Manning coefficients. The sensitivity study part (Section 4.4) discusses the effects of the Manning coefficients on model results. Refining the Manning coefficients could improve streamflow hydrographs. The increase of the Manning coefficient could affect flood extent, streamflow and river stages in local, upstream or downstream subbasins.

The text was revised as follows:

"*Following Getirana et al. (2012),* $n_{max}$ *and* $n_{min}$ *were set as 0.05 and 0.03, respectively. In addition, a few other studies of the Amazon Basin adopted similar values around the range of 0.03 – 0.05 for the Manning coefficient (e.g., Beighley et al., 2009; Paiva et al., 2013a; Yamazaki et al., 2011).*"

[C2-16]

2.7. Line 6. Why average manning of 0.03 ? You should use the average Manning from the reference simulation or use other approach to isolate the effect of variable vs constant manning.

Reply: The uniform Manning coefficient of 0.03 is used for two reasons: (1) the uniform Manning coefficient of 0.03 was used by Yamazaki et al. (2011); (2) it is the lowest value in the range 0.03 – 0.05. The spatially varying Manning coefficients are from 0.03 to 0.05 in the control simulation. So comparing the control simulation and the simulation "n003" (which uses the uniform Manning coefficient of 0.03) can reveal the impacts of Manning coefficient increases on modeled surface hydrology.

Following the reviewer's suggestion, we conducted a new simulation using the Manning coefficient of 0.04 (the average of 0.03 and 0.05) for all the channels (abbreviated as 'n004'). We added the Nash–Sutcliffe efficiency coefficients (NSEs) of streamflow of the simulation 'n004' into Table 4.

The description of the six contrasting scenario simulations was expanded and moved to Section 4 "Sensitivity study" in the revised manuscript. The description of the simulations "n003" and "n004" was added in the fourth paragraph of Section 4 (as follows).

*" A few previous studies at the Amazon Basin used a constant Manning coefficient for all the channels (e.g., 0.04 was used by Beighley et al., 2009; and 0.03 was used by Yamazaki et al., 2011). A constant Manning coefficient of 0.03 and 0.04 was used in the fifth and sixth simulations, respectively (abbreviated as "n003" and "n004"). "*

The description on the simulation comparison in Section 4.4 was revised (as follows).

*'The streamflow Nash–Sutcliffe efficiency coefficients (NSEs) of "CTL" were compared with those of "n003" and "n004" (Table 4). The NSEs of "CTL" are higher than those of "n004" at 10 of the 13*

*gauges (except Fazenda vista alegre, Itapeua and Manacapuru) and higher than those of "n003" at 12 of the 13 gauges (except Obidos). These results suggest that the spatially varying Manning coefficients are more appropriate than the uniform Manning coefficient of 0.03 or 0.04 for the simulations of this study.*

*The spatially varying Manning coefficients range from 0.03 to 0.05 and are equal to or larger than the Manning coefficient of 0.03. The spatially varying Manning coefficients result in larger flood extent than the uniform coefficient of 0.03 (Fig. 11). '*

[C2-17]

2.7. What is optimal combination? Was any calibration performed?

Reply: The original manuscript was not clear. It meant that in the control simulation, the preferred methodologies were used at each aspect. We did not try to calibrate parameters to improve the modeled results.

The text was expanded to be more specific in Section 2.7 "Control simulation" (as follows).

"*The aforementioned factors could have important impacts on modeling surface hydrology of the Amazon Basin. We configured a control simulation (abbreviated as "CTL") using the preferred methodologies for five aspects: (1) the inundation scheme was turned on; (2) vegetation-caused biases in the DEM data were alleviated; (3) the basin-wide channel geometry formulae were refined for different subregions; (4) the Manning coefficient varied with the channel size; (5) the diffusion wave method was used to represent river flow in channels. The control simulation was run for 14 years (1994 – 2007) and the results of 13 years (1995 – 2007) were evaluated against gauged streamflow data and remotely sensed river stage and inundation data.*"

[C2-18]

3.1. How the model performance compare to past modelling studies in the Amazon? Please discuss it in the manuscript.

Reply: The modeled streamflow results were compared with a few previous studies. The following text was added to the second paragraph of Section 3.1:

"*In general, the simulated streamflow results are comparable to those of a few previous studies (e.g., Getirana et al., 2012; Yamazaki et al., 2011) and slightly worse than those of Paiva et al. (2013a).*"

[C2-19]

3.2. Equation 7. Do you use this equation to estimate a parameter for simulation? If yes, this explanation should appear o section 2. Why this approach were selected? How it compares to previous studies? How this choice impact model results? See Paiva et al., 2013 for an analyses of impact of bed elevation errors on simulations.

Reply: The relative riverbed elevations from this equation can be deemed as parameters for channel routing computation. Actually, riverbed slopes ( $S_0$ in Equation (2)) are directly used in the channel routing computation in this study. This approach is the same as those of previous studies (Beighley et al., 2009; Getirana et al., 2012; Paiva et al., 2011, 2013a; Yamazaki et al., 2011).

The Equation (7) and the related descriptions was moved to the methodology part (Section 2.5).

In this study, the method for estimating the riverbed slope may be different from those of previous studies. The riverbed slopes of this study were directly derived from the DEM. Some previous studies first alleviated errors caused by water depths or vegetation heights, then used the corrected DEM to derive riverbed slopes (e.g., Paiva et al., 2011). So the method of our study has less physical mechanism and may have more uncertainties than those of some previous studies.

Paiva et al. (2013a) studied the sensitivities of streamflow, water depths and flooded area to riverbed elevations. In scenario simulations, riverbed elevations were perturbed by 3m, 1m, -1m, or -3m. In our understanding, the riverbed elevations of the entire basin were raised or lowered by a uniform value in any single simulation. So this treatment did not affect the riverbed slopes used in channel routing computation. Actually this treatment reduced or increased the channel depths, which decreased or enlarged the channel conveyance capacities. In our study, the impacts of channel cross-sectional geometry on surface hydrology were studied in a different way (Sections 2.5 “Channel geometry” and 4.3 “Refining channel geometry”).

[C2-20]

3.2. How model performance for river elevation compares to previous modelling studies in the amazon? Please discuss it in the manuscript.

Reply: The simulated river-stage results were compared to some previous studies. The following text was added to the third paragraph of Section 3.2:

" *Overall, in terms of the timing and magnitude of fluctuations, the modeled river stages of this study are comparable to those reported in some previous investigations (Coe et al., 2008; Getirana et al., 2012; Paiva et al., 2013a).* "

[C2-21]

3.3. How model performance for flood extent compares to previous modelling studies in the amazon? Please discuss it in the manuscript.

Reply: The modeled inundation results were compared to a few previous studies. The following text was added at the end of Section 3.3:

"*Although the GIEMS data have non-negligible uncertainties, it is useful to check how our results may differ from those of previous studies using the GIEMS data as the common benchmark. Overall compared to the GIEMS data, the spatial inundation patterns of this study were slightly better than those of Getirana et al. (2012), and comparable to those of Yamazaki et al. (2011) and Paiva et al. (2013a). In terms of monthly total flooded areas, Getirana et al. (2012), Paiva et al. (2013a) and this study were comparable at the whole-basin scale, while the results from Getirana et al. (2012) and this study were closer to the GIEMS data than those of Paiva et al. (2013a) at the subregion scale.* "

[C2-22]

4.1. How these analyses compare to previous analyses of impact of DEM and floodplains on Amazon simulations from previous modelling studies?

Reply: The vegetation-caused biases in DEM were alleviated with various approaches in a few previous modeling studies in the Amazon Basin. To our knowledge, most of those studies did not explicitly report the effects of the DEM correction on the modeled surface hydrology except Baugh et al. (2013). The following text was added to Section 4.2 "Correcting DEM" (previous Section 4.1 "Correction of DEM"):

"*The vegetation-caused biases in DEM data were alleviated with various approaches in a few previous studies modeling the surface hydrology in the Amazon Basin (Baugh et al., 2013; Coe et al., 2008; Getirana et al., 2012; Paiva et al., 2011, 2013a; Wilson et al., 2007; Yamazaki et al., 2011). Most of these studies did not examine and explicitly report the effects of the DEM correction on the modeled results. Baugh et al. (2013) demonstrated that alleviating vegetation-caused biases in DEM could improve the modeled water levels and inundation over floodplains adjacent to a 280-km reach of the central Amazon (in their Figs. 2 and 5).*"

Following the suggestion of both reviewers, in the revised manuscript we added a new section (Section 4.1 "Representing floodplain inundation") to report the impacts of using the inundation scheme on modeled surface hydrology. We also compared our methodology and results with those of a few previous studies (as follows).

*" Some previous studies also examined and reported the impacts of representing the floodplain inundation on the modeled surface hydrology in the Amazon Basin (Getirana et al., 2012; Paiva et al., 2013a; Yamazaki et al., 2011). Yamazaki et al. (2011) showed the impacts of floodplain inundation on the streamflow, water depths, and flow velocities at the Obidos gauge (in their Fig. 5) and the mainstem water surface profile (in their Fig. 7). Getirana et al. (2012) demonstrated the effects of floodplain inundation on streamflow of a few mainstem gauges (in their Fig. 16). When investigating the impacts of floodplain inundation on surface hydrology, these two studies used the kinematic wave river routing method that could not represent the important backwater effects in the Amazonia, while we used the diffusion wave river routing method that captured backwater effects. Backwater effects were also represented in the dynamic wave river routing method used by Paiva et al. (2013a) when they studied the impacts of floodplain inundation on streamflow of a few major tributary or mainstem gauges including Obidos and Manacapuru (in their Table 2 and Fig. 14). Besides streamflow, in this study we also examined and revealed the prominent impacts of floodplain inundation on the river stages near 11 major gauges or along the mainstem. "*

[C2-23]

4.2. It is not change in channel storage capacity that changes simulation. It is changes in channel conductance capacity.

Reply: "*channel storage capacity*" was revised to be "*channel conveyance capacity*" throughout the manuscript.

[C2-24]

4.2. How these analyses compare to previous analyses of channel geometry from previous modelling studies?

Reply: Some previous studies in the Amazon Basin (e.g., Paiva et al., 2013a; Yamazaki et al., 2011) also investigated the sensitivities of modeled surface hydrology to channel geometry. They pointed out the importance of channel geometry that motivated the analysis in our study. At the same time, the methods and results of our study had some new points: (1) channel-geometry changes were caused by the process of refining channel cross-sections and those changes were spatially varying (Table 1); (2) we examined

the effects of channel-geometry changes on modeled surface hydrology at spatially distributed locations (i.e., the 10 subregions, more than 10 tributary and mainstem gauges, and the mainstem); (3) some of our result-analyzing approaches were different from those of former studies.

The following text was added to the end of Section 4.3 "Refining channel geometry" (previous Section 4.2 "Adjustment of channel geometry"):

*" The sensitivities of modeled surface hydrology to channel geometry were also investigated by some former studies (e.g., Paiva et al., 2013a; Yamazaki et al., 2011). Yamazaki et al. (2011) perturbed the channel width or depth by a uniform percentage for all the channels and examined the effects of these channel-geometry changes on streamflow of the Obidos gauge and the flooded area over the central Amazon region (in their Fig. 13). Paiva et al. (2013a) perturbed the channel width by a uniform percentage or perturbed the channel-bottom level by a uniform height, which was equivalent to perturbing the channel depth by a uniform value, and investigated the effects of these channel-geometry changes on streamflow of the Obidos gauge, channel water depths of the Manacapuru gauge, and the total flooded area of the entire Amazon Basin (in their Fig. 10). These two studies showed the sensitivities of modeled surface hydrology to channel geometry, as well as the interactions between streamflow, water depths and inundation. They pointed out the importance of channel geometry and provided a foundation to this study. Here, channel-geometry changes were caused by the process of refining the channel cross-sections, and the changes varied spatially (Table 1). We examined the effects of channel-geometry changes on inundation of 10 subregions, streamflow of 13 gauges, river stages near 11 gauges, as well as the mainstem water surface profile. In addition, the effects of channel-geometry changes on modeled surface water dynamics were analyzed with approaches of which some were different from those of the former studies. "*

[C2-25]

4.3. I'm not sure if this analysis is conclusive. It is not possible to be sure that the differences in results are related to variable Manning or if it is because a specific value of 0.03 was chosen. This value may be different from the average value of the control simulation. I suggest the computation of the average Manning from control simulation and using this value for the new simulation.

Reply: Following the reviewer's suggestion, we conducted a new simulation "n004" which used a constant Manning roughness coefficient of 0.04 (i.e., the average of 0.03 and 0.05) for all the channels. We compared the streamflow Nash–Sutcliffe efficiency coefficients (NSEs) of three simulations ("CTL", "n004" and "n003"). In Section 4.4 "Varying Manning roughness coefficients" (previous Section 4.3 "Varying the Manning coefficients"), the second paragraph and the beginning of the third paragraph were revised as follows:

" *The streamflow Nash–Sutcliffe efficiency coefficients (NSEs) of "CTL" were compared with those of "n003" and "n004" (Table 4). The NSEs of "CTL" are higher than those of "n004" at 10 of the 13 gauges (except Fazenda vista alegre, Itapeua and Manacapuru) and higher than those of "n003" at 12 of the 13 gauges (except Obidos). These results suggest that the spatially varying Manning coefficients are more appropriate than the uniform Manning coefficient of 0.03 or 0.04 for the simulations of this study.*

*The spatially varying Manning coefficients range from 0.03 to 0.05 and are equal to or larger than the Manning coefficient of 0.03. The spatially varying Manning coefficients result in larger flood extent than the uniform coefficient of 0.03 (Fig. 11). … …*"

[C2-26]

## 4.3. How these analyses compare to previous analyses of Manning role from previous modelling studies?

Reply: A few former studies in the Amazon Basin (e.g., Paiva et al., 2013a; Yamazaki et al., 2011) also investigated the sensitivities of simulated surface hydrology to the Manning roughness coefficient. They revealed the importance of the Manning coefficient and motivated the analysis in our study. At the same time, the approaches and analyses of this study had some new points: (1) the Manning coefficient increase depended on the channel depth; (2) we examined the effects of Manning coefficient changes on modeled surface hydrology at spatially diverse locations (i.e., the 10 subregions, more than 10 tributary and mainstem gauges, and the mainstem).

The following text was added to the beginning of Section 4.4 "Varying Manning roughness coefficients" (previous Section 4.3 "Varying the Manning coefficients"):

" *A few studies for the Amazon Basin (e.g., Paiva et al., 2013a; Yamazaki et al., 2011) revealed some sensitivities of surface hydrology to the Manning coefficient. Yamazaki et al. (2011) perturbed the Manning coefficient by a uniform percentage for all the channels and examined the effects on streamflow of the Obidos gauge and the flooded area over the central Amazon region (in their Fig. 13). Using a similar approach, Paiva et al. (2013a) investigated the effects of the Manning coefficient on streamflow of the Obidos gauge, channel water depths of the Manacapuru gauge, and the total flooded area of the entire Amazon Basin (in their Fig. 10). These studies revealed that increasing the Manning coefficient could raise the river stage, expand the flooded area, and reduce and delay the flood peak. Instead of a uniform perturbation, we varied the Manning coefficient with the channel depth and examined the effects on flood extent of 10 subregions, streamflow of 13 gauges, river stages near 11 gauges, and the mainstem water surface profile.* "

[C2-27]

Figure 10. This figure is confusing. It's hard to understand the break in the profile. Please review it.

Reply: Figure 10 was replotted to avoid the break and to use the same y-axis for the entire river length.

[C2-28]

4.4. Line 20. See also analyses on the importance of backwater effects for amazon simulations from Paiva et al., 2013 WRR and Paiva et al., 2013 Hyd.Process. Please compare and discuss in the manuscript.

Reply: Paiva et al. (2013b, HP) demonstrated the important impacts of backwater effects on streamflow of the mainstem and tributaries, and discussed the important role of backwater effects in the inundation dynamics and river stages of the Amazon Basin. Paiva et al. (2013a, WRR) showed the important impacts of backwater effects on streamflow of eight mainstem or tributary gauges.

In a more comprehensive manner, we examined the impacts of backwater effects on flood extent in 10 subregions, streamflow of 13 gauges, river stages near 11 gauges, and the mainstem water surface profile.

The following text was added or revised:

"*Paiva et al. (2013b) used the dynamic wave method to represent river flow in the Solimoes River basin, which is the western upstream portion of the Amazon Basin. They discussed the important role of backwater effects in the inundation dynamics of the Amazon. In this study, we examined the impacts of backwater effects on flood extent in the 10 subregions constituting the Amazon Basin (Fig. 11), and demonstrated the spatial pattern of flood extent changes caused by backwater effects (Figs. 12j and 12k).*"

"*These backwater effects on hydrographs agree with the results of Paiva et al. (2013)*" was revised as "*These results agree with Paiva et al. (2013a, 2013b) which demonstrated the important role of the backwater effects in streamflow of the mainstem and tributaries of the Amazon Basin (Table 2 and Fig. 14 of Paiva et al., 2013a; Table 2 and Figs. 3, 4 and 9 of Paiva et al., 2013b).*"

"*In addition, to our knowledge, this phenomenon of backwater effects on the streamflow timing has not been discussed in previous modeling studies in the Amazon Basin.*"

"*In addition, the result of this study agreed with Paiva et al. (2013b), which discussed the backwater effects on river stages in the Solimoes River basin.*"

[C2-29]

Conclusions. Line 20. Review Yamazaki et al., 2013. WRR for discussion in Catchment vs grid based simulations.

Reply: Yamazaki et al. (2013, WRR) used a special computation unit, which had characteristics of both catchment unit and grid unit. Using their computation unit could preserve the river flow pathway better than using the grid unit. Their computation units were more even than catchment units in terms of area. The citation of their study was supplemented in the revised manuscript.

[C2-30]

Conclusions: I'm not sure if there are new conclusions /findings that were not addressed by the past modelling studies in the Amazon (e.g. Paiva et al., 2013, Getirana et al. 2012, Yamazaki et al., 2011, Beighley et al., 2009; Baugh et al., 2013). The past studies already pointed for the importance backwater effects and flooding, performed Sensitivity studies on the role of river geometry errors and DEM errors on amazon simulations. It is important to recognize that the analyses from this paper only reproduced similar conclusions from the past studies. And also clarify that the new contribution from this paper is mostly on updating/improving the parametrization of an specific model, i.e. MOSART model by including improvements tested or suggested by the previous studies.

Reply: We thank the reviewer for the constructive suggestions.

In the initial manuscript, the comparisons between our work and previous studies were not clear. The manuscript was improved at this aspect during the revising procedure. As discussed in our reply to the first comment [C2-1], on one hand, our work was based on the important foundation of previous studies; at the same time, our investigation also had a few new points in terms of methodologies, simulation results and sensitivity analyses.

Following the suggestion of both reviewers, the contribution of incorporating the inundation scheme into the MOSART model was described more clearly than before in the revised manuscript.

## References


Baugh, C. A., Bates, P. D., Schumann, G. and Trigg, M. A.: SRTM vegetation removal and hydrodynamic modeling accuracy, Water Resour. Res., 49(9), 5276–5289, doi:10.1002/wrcr.20412, 2013.

Beighley, R. E., Eggert, K. G., Dunne, T., He, Y., Gummadi, V. and Verdin, K. L.: Simulating hydrologic and hydraulic processes throughout the Amazon River Basin, Hydrol. Process., 23(8), 1221–1235, doi:10.1002/hyp.7252, 2009.

Coe, M. T., Costa, M. H., Botta, A. and Birkett, C.: Long-term simulations of discharge and floods in the Amazon Basin, J. Geophys. Res. Atmospheres, 107(D20), LBA 11-1, doi:10.1029/2001JD000740, 2002.

Coe, M. T., Costa, M. H. and Howard, E. A.: Simulating the surface waters of the Amazon River basin: impacts of new river geomorphic and flow parameterizations, Hydrol. Process., 22(14), 2542–2553, doi:10.1002/hyp.6850, 2008.

Getirana, A. C. V., Boone, A., Yamazaki, D., Decharme, B., Papa, F. and Mognard, N.: The Hydrological Modeling and Analysis Platform (HyMAP): Evaluation in the Amazon Basin, J. Hydrometeorol., 13(6), 1641–1665, doi:10.1175/JHM-D-12-021.1, 2012.

Junk, W. J., Piedade, M. T. F., Wittmann, F., Schöngart, J. and Parolin, P., Eds.: Amazonian Floodplain Forests, Springer Netherlands, Dordrecht. [online] Available from: http://link.springer.com/10.1007/978-90-481-8725-6 (Accessed 25 March 2016), 2011.

Li, H., Wigmosta, M. S., Wu, H., Huang, M., Ke, Y., Coleman, A. M. and Leung, L. R.: A Physically Based Runoff Routing Model for Land Surface and Earth System Models, J. Hydrometeorol., 14(3), 808–828, doi:10.1175/JHM-D-12-015.1, 2013.

O'Loughlin, F. E., Paiva, R. C. D., Durand, M., Alsdorf, D. E. and Bates, P. D.: A multi-sensor approach towards a global vegetation corrected SRTM DEM product, Remote Sens. Environ., 182, 49–59, doi:10.1016/j.rse.2016.04.018, 2016.

Paiva, R. C. D., Collischonn, W. and Tucci, C. E. M.: Large scale hydrologic and hydrodynamic modeling using limited data and a GIS based approach, J. Hydrol., 406(3–4), 170–181, doi:10.1016/j.jhydrol.2011.06.007, 2011.

Paiva, R. C. D., Buarque, D. C., Collischonn, W., Bonnet, M.-P., Frappart, F., Calmant, S. and Bulhões Mendes, C. A.: Large-scale hydrologic and hydrodynamic modeling of the Amazon River basin, Water Resour. Res., 49(3), 1226–1243, doi:10.1002/wrcr.20067, 2013a.

Paiva, R. C. D., Collischonn, W. and Buarque, D. C.: Validation of a full hydrodynamic model for large-scale hydrologic modelling in the Amazon, Hydrol. Process., 27(3), 333–346, doi:10.1002/hyp.8425, 2013b.

Wilson, M., Bates, P., Alsdorf, D., Forsberg, B., Horritt, M., Melack, J., Frappart, F. and Famiglietti, J.: Modeling large-scale inundation of Amazonian seasonally flooded wetlands, Geophys. Res. Lett., 34(15), L15404, doi:10.1029/2007GL030156, 2007.

Yamazaki, D., Kanae, S., Kim, H. and Oki, T.: A physically based description of floodplain inundation dynamics in a global river routing model, Water Resour. Res., 47(4), W04501, doi:10.1029/2010WR009726, 2011.

# Appendix

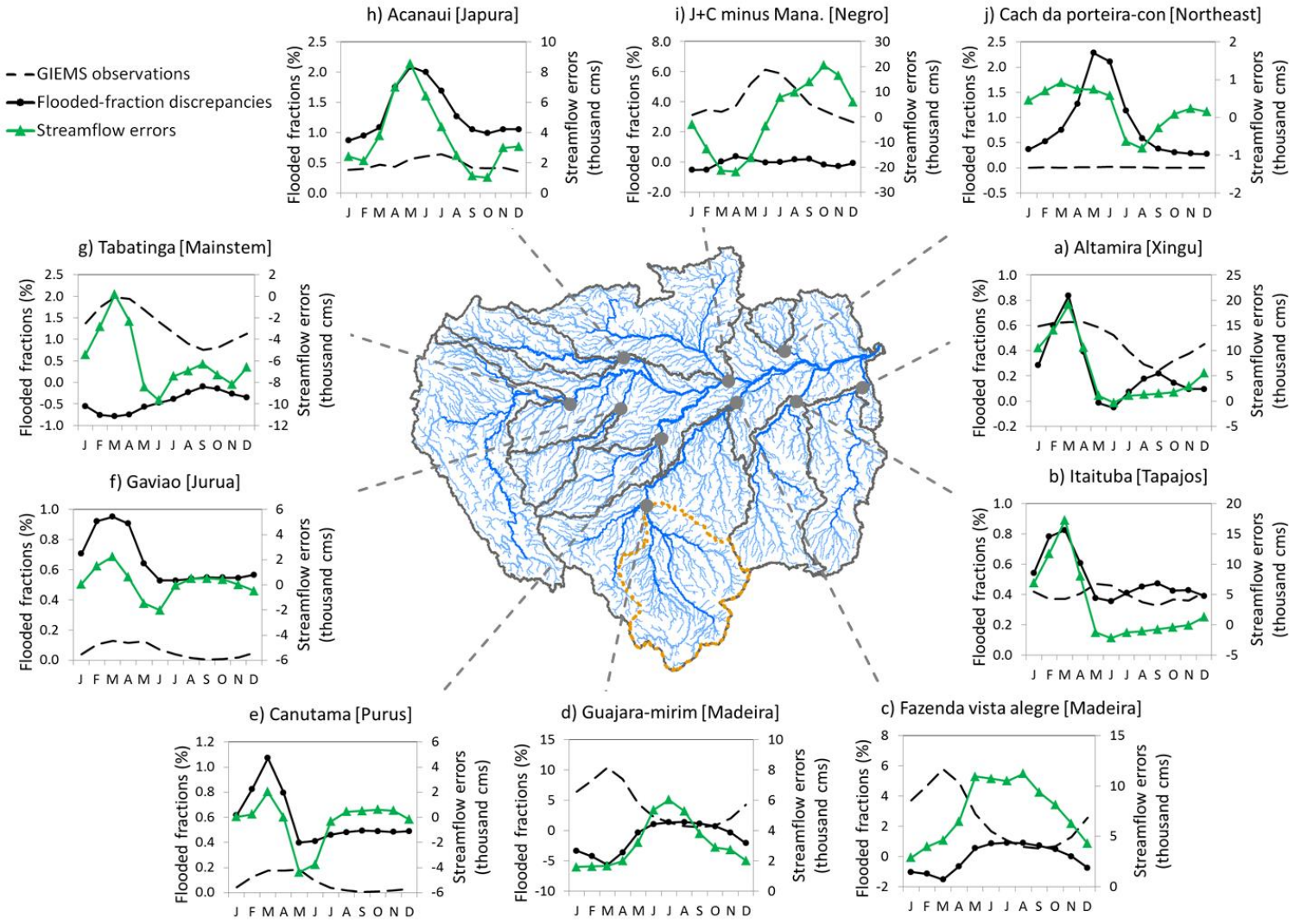


Averaged monthly streamflow errors and the flood extent discrepancies (i.e., the differences between simulated flood extent and the GIEMS data) in the area upstream of the gauge for 10 gauges during 12 years (1995 – 2006). Streamflow of the Negro subregion (panel (i) ) is approximated by the streamflow difference between the Jatuarana+Careiro gauge and the Manacapuru gauge. The upstream area of each gauge is enclosed by gray lines (or brown dotted lines for the Guajara-mirim gauge) in the basin map.

# Modeling surface water dynamics in the Amazon Basin using MOSART-Inundation-v1.0: Impacts of geomorphological parameters and river flow representation

Xiangyu Luo[1], Hong-Yi Li[1], L. Ruby Leung[1], Teklu K. Tesfa[1], Augusto Getirana[2], Fabrice Papa[3,4], Laura L. Hess[5]

[1] Pacific Northwest National Laboratory, Richland, Washington 99352, United States
[2] NASA Goddard Space Flight Center, Greenbelt, Maryland 20771, United States
[3] LEGOS/IRD, Universite de Toulouse, IRD-CNRS-CNES-UPS, Toulouse 31400, France
[4] Indo-French Cell for Water Sciences, IISc-NIO-IITM–IRD Joint International Laboratory, IISc, Bangalore, India
[5] University of California, Santa Barbara, California 93106, United States

*Correspondence to*: L. Ruby Leung (Ruby.Leung@pnnl.gov)

**Abstract**

In the Amazon Basin, floodplain inundation is a~~one~~ key~~important~~ component of ~~S~~surface water dynamics and plays an important role in water, energy and carbon cycles~~ of the Amazon Basin~~. The Model for Scale Adaptive River Transport (MOSART) was extended with ~~A~~a macro-scale inundation scheme ~~was integrated with a surface water transport model which could~~to represent floodplain inundation. ~~and t~~The extended model, named ~~as~~ "MOSART-Inundation", was ~~applied~~ used to simulate surface hydrology ~~in this vast basin~~of the entire Amazon Basin. Previous hydrologic~~al~~ modeling studies in the Amazon Basin identified and ~~used some methodologies to deal~~addressed ~~with~~ a few challenges ~~facing~~in simulating surface hydrology of this basin, including uncertainties of floodplain topography and channel geometry, and the representation of river flow in ~~mild slope~~ reaches with mild slopes. ~~We made efforts to addressed handle~~This study further addresse~~s~~d four aspects of ~~the~~ these challenges. First, ~~of improving basin-wide geomorphological parameters and river flow representation for large-scale applications. at four aspects: (1) We explicitly considered~~ the spatial ~~variation~~variability of vegetation-caused biases embedded in the HydroSHEDS DEM data were explicitly considered to~~while~~ alleviate~~ing~~ th~~os~~e biases in the DEM. ~~Vegetation-caused biases embedded in the HydroSHEDS DEM data were alleviated by using a~~ A vegetation height map of about 1-km resolution and a land cover dataset of about 90-m resolution were used in the DEM correction procedure~~.~~. This ~~which~~ resulted in an~~The~~ average elevation deduction ~~from the DEM correction was~~ of ~~about~~ 13.2 m for the entire basin and

~~could~~led to evident~~ly~~ changes in the floodplain topography~~.~~. Second,~~; (2)~~ b~~B~~asin-wide empirical formulae for channel cross-sectional ~~geometry~~ dimensions were ~~adjusted based on local information for the major portion of the basin~~refined for various subregions to improve the representation of spatial ~~variation~~variability in channel geometry~~. , which could significantly reduce the cross-sectional area for the channels of some subregions.~~.; ~~(3)~~ Third, the channel Manning roughness coefficient was allowed to ~~of the channel~~ vary~~ied~~ with the channel depth, ~~to reflect the general rule that the relative importance~~ as the effect of riverbed resistance ~~in~~ on river flow generally decline~~d~~s with ~~the~~ increase~~e~~ing ~~of~~ river size~~.~~. Lastly,~~; (4) The~~ backwater effects were accounted for to better represent river flow in mild-slope reaches. ~~The entire basin was discretized into 5395 subbasins (with an average area of 1091.7 km$^2$), which were used as computation units. The model was driven by runoff estimates of 14 years (1994 – 2007) generated by the ISBA land surface model.~~ The ~~simulated results~~ model ~~performance were~~ was evaluated against in situ streamflow records, and remotely sensed Envisat altimetry data and GIEMS inundation data. The streamflow hydrographs were reproduced fairly well for the majority of 13 major stream gauges. The river-stage hydrographs were modeled reasonably well ~~F~~for the 11 subbasins containing or close to 11 of the 13 stream gauges~~, the timing of river stage fluctuations was captured; for most of the 11 subbasins, the magnitude of river stage fluctuations was represented well~~. The inundation estimates were comparable to the GIEMS observations. In a sensitivity study, seven scenario simulations were compared to reveal the important roles of the newly incorporated inundation scheme, floodplain and channel geomorphology, and river flow representation in the ~~modeled~~ simulated surface water dynamics of the Amazon Basin. ~~We examined the S~~simulation results at~~of~~ various locations ~~spread over~~across the basin were examined, including inundation of 10 subregions, streamflow and river stages at both mainstem and tributary gauges, and the water surface profile along the mainstem. The ~~simulation~~ comparison showed that representing floodplain inundation could significantly improve the ~~modeled~~ streamflow and river stages. ~~Sensitivity analyses~~ ~~It was also demonstrated that r~~Refining floodplain topography, channel ~~morphology~~ geometry and Manning roughness coefficients, as well as accounting for backwater effects ~~could evidently affect local and upstream inundation, which consequently affected flood waves and inundation of the downstream area~~. ~~have~~ had evident impacts on the ~~modeled~~ surface hydrology in the Amazonia. ~~It was also shown that the river stage was sensitive to local channel morphology and Manning roughness coefficients, as well as backwater effects.~~ The understanding obtained in this study could be helpful ~~to~~ in improving modeling of surface hydrology in basins with evident inundation, especially at ~~the~~ regional ~~or~~to ~~larger scales~~continental scales.

**Keywords**

surface hydrology, hydrologic modeling, floodplain inundation, ~~modeling,~~ Amazon Basin, geomorphology, DEM biases, channel cross-sectional geometry, Manning roughness coefficient, backwater effects

## 1 Introduction

The terrestrial surface water dynamics have significant impacts on the water, energy and carbon cycles of the planet, as they influence energy and material exchange between the land surface and the atmosphere. For instance, surface water bodies are important natural sources of greenhouse gases (e.g., carbon dioxide and methane) (Bousquet et al., 2006; Richey et al., 2002). Extreme events such as river inundation have extraordinary effects on the land surface – groundwater interactions and the sediment and nutrient exchange between rivers and floodplains, and thereby influence land and aquatic ecosystems as well as their feedback to the atmosphere. Therefore, improving parameterizations of surface water dynamics is meaningful in studying the linkages between the land surface and climate.

Many previous studies of surface-hydrology modeling were conducted for the Amazon River, which is the largest river of the globe and accounts for about 18% of the total continental freshwater discharge to oceans (Dai and Trenberth, 2002). Seasonal floods occur every year and wetlands occupy a considerable proportion of the total area in this basin (Hess et al., 2003, 2015). River and inundation dynamics were simulated by using 2-D hydrodynamic models at the central Amazonia (e.g., Baugh et al., 2013; Wilson et al., 2007). Using fine-resolution grid cells (e.g., ~ 300 m) as computation units, 2-D hydrodynamic models could represent water flow over floodplains. They were not applied at regional or larger scales due to computational costs. On the other hand, some computationally efficient macro-scale inundation schemes were used in a few continental-scale hydrologic models for the entire Amazon Basin (Coe et al., 2008; Decharme et al., 2008; Getirana et al., 2012; Paiva et al., 2013a; Vörösmarty et al., 1989; Yamazaki et al., 2011). ~~While t~~These ~~models with macro-scale inundation schemes~~ could capture some aspects of surface water dynamics fairly well. These previous studies also identified and ~~used some methodologies to deal with~~addressed ~~,~~ a number of modeling challenges ~~have been identified~~, including uncertainties in model inputs of floodplain and channel morphology, flow parameterization for gentle-gradient ~~river~~ reaches, etc.

The Model for Scale Adaptive River Transport (MOSART) was developed to simulate terrestrial surface water flow from hillslopes to the basin outlet (Li et al., 2013). It was designed to be applicable at the local, regional or continental scale. Some details of this model are provided in Sect. 2.1. In this study, the MOSART model ~~has been~~was extended with a macro-scale inundation scheme ~~which can~~to represent floodplain inundation. The extended model, named ~~as~~ "MOSART-Inundation", was applied to the entire Amazon Basin. In addition, in this application we made efforts to ~~handle the~~further address four aspects of the aforementioned challenges ~~at~~

four aspects: (1) wWhile alleviating the vegetation-caused biases embedded in the DEM data, we explicitly considered the spatial variationvariability of those biases; (2) tThe approach for estimating channel cross-sectional dimensions was refined to improve its representation of the spatial variationvariability in channel geometry; (3) tThe Manning roughness coefficient of the channel was allowed to varyied with the channel depth; and (4) The backwater effects were accounted for to better represent river flow in gentle-gradient reaches.

Topography data are essential inputs in hydrologic modeling. At present the common practice is to use the digital elevation model (DEM) to represent topography. Because the coverage of high-accuracy DEM data (e.g., with elevation errors less than 1 m) is limited, hydrologic modeling at regional or larger scales uses DEM data obtained by spaceborne sensors. The Shuttle Radar Topography Mission (SRTM) DEM data have been widely used for hydrologic modeling, but some factors limit their accuracy. In forested regions such as the Amazon Basin, primary biases in SRTM DEM data were caused by vegetation cover because the radar signal was not able to penetrate the vegetation canopy (Sanders, 2007). Previous studies in the Amazon Basin adopted various approaches to alleviate the vegetation-caused biases embedded in SRTM data. In some modeling studies, elevation values were lowered by a constant in forested area of the entire basin, ignoring the spatial variability of vegetation heights (Coe et al., 2008; Paiva et al., 2013a). In a few hydrodynamic modeling studies for the central Amazonia, –the vegetation-caused biases in SRTM elevations were derived from spatially variedvarying vegetation heights. For example, Wilson et al. (2007) estimated the vegetation-height distribution based on their field surveyed heights of various vegetation types and a map of vegetation types (Hess et al., 2003); Baugh et al. (2013) utilized a global dataset of spatially distributed vegetation heights developed by Simard et al. (2011). These two studies estimated the vegetation-caused biases as products of spatially varying vegetation heights and a fixed percentage. In this study, we used the HydroSHEDS DEM data which were derived from SRTM data and inheriteding the vegetation-caused biases. To alleviate those biases, we used a method similar to that of Baugh et al. (2013). Besides the vegetation height map by Simard et al. (2011), we also used a land cover dataset for wetlands of the lowland Amazonia developed by Hess et al. (2003, 2015). A “bare-earth” DEM of the Amazonia was created and employed in the hydrologic modeling for the entire basin. To our knowledge, this was the first time that the spatial variability of vegetation-caused biases in the DEM data was explicitly considered while thein basin-wide hydrologic modeling was conducted in the Amazonia.

Channel cross-sectional geometry affects the estimation of channel flow velocity and channel storage conveyance capacity in the modeling of surface water dynamics. Distributed hydrologic modeling at regional or larger scales needs cross-sectional dimensions of all the channels that constitute the river network in the study

domain. Channel cross-sectional dimensions obtained from in situ measurements are reliable, but limited to a small number of locations. Therefore channel cross-sectional dimensions were usually estimated based on available basin characteristics by using empirical formulae. Modeling studies in the Amazon Basin employed relationships between channel geometry and streamflow statistics (Getirana et al., 2012; Yamazaki et al., 2011) or upstream drainage area (Beighley et al., 2009; Coe et al., 2008; Paiva et al., 2013a). T(those relationships are also referred to as "channel geometry formulae" in this article). In most of these studies, cross-sectional geometry of all the channels spread over the Amazon Basin were estimated by using one set of channel geometry formulae and corresponding parameters, which represented average characteristics of the entire basin. So for different subregions of the basin, channel cross-sectional dimensions derived from the same formulae and parameters contained biases of various magnitudes. Hydrologic modeling results were demonstrated to be sensitive to channel cross-sectional dimensions and shapes (Getirana et al., 2013; Neal et al., 2015; Paiva et al., 2013a; Yamazaki et al., 2011) so and improving the channel dimensions to be more representative representation of the actual channel morphology could be important. In this study, the basin-wide parameters for the channel geometry formulae were refined for various subregions of the Amazon Basin based on the channel morphology information of local locations to . Therefore the channel geometry formulae could better represent the spatial variability in channel morphology.

The Manning formula has been used for estimating flow velocities of rivers in many continental or global scale hydrologic models. In this formula, the Manning roughness coefficient (also abbreviated to "Manning coefficient" hereinafter; in this article, the "Manning roughness coefficient" discussed is for river channels) is a key and sensitive parameter (Paiva et al., 2013a; Yamazaki et al., 2011) which, however,that can only be estimated empirically. In previous studies of the Amazon Basin, the Manning coefficient was determined using various approaches: (a) a constant value for the entire basin (Beighley et al., 2009; Yamazaki et al., 2011); (b) different values for different subregions calibrated as a result of calibration using hydrographs at stream-gauge locations of major rivers (Paiva et al., 2013a); (c) diverse values dependent on the channel cross-sectional dimensions that vary spatially (Getirana et al., 2012, 2013). For natural river channels, the Manning coefficient depends on many factors, including riverbed roughness, cross-sectional geometry and channel sinuosity (Arcement and Schneider, 1989). The significant variations of these factors within a basin undermine the rationale of a uniform Manning coefficient across the entire basin or a few Manning coefficients for different subregions of the basin. The aforementioned approaches used inof the category (c) reflects the general

phenomenon that the relative importance of riverbed friction in river flow becomes smaller for larger rivers, ~~whic. This approachh ,~~ and can be used to represent the ~~major aspect of the~~dominant spatial ~~variation~~variability of the Manning coefficients. ~~In this study …~~We adopted a method of ~~the~~ category (c) ~~, which was~~ similar to those of Decharme et al. (2010) and Getirana et al. (2012) ~~,~~ to estimate the spatially varying Manning coefficients for different channels of the Amazon Basin.

The Amazonia is characterized by flat gradients and backwater effects are evident in river flows ~~-~~(Meade et al., 1991). Trigg et al. (2009) analyzed the characteristics of flood waves and conducted hydraulic modeling for reaches of the central Amazonia. They demonstrated that it was necessary to account for backwater effects and the diffusion wave method was valid for modeling the Amazon flood waves. The backwater effects were also represented in some continental-scale models applied in this basin. Yamazaki et al. (2011) used both the kinematic wave and diffusion wave methods to simulate river flow, with the latter capable of simulating backwater effects. Paiva et al. (2013a, 2013b) used the full Saint-Venant equations (or the dynamic wave method) to represent water flow of river reaches with gentle riverbed slope and large floodplains. These studies showed that accounting for backwater effects could evidently improve the modeling of surface water dynamics in this basin. In this study, river flow was modeled with the diffusion wave method ~~which~~that could represent backwater effects. Moreover, the impacts of backwater effects on surface hydrology of the Amazon Basin were investigated through numerical experiments in a comprehensive manner.

~~In this study, a surface-water transport model was extended with a macro-scale inundation scheme, and the extended model was applied in the Amazon Basin. Efforts were made to refine model geomorphological parameter inputs, which have important effects on inundation but are difficult to determine for basin-scale simulations. We focused specifically on floodplain topography and channel cross-sectional geometry. The vegetation-caused biases in the DEM data were estimated based on spatially varied vegetation heights for the entire Amazon Basin. The channel geometry biases were alleviated by adjusting the basin-wide channel geometry formulae for different subregions based on channel morphology information of local locations. We also aimed to improve the river flow representation and its parameters. The Manning roughness coefficient depended on the river size and its spatial variation was represented. The diffusion wave method was chosen to model river flow in channels and the backwater effects were accounted for.~~

The ~~above~~ four factors described above ~~which~~ could have important impacts on modeling~~ed~~ surface hydrology in the Amazonia and were accounted for in the simulations conducted with the MOSART-Inundation model.

The model performance was evaluated against gauged streamflow data, as well as river-stage and inundation data obtained by satellites. ~~Sensitivity analyses were conducted to investigate the impacts of improving floodplain topography, channel morphology, and Manning roughness coefficients, as well as accounting for backwater effects on surface water dynamics.~~ In a sensitivity study, the roles of the following factors in ~~the~~ hydrologic modeling of~~for~~ the Amazon Basin were separately examined and demonstrated: (1) representing floodplain inundation; (2) alleviating vegetation-caused biases in the DEM data; (3) refining channel cross-sectional geometry; (4) adjusting Manning roughness coefficients; and (5) representing backwater effects. The results of this study were also compared with those of a few previous studies on modeling surface hydrology in the Amazonia.

## 2 Methods and data

### 2.1 ~~Surface water transport~~ MOSART model

~~The Model for Scale Adaptive River Transport (MOSART) was developed to simulate terrestrial surface water flow from hillslopes to the basin outlet.~~ In the MOSART model, each computation unit (subbasin or grid cell) has a major channel (or main channel) and a tributary subnetwork that~~which~~ represents the combined equivalent transport capacity of ~~includes~~ all the tributaries within the~~is~~ computation unit. Two simplified forms of the one-dimensional Saint-Venant equations (i.e., kinematic wave or diffusion wave methods) are used to represent water flow over hillslopes, in ~~minor tributaries (named as~~ the tributary subnetwork~~)~~, or in ~~major~~ main channels. The MOSART model is driven by runoff estimates from the land surface model. Surface runoff is treated as input of overland flow, which is represented with the kinematic wave method and enters the tributary subnetwork, while subsurface runoff directly enters the tributary subnetwork. Water flow in the tributary subnetwork is also represented with the kinematic wave method and the outflow finds its way to the ~~major channel (or~~ main channel~~)~~. Either the diffusion wave method or kinematic wave method could be used to simulate water flow in main channels. The two methods use the same continuity equation, and differ in the momentum equation and Manning's equation.

The continuity equation is expressed as (Chow et al., 1988):

$$\frac{\partial(v \cdot y \cdot w)}{\partial x} + \frac{\partial(y \cdot w)}{\partial t} = q \quad (1)$$

where $v$ is the flow velocity [unit: m $s^{-1}$]; $y$ is the water depth in the channel [unit: m]; $w$ is the channel width [unit: m]; $x$ is the distance along the river [unit: m]; $t$ is time [unit: s]; and $q$ is the lateral inflow per unit length of channel [unit: $m^2$ $s^{-1}$].

In the diffusion wave method, the momentum equation is expressed as (Chow et al., 1988):

$$g\frac{\partial y}{\partial x} - gS_0 + gS_f = 0$$

$$\frac{\partial y}{\partial x} - S_0 + S_f = 0 \quad (~~1~~2)$$

where $g$ ~~is the gravitational acceleration [unit: m $s^{-2}$];~~ $y$ ~~is the water depth in the channel [unit: m];~~ $x$ ~~is the distance along the river [unit: m];~~ $S_0$ is the riverbed slope [dimensionless] and $S_f$ is the friction slope [dimensionless], which could be positive or negative. ~~-~~$g\frac{\partial y}{\partial x}$ ~~is the pressure force term,~~ $gS_0$ ~~is the gravity force term and~~ $gS_f$ ~~is the friction force term.~~

The Manning's equation is expressed as:

$$v = \frac{S_f}{|S_f|} n^{-1} R^{\frac{2}{3}} |S_f|^{\frac{1}{2}} \quad (~~2~~3)$$

where~~-~~ $n$ is the Manning roughness coefficient [unit: $s \cdot m^{-1/3}$ ] and $R$ is the hydraulic radius [unit: m].

The continuity equation, momentum equation and Manning's equation are combined to determine the flow velocity, channel water depth and friction slope. The friction slope depends on water depth variation along the channel so it is affected by the river stage of the downstream channel. This way, backwater effects are represented. One extreme phenomenon caused by backwater effects is that when the downstream river stage is

higher than the river stage of the current channel and hence ~~-~~ $S_f$ is negative, the flow velocity from Eq. (~~2~~3) is also negative, so water flows from downstream to upstream.

In the kinematic wave method, the ~~pressure force~~ term $\frac{\partial y}{\partial x}$ is neglected from the momentum equation. With this simplification, the friction slope equals the riverbed slope and backwater effects are not represented.

In this model, the equations are solved with the explicit finite difference method. Either square grid cells or irregular subbasins can be used as computation units. The time-step size is chosen~~needs~~ to satisfy the Courant condition to ensure stable computation (Cunge et al., 1980).

### 2.2 Macro-scale inundation scheme

In this study the MOSART model was extended with a macro-scale inundation scheme and the extended model was named "MOSART-Inundation". ~~River~~ Floodplain inundation dynamics was represented by macro-scale inundation schemes in a few previous studies (Coe et al., 2008; Decharme et al., 2008; Getirana et al., 2012; Paiva et al., 2013a; Yamazaki et al., 2011). Those studies used relatively coarse computation units with the area magnitude ranging from 100 to 10,000 km$^2$. The main feature of their macro-scale inundation schemes was that the water level–inundated area relationship for the computation unit was used to estimate flood extent. The inundation scheme of this study is similar to those of Yamazaki et al. (2011) and Getirana et al. (2012). In this scheme, each computation unit (a ~~squared~~ square grid or a subbasin) has a main channel and a floodplain reservoir (Fig. 1a). Flooding water can spill out of the main channel and enter the floodplain reservoir, or recede from the floodplain reservoir to the main channel. The water storage within each computation unit is used with a water stage versus flooded area curve (referred to as "elevation profile") to estimate the flooded area within the unit. The elevation profile is derived from DEM data within the computation unit (Fig. 1b). The channel – floodplain exchange is assumed to be instantaneous for each time step (i.e., the channel stage and the floodplain stage are level at the end of each time step). In the model computation, the channel – floodplain exchange is incorporated into the lateral inflow term of the continuity equation (i.e., ~~-~~Eq.(1)~~-~~).

The channel area is implicitly included in an elevation profile, which is developed from all the elevations of the fine-resolution DEM within the computation unit (Fig. 1b: the brown solid line). Getirana et al. (2012) proposed an amended elevation profile in which the channel area was distinguished from the non-channel area.

Their method was adopted in this study. It is assumed that the main channel consists of the lowest pixels of the DEM within a computation unit. So the main channel and the rest of the computation unit (including the floodplain) are represented by the lower part and the upper part of the elevation profile, respectively. The dividing point corresponds to the fraction of channel area, which is estimated as the product of the channel length derived from DEM data and the channel width calculated with empirical formulae (Sect. 2.5). The elevation of the dividing point corresponds to the channel bank top. If the channel cross-sectional shape is assumed to be a rectangle, the channel part of the elevation profile changes to be the green dash line in Fig. 1b~~:~~. The channel bed elevation equals the difference of the bank top elevation and the channel depth, which is estimated in Sect. 2.5. The channel bed could be lower than the lowest DEM pixel of the computation unit because the DEM does not reflect the channel bed elevation. ~~w~~When the river stage is lower than the bank top, the water surface area does not change with the river stage and always equals the channel area. As the river stage exceeds the bank top, the total water storage is used with the amended elevation profile to estimate the total water surface area (including the channel area and the flooded area in the floodplain).

### 2.3 Application in the Amazon Basin

The MOSART-Inundation model was applied to the entire Amazon Basin. The 3- arc-seconds ~~resolution~~ HydroSHEDS DEM data developed by United States Geological Survey (USGS) (http://hydrosheds.cr.usgs.gov/) ~~were~~ was used in this study. The hydrologically conditioned HydroSHEDS DEM was used to generate the digital river network and subbasins. ~~Compa~~Rel~~r~~atively coarse resolution subbasins were adopted ~~due to the consideration of computational costs~~as MOSART-Inundation is intended for global earth system modeling, which is constrained by computational cost. The study domain of 5.89 million km$^2$ was divided into 5395 subbasins (the average area is 1091.7 km$^2$ and the standard deviation is 921.5 km$^2$), which were used as computation units (Figs. 2a and 2b). Each subbasin has a main channel and the entire river network consists of 5395 main channels (Fig. 2a). To ensure stable computation, the time-step size was determined based on the Courant condition and ~~some experiment~~numerical tests~~simulation~~s. The time step of one minute was used for all the simulations.

In order to analyze the spatially ~~varied~~ varying characteristics of inundation results, the Amazon Basin was ~~also~~ divided into 10 subregions (Fig. 2c). Twenty eight ~~major~~ large tributary catchments were first delineated and ~~some neighboring major tributary catchments were combined so the 28 catchments were~~ then aggregated to ~~9~~nine

tributary subregions. Initially~~At first~~, seven major catchments (i.e., Xingu, Tapajos, Madeira, Purus, Jurua, Japura and Negro) were selected as subregions or the major part of a subregion.~~;~~ Then the Upper-Solimoes catchments were combined as one subregion, ~~and~~ the northeast catchments were combined as another subregion, and ~~; After that,~~ the remaining five large catchments were incorporated into their adjacent tributary subregions. T~~In t~~his way, ~~the~~ nine tributary subregions were delineated. L~~At l~~astly, ~~A~~all the ~~minor~~ small tributary catchments and the area draining directly to the mainstem were aggregated to be the tenth subregion (i.e., the mainstem subregion).

The inputs of surface and subsurface runoff, which were of 1-degree resolution, were produced by the ISBA land surface model (Getirana et al., 2014) driven by the ORE-HYBAM precipitation dataset (Guimberteau et al., 2012). The area-weighted averaging method was used to convert ~~T~~the grid based runoff data ~~were converted~~ to subbasin based runoff data ~~using area-weighted averaging method~~ for driving the simulations of this study.

~~The inputs of DEM data, channel cross-sectional geometry and Manning roughness coefficients, as well as the setup of simulations are described in the following subsections.~~

### 2.4 Vegetation-caused biases in DEM

~~The 3-second resolution HydroSHEDS DEM data developed by United States Geological Survey (USGS) (http://hydrosheds.cr.usgs.gov/) were used in this study. The HydroSHEDS DEM data included void-filled DEM data and hydrologically conditioned DEM data. The conditioned DEM was used to generate the digital river network and subbasins, and the~~The void-filled HydroSHEDS DEM ~~after the correcting the~~on of vegetation-caused biases ~~was used to generate the elevation profiles of all the subbasins.~~

The conditioned DEM was not suitable for representing floodplain topography and generating elevation profiles. In the DEM conditioning process, the elevation values of pixels for river channels and their buffer zones were lowered by non-negligible amounts that could be larger than 20 m in the lower mainstem area of the Amazon Basin. So the channels and their adjacent areas in the conditioned DEM could hold more water than the actual counterparts, which would lead to underestimation of flood extent.

The HydroSHEDS DEM data were derived from the SRTM data and inherited the vegetation-caused biases. Before being used for producing elevation profiles, the void-filled HydroSHEDS DEM was processed to alleviate the biases caused by vegetation. The vegetation height data with ~ 1-km resolution developed by Simard et al. (2011) was used. For vegetated areas, the original void-filled DEM represented elevations of locations within the

vegetation canopy. So, part of the vegetation height needed to be deducted from the original elevation. Baugh et al. (2013) found that deducting 50 – 60% of the vegetation height of the Simard et al. (2011) data from the original DEM achieved the greatest improvements to hydrodynamic model accuracy in the Amazon floodplain. A deduction ratio of 50% was used for the vegetated area in this study.

The resolution of the vegetation height data was coarser than that of the DEM data. It might not be appropriate to assume a uniform vegetation height for all the DEM pixels within the grid cell of the vegetation height dataset. Hess et al. (2003, 2015) developed a high resolution (3 arc-seconds) land cover dataset for floodplains (or wetlands) located in the lowland Amazon Basin (i.e., areas with elevations lower than 500 m). This land cover dataset was used in our DEM correction process. In the floodplains of the lowland Amazon Basin, vegetation height removal was conducted differently for different land cover classes. For DEM pixels with forest or woodland classes, 50% of the vegetation height was deducted from the original DEM. In the high resolution land cover dataset, shrubs were defined to be less than 5 m tall (Junk et al., 2011). ~~If the vegetation height was larger than 5 m~~ So for DEM pixels with ~~the~~ shrubs ~~class~~, the vegetation height was ~~reduced to be 5 m if it was larger than 5 m~~ determined by the vegetation height data, but with an upper limit of 5 m. ~~Therefore, for shrub DEM pixels with vegetation heights equal to or higher than 5 m, the elevations were lowered by 2.5 m, but if the vegetation heights were less than 5 m,~~ After this correction, the elevations were lowered by 50% of the vegetation heights for shrub DEM pixels. For DEM pixels with other land cover classes (e.g., open water, bare soil, etc.), the elevations were not modified. For areas outside of the floodplains of the lowland basin, a uniform vegetation height was applied for all the DEM pixels ~~that overlap with the~~ within each vegetation height pixel. This approximation was not expected to have obvious effects on inundation modeling since most inundation occurred within the floodplains of the lowland basin.

The DEM correction obviously changed the topographic features in the DEM data. The average elevation deduction in each subbasin ranges from 0 to 21 m (Fig. 2d). After the DEM correction, the average elevation in each subbasin ranges from 0 to 4772 m (Fig. 2e). For all the subbasins, the ratio of the average elevation deduction to the subbasin elevation difference (i.e., the difference between the highest and lowest elevations in the subbasin) ranges from 0 to 52.9% (average: 9.2%; standard deviation: 7.1%). The average elevation profile of the Amazon Basin was generated for the original DEM and corrected DEM, respectively (Fig. 2f). At first, the normalized elevation profile was produced for each subbasin. For each DEM pixel within a subbasin, the elevation relative to the lowest pixel of the subbasin was divided by the subbasin elevation difference to give the normalized elevation, which was used to generate the normalized elevation profile. Then the normalized

elevation profiles of all subbasins were averaged to give the average elevation profile of the entire basin. Figure 2f illustrates that the DEM processing evidently lowers the average elevation profile.

O'Loughlin et al. (2016) estimated the vegetation-caused biases in the SRTM DEM data based on vegetation height data, canopy density data and the distribution of five climatic zones (i.e., Tropical, Arid, Temperate, Cold and Polar). They created the first global 'Bare-Earth' high resolution (3 arc-seconds) DEM from the SRTM DEM data. They ~~also~~ compared their method with the static correction method (i.e., estimating the vegetation-caused bias as the product of vegetation height and a fixed percentage) ~~which was~~ used by Baugh et al. (2013) and this study, and ~~stat~~noted that the static correction method was effective but moderately worse than their method.

## 2.5 Channel ~~cross-sectional~~ geometry

At regional or larger scales, channel cross-sectional shape is usually simplified to be a rectangle since the channel top width is much larger than the channel depth (or bank height). The channel cross-section can be determined by channel width and channel depth. Beighley and Gummadi (2011) presented a methodology for estimating channel cross-sectional dimensions (i.e., channel width and channel depth) at stream-gauge locations by using stage – discharge relationship data and Landsat imagery. They implemented the approach to derive channel cross-sectional dimensions of 82 streamflow gauging locations spread over the Amazon Basin, which were further used to develop the general relationships between channel cross-sectional dimensions and upstream drainage area (or channel geometry formulae) for the entire basin. Their channel geometry formulae are listed as follows.

$$w = 1.956A^{0.413} \quad (A < 10{,}000 km^2) \qquad (3\underline{4})$$

$$w = 0.403A^{0.600} \quad (A \geq 10{,}000 km^2) \qquad (4\underline{5})$$

$$d = 0.245A^{0.342} \qquad (5\underline{6})$$

where $w$ is channel width (unit: m); $d$ is channel depth (unit: m); $A$ is upstream drainage area (unit: km$^2$). Beighley and Gummadi (2011) showed that the channel cross-sectional dimensions estimated from their channel geometry formulae agreed well with those from the formulae by Coe et al. (2008). Based on extensive river morphology data obtained from stations spread throughout the Amazon and Tocantins basins, Coe et al. (2008)

derived the general channel geometry formulae for the Amazon Basin and, in their formulae, channel cross-sectional dimensions were also expressed as power functions of upstream drainage area.

The channel geometry formulae of Beighley and Gummadi (2011) were obtained through regression analysis of data from 82 locations over the Amazon Basin, and reflected the average feature of the basin. Directly applying the same formulae and parameters to the entire basin could cause large biases in the estimated channel cross-sectional dimensions for some subregions. In order to reduce those biases, in this study the coefficients in the basin-wide channel geometry formulae of Beighley and Gummadi (2011) were adjusted for a majority of the 10 subregions (Fig. 2c) based on channel cross-sectional dimensions of local locations. The 82 streamflow gauging locations scattered over the Amazon Basin and each subregion contained a few streamflow gauging locations. For the streamflow gauging locations of the same subregion, the root-mean-square error (RMSE) between the channel cross-sectional dimensions estimated with the channel geometry formulae and the corresponding dimensions presented in Beighley and Gummadi (2011) could be calculated. During the adjustment process, the coefficient of the channel geometry formula (i.e., 1.956, 0.403 or 0.245 in Eqs. (~~3~~4)–(~~5~~6)) was multiplied by a factor to reduce the RMSE. The factor values for the 10 subregions are listed in Table 1. The ranges for the channel width and depth of each subbasin are shown in Figs. 2g and 2h, respectively.

It is worth mentioning that Paiva et al. (2013a) also accounted for spatial variability of channel geometry formulae and used various coefficients in their formulae for six zones of the Amazon Basin. In this study, we used both the basin-wide channel geometry formulae and the diverse formulae for various subregions, and investigated the effects of ~~adjusting~~ refining channel geometry on modeled surface water dynamics.

In order to convert the calculated channel water depths to river stages, we estimated ~~T~~the riverbed elevations ~~was estimated~~ by using the following equation since observed data were not available.

$$E_c = E_{mouth} + \sum_{i=1}^{n} L_i S_i + \frac{1}{2} L_c S_c \qquad (7)$$

where $E_c$ is the average riverbed elevation of the current channel [unit: m]; $E_{mouth}$ is the riverbed elevation at the mouth of the Amazon River [unit: m]; $n$ is the total number of ~~the~~ downstream channels; $L_i$ is the flow length of a~~one~~ downstream channel $i$ [unit: m]; $S_i$ is the average riverbed slope of a~~one~~ downstream channel $i$ [dimensionless]; $L_c$ is the flow length of the current channel [unit: m] and $S_c$ is the average riverbed slope of

the current channel [dimensionless]. $E_{mouth}$ is assumed to be the negative channel depth at the mouth of the Amazon River, which is calculated with Eq. (6).

### 2.6 Manning roughness coefficients for channels

The Manning roughness coefficient for channels reflects the resistance to water flows in channels and is determined by many factors, such as roughness of riverbed and riverbank, shape and size of channel cross-sections and channel meanderings. In general, within a basin these factors have considerable spatial heterogeneities. Therefore it is more reasonable to use spatially ~~varied~~ varying coefficients estimated based on these factors than using a constant coefficient. However, distributed hydrologic modeling requires a channel Manning coefficient ~~value~~ for each subbasin~~,~~. ~~which~~ It is not realistic to separately estimate each of th~~os~~e Manning coefficients given the lack of information. For continental ~~or global~~ scale studies, the river network consists of river channels of distinct magnitude orders. Riverbed resistance plays a relatively smaller role in water flows of larger channels. Assuming that the Manning coefficient decreases linearly with the channel top width, Decharme et al. (2010) showed that the assumed relationship produced acceptable variation in flow velocity in a global application of the ISBA-TRIP continental hydrologic~~al~~ modeling system. Getirana et al. (2012) expressed the Manning coefficient as a power function of the channel depth in their study of inundation dynamics in the Amazon Basin. In ~~this~~ our study, the Manning coefficient also depended on the channel depth and was estimated using the following function:

$$n = n_{\min} + (n_{\max} - n_{\min})\left(\frac{h_{\max} - h}{h_{\max} - h_{\min}}\right) \quad (6\text{~~}8)$$

where the maximum Manning coefficient $n_{\max}$ is for the channel with the shallowest channel depth and the minimum Manning coefficient $n_{\min}$ is for the channel with the largest channel depth. Following Getirana et al. (2012), $n_{\max}$ and $n_{\min}$ were set as 0.05 and 0.03, respectively~~, based on the literature~~. In addition, a few other studies of the Amazon Basin adopted similar values around the range of 0.03 – 0.05 for the Manning coefficient (Beighley et al., 2009; Paiva et al., 2013a; Yamazaki et al., 2011). In Eq.(8), $h_{\max}$ and $h_{\min}$ are the maximum and minimum channel depths in all the channels, and were estimated to be 50.64 and 0.96 m, respectively, using

the method described in ~~the previous subsection~~ Sect. 2.5. The variable ~~-~~ $h$ is the depth of the current channel. The spatial distribution of the channel Manning coefficient is shown in Fig. 2i.

In this study, ~~T~~the function of the Manning coefficient (i.e., Eq. (~~6~~8)) was compared to those of Decharme et al. (2010) and Getirana et al. (2012) ~~in this study~~. In general, compared to the equations of the two previous studies, Eq. (~~6~~8) gave smaller Manning coefficients and resulted in better simulation of~~ed~~ hydrographs, which suggested that Eq. (~~6~~8) was more appropriate for the simulations of this study.

### 2.7 ~~Setup of~~ Control simulation~~s~~

The aforementioned factors could have important impacts on modeling~~ed~~ surface hydrology of the Amazon Basin. ~~Five simulations were conducted in this study (Table 2).~~

~~The first simulation used the optimal combination of the four factors (i.e., DEM, channel cross-sectional geometry, Manning roughness coefficients and the parameterization for channel water flow) and was set as~~ We configured ~~the~~ a control simulation (abbreviated as "CTL") ~~where~~using the preferred methodologies ~~were used~~ for~~at~~ five aspects: (1) the inundation scheme was turned on; (2) vegetation-caused biases in the DEM data were alleviated; (3) the basin-wide channel geometry formulae were refined for different subregions; (4) the Manning ~~roughness~~ coefficient varied with the channel size; (5) the diffusion wave method was used to represent river flow in channels. The control simulation was run for 14 years (1994 – 2007) and the results of 13 years (1995 – 2007) were evaluated against gauged streamflow data and remotely sensed river stage and inundation data.

~~For the purpose of investigating the effects of each of the four factors on surface water dynamics, only one factor was changed in each of the other four simulations. In the second simulation, the original HydroSHEDS DEM data without the correction of vegetation-caused biases were used; in the third simulation, the basin-wide channel geometry formulae were not adjusted for the subregions and were directly used for the entire basin;~~

~~in the fourth simulation, the spatially varied Manning roughness coefficients for channels were replaced with a constant coefficient of 0.03; lastly the diffusion wave method was replaced by the kinematic wave method for representing water flow through channels in the fifth simulation. All simulations were run for 14 years (1994 – 2007) and the results of 13 years (1995 – 2007) were analyzed. The results of the control simulation were used in model evaluation and the results of all simulations were utilized for sensitivity analysis.~~

## 3 Model evaluation

### 3.1 Streamflow

The observed daily streamflow data for model evaluation were from 13 stream gauges operated by the Brazilian Water Agency. Eight of the 13 gauges either control the major area of a tributary subregion or are typical gauges in their tributary subregions. None of the 13 gauges is located in the tributary subregion "Upper-Solimoes tributaries" in the western Amazon Basin. ~~Streamflow of this subregion can be approximately represented by that of~~ Most of this subregion is controlled by the Santo antonio do ica gauge at the upper mainstem. The remaining four gauges are located along the middle or lower mainstem.

The simulated daily streamflow results were compared with the observed data for a 12-year period (1995 – 2006) at the 13 stream gauges (Fig. 3). The Nash–Sutcliffe efficiency coefficient (NSE) and the relative error of mean annual streamflow (RE) were calculated for each gauge (Fig. 3). For the majority of the 13 gauges, daily streamflow values were reproduced fairly well. The NSE value is higher than 0.62 at seven gauges. The four gauges with NSE values lower than 0.5 have high absolute values of RE (i.e., > 0.20), which suggests that large biases in runoff inputs for the areas upstream of those gauges degrade the streamflow results. Overall, runoff inputs have large negative biases in the western portion of the Amazon Basin, and large positive biases in the southern and southeastern portions. The runoff biases could be caused by errors in the precipitation forcing dataset or errors in the land surface water fluxes calculated by the land surface model (e.g., canopy evaporation, plant transpiration, and soil evaporation). In general, the simulated streamflow results are comparable to those of a few previous studies (e.g., Getirana et al., 2012; Yamazaki et al., 2011) and slightly worse than those of Paiva et al. (2013a).

### 3.2 River stage

The observed river stages were based on altimetry data obtained by the Envisat satellite. The altimetry data were stored in the Hydroweb server (http://ctoh.legos.obs-mip.fr/products/hydroweb). This study utilizes river stages of 11 virtual stations which correspond to 11 of the 13 stream gauges used in Sect. 3.1. Each of the 11 virtual stations is close to one gauge: the virtual station and the gauge are located in either the same subbasin or two neighboring subbasins. There is no virtual station close to the Altamira or Cach da porteira-con gauges.

The simulated river stages are relative elevations as they were calculated from the riverbed elevation and the channel water depth. The method for estimating the riverbed elevation is described in Sect. 2.5. Considerable uncertainties in the riverbed elevation are expected due to the large uncertainties in the riverbed elevation at the mouth and the riverbed slopes. Therefore the simulated river stage of a channel is negatively affected by parameter biases of downstream channels and cannot be directly compared to the observations. ~~The riverbed elevation was estimated by using the following equation since observed data were not available.~~

$$E_c = E_{mouth} + \sum_{i=1}^{n} L_i S_i + \frac{1}{2} L_c S_c \qquad (7)$$

~~where $E_c$ is the average riverbed elevation of the current channel [unit: m]; $E_{mouth}$ is the riverbed elevation at the mouth of the Amazon River [unit: m]; $n$ is the total number of the downstream channels; $L_i$ is the flow length of one downstream channel $i$ [unit: m]; $S_i$ is the average riverbed slope of one downstream channel $i$ [dimensionless]; $L_c$ is the flow length of the current channel [unit: m] and $S_c$ is the average riverbed slope of the current channel [dimensionless]. The method for estimating the riverbed elevation is described in Sect. 2.5. Considerable uncertainties in the riverbed elevation are expected due to the large uncertainties in the riverbed elevation at the mouth ($E_{mouth}$) and the riverbed slope. Therefore the simulated river stage of a channel is negatively affected by parameter biases of downstream channels and cannot be directly compared to the observations.~~

The timing and magnitude of simulated river stage fluctuations were compared to those of observed data. The comparison was conducted at the daily scale during a 6-year period (2002 – 2007) for the 11 subbasins ~~which~~ containing~~ed~~ the 11 virtual stations (Fig. 4). For better visual comparison, the simulated river stages of ~~one~~ the same subbasin were shifted by a uniform height to coincide with the observations. The Pearson correlation coefficient between the simulated river stages and the observed data~~, as well as standard deviation for simulated and observed river stages~~ were calculated. The timing of the simulated river stage fluctuations is in good agreement with the observations in all 11 subbasins, with Pearson correlation coefficients ranging from 0.830 to 0.960. Moreover, the standard deviations for the simulated and observed river stages were also calculated. The river stage fluctuations are captured well in the majority of the 11 subbasins, and overestimated for the subbasins of 4 gauges (i.e., Canutama, Acanaui, Serrinha and Santo antonio do ica): the standard deviation of the simulated

river stages is much larger than that of the observed data, which could be primarily due to a few reasons: (1) overestimation of streamflow peaks (e.g., Canutama and Acanaui), which could be caused by biases of runoff inputs or underestimation of flood extent in the upstream area; (2) uncertainties in model parameters of channel cross-sectional geometry, channel Manning coefficients, etc. Overall, in terms of the timing and magnitude of fluctuations, the modeled river stages of this study are comparable to~~with~~ those reported in some previous investigations (Coe et al., 2008; Getirana et al., 2012; Paiva et al., 2013a).

### 3.3 Flood extent

The simulated flood extent results were evaluated using the Global Inundation Extent from Multi-Satellite (GIEMS) data (Papa et al., 2010; Prigent et al., 2007, 2012). The GIEMS data contained monthly surface water area during a 15-year period (1993 – 2007) for each of the land pixels of equal area (i.e., 773 $km^2$). The area-weighted averaging method was used to convert ~~-~~the grid based surface water extent data to subbasin based data for using in this study. Lake area was not deducted from the GIEMS data because in the Amazon Basin the lakes usually were located in the low portion of one subbasin and the simulated inundated area also contained lake~~ area~~ areas.

The simulated monthly flood extent results (including channel surface area and flooded area over floodplains) were compared to the GIEMS data during a 13-year period (1995 – 2007) for 10 subregions and the entire Amazon Basin (Fig. 5). The Pearson correlation coefficient and the mean annual relative difference between the simulated flood extent results and the observations were calculated. The timing of inundation was reproduced well for most area of the Amazon Basin: the Pearson correlation coefficient is equal to or larger than 0.727 at seven of the ten subregions and the entire basin. The mean annual value of simulated flood extent is comparable to that of the GIEMS observations for major portion of the basin: the absolute value of the mean annual relative difference is less than 0.23 at seven of the ten subregions and the entire basin.

The spatial pattern of simulated flood extent was also compared to that of the GIEMS observations for high-water and low-water seasons (Fig. 6). For each subbasin, the simulated or observed flooded fractions of 13 years (1995 – 2007) were averaged for the high-water season (April, May and June) and low-water season (October, November and December), respectively~~ (Fig. 6)~~. ~~The spatial pattern of observed flood extent was reproduced reasonably well for the high-water and low-water seasons.~~ Both the observations and the simulated results show evident inundation in the regions near the middle and lower mainstem. The observed inundation in the upper

Madeira subregion and middle Negro subregion is partially captured by the model. The comparison also shows spatially varying differences between the modeled and observed flood extent (Figs. 6e and 6f). The modeled flood extent exceeds the observations in the lower Madeira subregion near the mainstem and around the major reaches in the middle Negro subregion. At the same time, the modeled flood extent is lower than the observations for some subbasins in the mainstem, upper Madeira, Upper-Solimoes and middle Negro subregions.

~~Figures 5 and 6 show some~~ The aforementioned discrepancies between the simulated flood extent and the GIEMS data~~. Those differences~~ could be related to biases of runoff inputs, which have important effects on the streamflow simulation, as noted earlier. The runoff biases (i.e., the differences between runoff inputs and "actual" runoff) in the upstream area of a stream gauge could be inferred from the long-term mean streamflow errors. Comparing the annual streamflow errors to the flood extent errors upstream of the gauge from year 1995 to 2006 (Fig. 7) shows that runoff biases could be the partial cause for the flood extent discrepancies. For three of the ten gauges (i.e., (b) Itaituba, (g) Tabatinga and (h) Acanaui), the upstream flood-extent discrepancies are consistent with the streamflow errors (i.e., both are positive or negative) in all 12 years. For the other seven gauges, upstream flood-extent discrepancies and streamflow errors are consistent for some years, but contradictory for other years. This result suggests that flood extent discrepancies were also caused by other factors such as (1) uncertainties in model parameters including floodplain topography, channel cross-sectional geometry, channel Manning coefficients, the riverbed slope, etc.; (2) surface water bodies (e.g., lakes and swamps) not represented by the model were lumped into the inundated floodplains; (3) subsurface processes and wetlands sustained by groundwater were not simulated; and (4) inundation could be underestimated or overestimated in the GIEMS data which were of comparatively low resolution (Hess et al., 2015; Prigent et al., 2007). The effects of model parameters (including floodplain topography, channel cross-sectional geometry and channel Manning coefficients) on the inundation results were investigated in the sensitivity study.

~~The flood extent results were compared with those reported in~~of a few ~~previous studies which~~that ~~also used the GIEMS data. As mentioned above,~~ Although the GIEMS data ~~had~~ have non-negligible uncertainties, ~~s. So the comparison to this data should not be deemed as~~it may not be strictly used to ~~differentiate the skill of a criterion for judging different modeling approaches~~studies it is useful to check how our results may differ from those of previous studies using the GIEMS data as the common benchmark. Overall compared to the GIEMS data, t~~T~~he spatial inundation patterns of this study were slightly better than those of Getirana et al. (2012), and comparable to those of Yamazaki et al. (2011) and Paiva et al. (2013a). In terms of monthly total flooded areas, Getirana et al. (2012), Paiva et al. (2013a) and this study were comparable at the whole-basin scale, ~~with~~ while the results from ~~;~~

Getirana et al. (2012) and this study were closer to the GIEMS data than those of Paiva et al. (2013a) at the subregion scale.

## 4 Sensitivity study

~~To investigate the impacts of floodplain topography, channel cross-sectional geometry, channel Manning coefficients and backwater effects on surface water dynamics of the Amazon Basin, the control simulation was compared to the four contrasting simulations in Table 2 for streamflow, river stages and inundation extent (Figs. 8 – 12).~~A sensitivity study was carried out to investigate the roles of the following factors in ~~the~~ modeling of surface hydrology of the Amazon Basin: (1) representing floodplain inundation; (2) alleviating vegetation-caused biases in the DEM; (3) refining channel geometry; (4) adjusting Manning coefficients; and (5) accounting for backwater effects. Six scenario simulations were so designed that for each simulation only one of the above five factors was changed from the control simulation described in Sect. 2.7 (Table 2). All simulations were run for 14 years (1994 – 2007) and the results of 13 years (1995 – 2007) were analyzed. The results of the control simulation were compared with those of each scenario simulation to separately examine the impacts of each factor on the modeled streamflow, river stages and inundation.

The inundation scheme was turned off (i.e., river water could not spill out of the main channel and enter the floodplain) in the second simulation (abbreviated as "NoInund") of Table 2. The results of the control simulation were compared to those of the simulation "NoInund" to reveal the role of the inundation scheme in improving the modeled streamflow and river stages (Sect. 4.1).

The original HydroSHEDS DEM data without the correction of vegetation-caused biases were used in the third simulation (abbreviated as "OriDEM"); the basin-wide channel geometry formulae were not refined for different subregions and were directly used for the entire basin in the fourth simulation (abbreviated as "OriSec"). The results of these two simulations were contrasted with those of the control simulation to show the effects of geomorphological parameters on modeling~~ed~~ surface water dynamics (Sect. 4.2 and 4.3).

A few previous studies at the Amazon Basin used a constant Manning coefficient for all the channels (e.g., 0.04 was used by Beighley et al., 2009; and 0.03 was used by Yamazaki et al., 2011). A constant Manning coefficient of 0.03 and 0.04 was used in the fifth and sixth simulations, respectively (abbreviated as "n003" and "n004"). The diffusion wave method was replaced by the kinematic wave method for representing water flow

through channels in the seventh simulation (abbreviated as "KW"). These three simulations were compared with the control simulation to reveal the impacts of river flow representations on modeled surface hydrology (Sect. 4.4 and 4.5).

~~Figure 8 shows the average seasonal cycles of observed and simulated streamflow during a period of 12 years (1995 – 2006) at 13 stream gauges. Figure 9 shows the observed and modeled river stages at daily scale in year 2007 for 11 subbasins containing or close to 11 of the 13 gauges. Figure 10 illustrates the simulated average river surface profiles along the mainstem in the four seasons (i.e., rising flood, high water, falling flood and low water) of year 2007. Figure 11 demonstrates the average seasonal cycles of observed and simulated flood extent during 13 years (1995 – 2007) for the 10 subregions and the entire basin. In Figs. 8 – 11, the results of all five simulations are included. Figure 12 reveals the differences in average inundation spatial patterns of 13 years (1995 – 2007) between the control simulation and the four contrasting simulations for the high water and low water seasons, respectively.~~In the comparisons between the control simulation and the contrasting scenario simulations, we examined the model results of various locations spread over the Amazon Basin, including streamflow at 13 major mainstem or tributary gauges (Fig. 8), river stages near 11 major gauges (Fig. 9), the mainstem water surface profile (Fig. 10), inundation of 10 subregions (Fig. 11), and spatial patterns of inundation differences for the entire basin (Fig. 12). In the following discussions, Figs. 8 – 12 are used jointly to reveal the impacts of the ~~four~~ five factors on surface water dynamics.

### 4.1 Representing floodplain inundation

The comparison of streamflow results between the control simulation "CTL" and the simulation "NoInund" shows that incorporating the inundation scheme evidently improves the modeled streamflow. More specifically, ~~:~~ streamflow peaks are reduced and delayed, and the streamflow hydrographs become smoother (Fig. 8). The impacts are especially prominent in the subregions with evident inundation (e.g., Fig. 8c) and at the gauges on the middle and lower mainstem (Figs. 8j – 8m). This result demonstrates that floodplains play a significant role in regulating streamflow of the Amazon Basin.

Fig. 9 shows that incorporating the inundation scheme has prominent impacts on the modeled river stages of most of the 11 subbasins examined in this study: the river-stage peaks are attenuated and ~~postpon~~delayed, and the river-stage timing and fluctuation magnitude are improved. The impacts are most obvious in the subregions with evident inundation (e.g., Fig. 9b) and in the middle and lower mainstem (Figs. 9h – 9k). One exception is that the

large improvement of river stages near the Itaituba gauge (Fig. 9a) is primarily caused by the improvement of mainstem river stages because the Itaituba gauge is close to the lower mainstem and its river stages are influenced by the mainstem through backwater effects.

Including the inundation scheme brings about changes of the mainstem water surface profile and the changes are more evident in the rising-flood season than in other seasons (Fig. 10). In the rising-flood season, the average water surface profile is lowered for the entire mainstem section examined here and the large river-stage differences occur in the middle mainstem with magnitude up to more than 5 m (Fig. 10a). In the high-water season, the average water surface profile is also lowered (Fig. 10b). However, Figure 10c shows that in the falling-flood season the mainstem river stages are raised because water stored in the floodplains returns to the river channels. Similar to the rising-flood season, ~~the~~ large river-stage differences appear in the middle mainstem with magnitude of about 3 m. In the low-water season, the average water surface profile is slightly lowered (Fig. 10d). ~~But actually~~It ~~is interesting to~~ should be noted that the mainstem river stages are first raised and then lowered during the three months (Figs. 9h – 9k).

The above comparisons and analyses reveal that incorporating the inundation scheme into ~~the~~ hydrologic modeling has prominent impacts on the simulated surface hydrology in the Amazon Basin and significantly improves both the streamflow and the river-stage hydrographs, especially at reaches whose upstream area involves large floodplains. This result suggests that floodplain inundation is an important component of the surface water dynamics in the Amazon Basin and should be represented in ~~the~~ hydrologic modeling for this basin.

Some previous studies also examined and reported the impacts of representing the floodplain inundation on the modeled surface hydrology in the Amazon Basin (Getirana et al., 2012; Paiva et al., 2013a; Yamazaki et al., 2011). Yamazaki et al. (2011) showed the impacts of floodplain inundation on the streamflow, water depths, and flow velocities at the Obidos gauge (in their Fig. 5) and the mainstem water surface profile (in their Fig. 7). Getirana et al. (2012) demonstrated the effects of floodplain inundation on streamflow of a few mainstem gauges (in their Fig. 16). When investigating the impacts of floodplain inundation on surface hydrology, these two studies used the kinematic wave river routing method that~~which~~ could not represent the important backwater effects in the Amazonia, while we used the diffusion wave river routing method ~~which~~that ~~could represent~~capture~~s~~d backwater effects. Backwater effects were also represented in the dynamic wave river routing method used by Paiva et al. (2013a) when they studied the impacts of floodplain inundation on streamflow of a few major tributary or mainstem gauges including Obidos and Manacapuru (in their Table 2 and Fig. 14). Besides

streamflow, in this study we also examined and revealed the prominent impacts of floodplain inundation on the river stages near 11 major gauges or along the mainstem.

### 4.~~1~~2 Correct~~ion~~ing ~~of~~ DEM

The vegetation-caused biases in the HydroSHEDS DEM data were alleviated via DEM correction. This lowered the floodplain elevations and changed the slope of the elevation profile, which could lead to changes in simulated flood extent. Figure 11 shows that the DEM correction increases flood extent in all 10 subregions. The increase of inundation postpones and lowers streamflow peaks in the downstream channels, especially in the middle and lower mainstem (Figs. 8 j – m).

The increase of inundation also brings about changes in river stages: the magnitude of river stage fluctuations is reduced in the 11 subbasins (Fig. 9). In the middle mainstem~~-~~, the river stages averaged over three months is lowered in the rising-flood and high-water seasons (Figs. 10a and 10b) and elevated in the falling-flood and low-water seasons (Figs. 10c and 10d), with magnitude up to about 1 m.

Figures 12a and 12b show that DEM correction leads to inundation changes in many subbasins: while flood extent is mostly enlarged, DEM correction could increase the slope of the elevation profile in some subbasins and reduce flood extent.

The vegetation-caused biases in DEM data were alleviated with various approaches in a few previous studies ~~of~~ modeling the ~~the~~ surface ~~water dynamics~~ hydrology in the Amazon Basin (Baugh et al., 2013; Coe et al., 2008; Getirana et al., 2012; Paiva et al., 2011, 2013a; Wilson et al., 2007; Yamazaki et al., 2011). Most of these studies did not examine and explicitly report the effects of the DEM correction on the modeled results. Baugh et al. (2013) demonstrated that alleviating vegetation-caused biases in DEM could improve the modeled water levels and inundation over floodplains adjacent to a 280-km reach of the central Amazon (in their Figs. 2 and 5).

### 4.~~2~~3 ~~Adjustment of~~ Refining channel geometry

Adjusting channel cross-sectional geometry could evidently affect the simulated surface water area (Fig. 11) ~~from two aspects~~ and the changes are caused by two mechanisms: (1) reducing channel cross-sectional area, which is equivalent to reducing channel ~~storage~~conveyance capacity, could increase flooded area over

floodplains, and vice versa; (2) broadening the channel width, hence increasing channel surface area, ~~–~~and vice versa. The nine tributary subregions can be placed in five categories according to the changes of channel cross-sectional area, the channel width and the total surface water area (Table 3). The channel geometry of the mainstem is not adjusted. The inundation changes in the tributary subregions affect streamflow in the mainstem and slightly delays and attenuates the inundation peak there (Fig. 11j).

Figure 8c shows that channel geometry changes significantly postpone and lower the streamflow peak at the gauge in the lower Madeira subregion. The reason is that ~~channel geometry changes~~ the channel cross-sectional area is multiplied by a factor of 0.36 (Table 1), which evidently advances inundation in this subregion (Fig. 11c). S~~The s~~imilar phenomenon is observed at the gauge "Cach da porteira-con" in the Northeast subregion (Fig. 8h), where the channel cross-sectional area is multiplied by a factor of 0.48. Inundation changes caused by refining channel geometry in other subregions are comparatively smaller than ~~that~~ those of the Madeira and Northeast subregions, and do not result in significant ~~-~~alterations in streamflow (Fig. 8).

Adjustment of channel geometry could have evident effect on the river stage of the local channel. The mechanism for channel geometry changes to affect river stages is not straightforward. For instance, reducing the channel width could raise the river stage and hence increase the flow velocity or inundation, which, in turn tend to lower the river stage (Fig. 13). The simulated results of this study show that, in most circumstances, reducing the channel width raises the river stage of the local channel (Figs. 9b, 9c and 9d) and vice versa (Figs. 9e and 9f). In Fig. 9a, this rule does not apply from about day ~~170~~160 to ~~330~~350, which could be caused by backwater effects: the river stage of this channel is influenced by that of the mainstem section downstream of the Obidos gauge.

Channel geometry changes could also influence river stages of remote downstream channels. The channel morphology of the mainstem is not adjusted. So the river stage changes along the mainstem are caused by inundation changes in the upstream area. The channel-geometry adjustment of this study advances inundation in the major portion of the Amazon Basin, which influences river stages along the mainstem, particularly in the middle reaches: the river stages averaged over three months are lowered in the rising-flood and high-water seasons (Figs. 10a and 10b) and elevated in the falling-flood and low-water seasons (Figs. 10c and 10d), with magnitude up to about 1 m. The phenomenon can also be observed in Figs. 9h–k.

The sensitivities of modeled surface hydrology to channel geometry were also investigated by some former studies (Paiva et al., 2013a; Yamazaki et al., 2011). Yamazaki et al. (2011) perturbed the channel width or depth

by a uniform percentage for all the channels and examined the effects of these channel-geometry changes on streamflow of the Obidos gauge and the flooded area over the central Amazon region (in their Fig. 13). Paiva et al. (2013a) perturbed the channel width by a uniform percentage or perturbed the channel-bottom level by a uniform height, which was equivalent to perturbing the channel depth by a uniform value, and investigated the effects of these channel-geometry changes on streamflow of the Obidos gauge, channel water depths of the Manacapuru gauge, and the total flooded area of the entire Amazon Basin (in their Fig. 10). These two studies showed the sensitivities of modeled surface hydrology to channel geometry, as well as the interactions between streamflow, water depths and inundation. Theyese previous studies pointed out the importance of channel geometry and provided a foundation to this study. HereIn this study, channel-geometry changes were caused by the process of refining the channel cross-sections, –and those changes varyied were spatially varied varying (Table 1). We examined the effects of channel-geometry changes on inundation of 10 subregions, streamflow of 13 gauges, river stages near 11 gauges, as well as the mainstem water- surface profile. In addition, the effects of channel-geometry changes on modeled surface water dynamics were analyzed with approaches of which some were different from those of the former studies.

### 4.34 Varying the Manning roughness coefficients

A few studies for the Amazon Basin (e.g., Paiva et al., 2013a; Yamazaki et al., 2011) revealed some sensitivities of surface hydrology to the Manning coefficient. Yamazaki et al. (2011) perturbed the Manning coefficient by a uniform percentage for all the channels and examined the effects on streamflow of the Obidos gauge and the flooded area over the central Amazon region (in their Fig. 13). Using a similar approach, Paiva et al. (2013a) investigated the effects of the Manning coefficient on streamflow of the Obidos gauge, channel water depths of the Manacapuru gauge, and the total flooded area of the entire Amazon Basin (in their Fig. 10). These studies revealed that increasing the Manning coefficient could raise the river stage, expand the flooded area, and reduce and delay the flood peak. Instead of a uniform perturbation, we varied the Manning coefficient with the channel depth and examined the effects on flood extent of 10 subregions, streamflow of 13 gauges, river stages near 11 gauges, and the mainstem water surface profile.

–The streamflow Nash–Sutcliffe efficiency coefficients (NSEs) of the simulation ‘“CTL-” were compared with those of the simulations ‘ -“n003-” and “n004” (Table 4). It is shown that tThe NSEs of the simulation ‘ “CTL-” are evidently higher than those of the simulation “n004” at 10 of the 13 gauges (except Fazenda vista

alegre, Itapeua and Manacapuru)~~;~~ and higher than those of ~~the simulation "~~"n003~~"~~" at 12 of the 13 gauges (~~the NSE decreases slightly from 0.931 to 0.911 at the~~ except Obidos ~~gauge~~)~~,~~. ~~which~~These~~is~~ results suggest~~s~~ that the spatially ~~varied~~ varying Manning coefficients are more appropriate than the uniform Manning coefficient ~~(i.e., 0.03)~~of 0.03 or 0.04 for the simulations of this study.

The spatially ~~varied~~ varying Manning coefficients range from 0.03 to 0.05 and are equal to or larger than the ~~uniform coefficient~~ Manning coefficient of 0.03. ~~The results of the simulation "CTL" are compared to those of the simulation "n003" to reveal the effects of Manning coefficient increasevalues on the modeled surface water dynamics.~~

The spatially ~~varied~~ varying Manning coefficients result~~ed~~ in larger flood extent than the uniform coefficient of 0.03 (Fig. 11). ~~The spatially varied coefficients range from 0.03 to 0.05 and are equal to or larger than the uniform coefficient.~~ The larger Manning coefficient leads to the lower flow velocity, larger wet cross-sectional area and thereby higher river stage (Fig. 9), which advance local inundation, as well as upstream inundation due to backwater effects. Inundation increases in the upstream area postpone and attenuate flood waves at the downstream gauges (Fig. 8).

Increases of the Manning coefficients not only affect local and upstream river stages as discussed above, but also influence downstream river stages. Inundation increases in the upstream area have impact on streamflow rates and hence river stages in the downstream channels. Therefore river stages are influenced by not only downstream and local Manning coefficients, but also upstream Manning coefficients. Figure 9 shows that the ~~varied~~ Manning coefficient~~s~~ increases result in rise of river stages in most circumstances, which suggests that the local and downstream effects play a dominant role: increases of Manning coefficients reduce flow velocities, enlarge wet cross-sectional area and hence elevate river stages. However, in the lower mainstem the upstream effects may overwhelm the local and downstream effects. For instance, Fig. 9k shows that, during the rising-flood period (before about the day 150), the ~~varied~~ Manning coefficient~~s~~ increases reduce river stages at the Obidos gauge. The main reason is that the ~~varied~~ Manning coefficient~~s~~ increases ~~increase~~ advance inundation in the upstream area, which results in smaller streamflow rates in the lower mainstem for the rising-flood period.

### 4.45 Backwater effects

Besides the above factors, backwater effects also play a significant role in the surface water dynamics of the Amazon Basin, particularly in the middle and lower portions of this basin thatwhich have very mild topography (e.g., Fig. 10e). In this study, backwater effects were represented by in using the diffusion wave routing method to simulate water flow through channels in for four six of the five seven simulations (including the control simulation). In the remaining simulation (i.e., KW), the diffusion wave method was replaced with the kinematic wave method thatwhich could not represent backwater effects. The results of the control simulation were compared with those of the simulation KW to reveal backwater effects on surface water dynamics.

(1) Backwater effects on flood extent.

In the diffusion wave method, backwater effects could decrease the friction slope and hence reduce the flow velocity (Eqs. (12) and (23)), and vice versa. For the same streamflow rate, reduction of the flow velocity leads to larger wet cross-sectional area and thereby higher river stage, which could increase local inundation if the river stage exceeds the bank top, as well as increase upstream inundation due to backwater effects. This mechanism is similar to the aforementioned mechanism that increases of the Manning roughness coefficients could advance local and upstream inundation. Using the same reasoning, backwater effects also could increase the flow velocity and eventually reduce inundation. Figure 11 shows that the flood extent of the control simulation is evidently larger than that of the simulation KW for nine of the ten subregions and the entire Amazon Basin, which suggests that the dominant role of backwater effects is to advance inundation for this basin. However, backwater effects also could reduce inundation as demonstrated in the subregion "Upper-Solimoes tributaries" (Fig. 11f). Figures 12j and 12k illustrate that backwater effects tend to advance inundation in the middle and lower mainstem, lower Negro and lower Madeira subregions, where the topography is flat and the streamflow rate is comparatively high. Yamazaki et al. (2011) showed the backwater effects on the flooded area over the central Amazon region (in their Fig. 9). In their results, backwater effects promoted the flooded area to a lesser extent as compared to our study, which may be due to the differences in the channel or floodplain geomorphology data betweenused in the two studies. Paiva et al. (2013b) used the dynamic wave method to represent river flow in the Solimoes River basin, which is the western upstream portion of the Amazon Basin. They discussed the important role of backwater effects in the inundation dynamics of the Amazon. In this study, we examined the impacts of backwater effects on flood extent in the 10 subregions constituting the Amazon Basin (Fig. 11), and demonstrated the spatial pattern of flood extent changes caused by backwater effects (Figs. 12j and 12k).

(2) Backwater effects on streamflow

Backwater effects bring about inundation increases in the subbasins of the upstream area, which have impact on streamflow in the downstream channels. Inundation increases in the upstream area could delay and attenuate hydrographs in the middle and lower mainstem (Figs. 8k–m). ~~These backwater effects on hydrographs agree with the results of Paiva et al. (2013).~~ These results agree with Paiva et al. (2013a, 2013b) which demonstrated the important role of the backwater effects in streamflow of the mainstem and tributaries of the Amazon Basin (Table 2 and Fig. 14 of Paiva et al., 2013a; Table 2 and Figs. 3, 4 and 9 of Paiva et al., 2013b).

Backwater effects could increase the friction slope and hence advance the flow velocity, which resulted in changes of the hydrograph. For instance, Fig. 8c shows that at the lower Madeira River the flow peak of the control simulation is about 20 days earlier than that of the simulation 'KW'. The Madeira River reaches its highest stage about 1 – 2 months earlier than the mainstem (compare Fig. 9b and Fig. 9j; also see Meade et al., 1991). This time difference in peak stage makes the slope of the river surface steep in the rising-flood period of the Madeira River, which advances the flow velocity and brings the streamflow peak to an earlier time. This phenomenon of backwater effects on the streamflow timing cannot be captured in the simulation 'KW' because in the kinematic wave method the flow velocity depends on the riverbed slope instead of the river surface slope. In addition, to our knowledge, this phenomenon of backwater effects on the streamflow timing has not been discussed in ~~the~~ previous modeling studies in the Amazon Basin.

(3) Backwater effects on river stages

It is discussed above that backwater effects could influence local and upstream river stages by changing the local flow velocity, but they could also affect downstream flow rates, which consequently influence downstream river stages. Therefore the river stage of a channel is influenced by not only the local and downstream backwater effects, but also the backwater effects in the upstream area. The combined impact significantly attenuates both temporal (Fig. 9) and spatial (Fig. 10) river stage fluctuations. This result is consistent with that of Yamazaki et al. (2011), which primarily discussed the ~~river stages~~ water depths at the Obidos gauge (in their Fig. 5b) and the mainstem ~~river~~water surface profile~~s of the mainstem~~ in one month (in their Fig. 7a), while this study examined river stages ~~of~~ near 11 major gauges on tributaries or the mainstem (Fig. 9), and the mainstem ~~river~~ water surface profiles ~~of the mainstem~~ in four seasons (Fig. 10). Moreover, in the results of Yamazaki et al. (2011), the backwater effects on river stages were not as prominent as those simulated in~~of~~ this study, which may be due to

the discrepancies in channel geometry or floodplain topography between the two studies. ~~However~~ In addition, t~~T~~he result of this study ~~also~~ agree~~s~~d with Paiva et al. (2013b), which discussed the backwater effects on river stages in the Solimoes River basin.

Figure 10 also shows that the river stages of the middle and lower mainstem drop significantly when backwater effects are not represented, especially during the rising-flood, falling-flood and low-water periods (Figs. 10a, 10c and 10d). The sea level was used as the boundary condition at the basin outlet when the diffusion wave method was employed to simulate water flow in channels. The river stages of the middle and lower mainstem were influenced by the sea level via backwater effects. In this study the sea level was assumed to be fixed, which was similar to the approach of Yamazaki et al. (2011). In reality, the sea level rises and falls regularly, which exerts varying impact on river flow (e.g., Yamazaki et al., 2012). The effect of sea level variation on river hydrology ~~could~~ can be represented ~~after~~ when the surface-water transport model is coupled with an Earth system model. Furthermore, this modeling framework could be used to investigate the potential impact of sea level rise on the terrestrial hydrologic cycle due to climate change.

## 5 ~~Discussion and conclusion~~ Summary and discussion

~~**Continental-scale modeling of surface hydrology in the Amazon Basin faced a few challenges including uncertainties in parameters of floodplain and channel morphology, and representation of river flow over flat-gradient topography. This study aimed to tackle those uncertainties and improve the continental-scale modeling of surface water dynamics in this vast basin. A macro-scale inundation scheme was integrated with the MOSART surface-water transport model and the extended model was utilized. Vegetation-caused biases embedded in the HydroSHEDS DEM data were alleviated by using a vegetation height map at about 1-km resolution (Simard et al., 2011) and a land cover dataset at about 90-m resolution for wetlands of the lowland Amazon Basin (Hess et al., 2003, 2015). Channel cross-sectional geometry was estimated by using relationships between channel cross-sectional dimensions and upstream drainage area (referred to as channel geometry formulae). The general channel geometry formulae for the entire basin (Beighley and Gummadi, 2011) were adjusted for most subregions based on channel morphological information of local locations. The Manning roughness coefficient for the channel depended on the channel depth to reflect the general rule that the relative importance of riverbed resistance in river flow declined with the increase of river size.**~~

Floodplain inundation is a~~one~~ key~~important~~ component of surface water dynamics in the Amazon Basin. A macro-scale inundation scheme for representing floodplain inundation was incorporated into the Model for Scale Adaptive River Transport (MOSART) and the extended model was applied to ~~for~~ the entire Amazonia. Efforts were made to deal with a few challenges ~~facing the~~ in continental-scale modeling of surface hydrology in this

vast basin: (1) we refined the floodplain topography ~~through~~by alleviating the spatially varying vegetation-caused biases in the HydroSHEDS DEM data. To our knowledge, this was the first time that the spatial variability of vegetation-caused biases in the DEM data was explicitly considered in ~~the~~ hydrologic modeling for the entire Amazon Basin; (2) we improved the representation of spatial variability in channel cross-sectional geometry by refining the basin-wide channel geometry formulae for various subregions; (3) the Manning roughness coefficient varied with the channel depth to reflect the general rule that the relative importance of riverbed resistance in river flow declined with the increase of river size; (4) we accounted for the backwater effects in the river routing method to better represent river flow in gentle-slope reaches.

The ~~simulated~~ model results were evaluated against in situ streamflow data as well as remote sensing river-stage and inundation data. The simulated streamflow results were compared with the observed data from 13 major stream gauges (Fig. 3). The streamflow hydrographs were reproduced fairly well for the majority of the 13 gauges. The simulated river stages were compared to the altimetry data obtained by the Envisat satellite ~~F~~for the 11 subbasins containing or close to 11 of the 13 gauges (Fig. 4)~~, the simulated river stages were compared to the altimetry data obtained by the Envisat satellite~~. ~~The timing (magnitude) of river stage fluctuations was captured well for all (the majority) of the 11 subbasins.~~The timing of river stage fluctuations was captured well for all ~~the~~ 11 subbasins and the magnitude of river stage fluctuations was reproduced well for most of the 11 subbasins. ~~For the 10 subregions and the entire basin, t~~The simulated ~~inundation~~ monthly flood extent results were compared against the GIEMS satellite data ~~(Papa et al., 2010; Prigent et al., 2007, 2012)~~ for the 10 subregions and the entire basin (Fig. 5). For the time series of the lumped flood extent, ~~T~~the ~~simulated inundation~~ model results were comparable to the GIEMS observations ~~for the major portion~~ in most subregions of the basin. The spatial pattern of modeled inundation was also contrasted with that of the GIEMS observations (Fig. 6). While the model results resemble the overall spatial pattern of the observed inundation, the comparison also shows spatially varying ~~The~~ flood extent discrepancies between the simulation and observations which could be partially explained by the biases of runoff inputs (Fig. 7). Those discrepancies could also be due to uncertainties in geomorphological parameters, missing representations of some potentially important hydrologic processes, as well as biases of the GIEMS data.

~~Sensitivity analyses were conducted to investigate the impacts on surface water dynamics of the Amazon Basin by improving floodplain topography, channel morphology and Manning coefficients, as well as accounting for backwater effects. The results showed that all four factors could have an evident effect on inundation, although through different mechanisms: DEM correction changes the floodplain elevations and slope; adjusting~~

~~channel cross-sectional geometry changes the channel storage conveyance capacity; Manning coefficient variations or backwater effects affect the flow velocity and hence the river stage. Inundation changes in the upstream area affected the downstream surface water dynamics, particularly along the middle and lower mainstem Amazon, by delaying flood waves, as well as attenuating fluctuations of streamflow and river stages, which consequently brought about inundation changes in the downstream area. Channel cross-sectional geometry, the Manning coefficient and backwater effects had impacts on the river stage of the local channel, and potential influence on surface water dynamics of the upstream area due to backwater effects.~~

In the sensitivity study, the results of the control simulation were compared with those of a few scenario simulations for investigating the roles of the following factors in the hydrologic modeling for the Amazon Basin.

(1) Representing floodplain inundation. It was shown that representing floodplain inundation could evidently improve the modeled streamflow at 13 major gauges (Fig. 8). It was also demonstrated that representing floodplain inundation could improve the river-stage timing and fluctuation magnitude near 11 major gauges (Fig. 9), and have prominent impacts on the modeled water surface profile along the mainstem (Fig. 10). These results showed that floodplain inundation played an important role in surface hydrology of the Amazon Basin and should be represented in the hydrologic modeling for this basin.

(2) Alleviating vegetation-caused biases in the DEM. The DEM correction leaded to evident inundation changes, of which most were inundation increases, in many subbasins (Figs. 11, 12a and 12b). The DEM correction ~~also~~ could lower and postpone streamflow peaks, especially at the mainstem (Fig. 8) and attenuate river-stage fluctuations in the tributaries and the mainstem (Figs. 9 and 10). To our knowledge, for ~~the~~ hydrologic modeling of~~in~~ the entire Amazon Basin, the impacts of correcting vegetation-caused biases in the DEM on the modeled surface hydrology were not reported in the past.

(3) Refining channel cross-sectional geometry. The channel geometry refinements could evidently increase or decrease the inundation area for various locations of the basin (Figs. 11, 12d and 12e). Those refinements could obviously improve the streamflow hydrograph (Figs. 8c and 8h), and raise or lower river stages in the tributaries and the mainstem (Figs. 9 and 10). These results demonstrated the importance of improving the representation of spatial variability in channel geometry.

(4) Adjusting Manning coefficients. The streamflow hydrographs of the scenario simulations suggested that the spatially varying Manning coefficients were more appropriate than the uniform Manning coefficient of 0.03 or 0.04 for the hydrologic modeling of this study. The comparison between the control simulation, where the

Manning coefficient varied from 0.03 to 0.05, and the simulation using the uniform Manning coefficient of 0.03 revealed that increasing the value of the Manning coefficient ~~increases~~ could obviously advance inundation (Figs. 11, 12g and 12h), reduce and delay streamflow peaks (Fig. 8), and mostly raise river stages (Figs. 9 and 10). One exception was that an increase in the Manning coefficient ~~increases~~ could lower the river stages in the lower mainstem during the rising-flood period (Fig. 9k).

(5) Representing backwater effects. The comparison between scenario simulations showed that the backwater effects could prominently advance inundation in most of the 10 subregions, especially in the area near the middle and lower mainstem and in the lower Negro basin (Figs. 11, 12j and 12k)~~.~~, ~~The backwater effects also could also~~ and reduce inundation in some circumstances (Figs. 11f, 12j and 12k).

~~The simulation comparison demonstrated that r~~Representing backwater effects could evidently lower and delay streamflow peaks ~~and~~, improve the hydrographs in the middle and lower mainstem (Figs. 8k–m)~~.~~, ~~In addition, model results showed that representing backwater effects could~~ and bring the streamflow peak to an earlier time (e.g., Fig. 8c), of which the last was not reported in ~~the past~~previous studies.

It was also illustrated that representing backwater effects could significantly attenuate the modeled river stage fluctuations in the mainstem and tributaries (Fig. 9), and smooth the mainstem water surface profile (Fig. 10).

~~We compared this sensitivity study with those of~~ Building on ~~a few~~ previous studies (Baugh et al., 2013; Getirana et al., 2012; Paiva et al., 2013a, 2013b; Yamazaki et al., 2011) that modeled surface hydrology in the Amazon Basin and examined sensitivity of their simulations to the factors discussed above~~.~~, ~~Our study was based on the important foundation of the previous investigations and~~ some of our analysis results agreed with ~~their~~ the findings reported earlier. At the same time, ~~we used some new~~ expanding on the methodologies explored in previous studies and performing a more comprehensive examination of the simulations, ~~and obtained~~ this study yielded some new results~~, which~~ that were either not reported before or different from those of the former studies. More detailed comparisons between our study and former studies were discussed in Sect. 4.

The understanding obtained in this study could be helpful to improving the modeling of terrestrial surface water dynamics at the global scale. Besides the Amazon Basin, alleviating the vegetation-caused biases in the DEM data is also worthwhile for other basins with considerable inundation and extensive forested area, such as the Congo Basin. The ~~simple method we developed~~ DEM correction can be tested globally for its impacts on

~~inundation~~ surface hydrologic modeling. It is shown that a simple method can improve the representation of channel cross-sectional geometry and consequently the modeled surface hydrology, which implies that representing the spatial ~~diversity~~ variability of channel morphology should be emphasized in applications for other regions. The future Surface Water and Ocean Topography (SWOT) mission (Alsdorf et al., 2007) is expected to bring notable advancement in this aspect. It is also demonstrated that spatially ~~varied~~ varying Manning ~~roughness~~ coefficients depending on the channel depth result in streamflow hydrographs better than those of the uniform Manning coefficient of 0.03 or 0.04 in the model simulations of this study. It is worth investigating the application of this method to other regions, although the Manning coefficient is empirical and model dependent. Besides the Amazon River, ~~it is very likely that~~ backwater effects also play a significant role in many other rivers, such as the Yangtze River and Mississippi River (Meade et al., 1991). Therefore backwater effects should be accounted for in the global applications where river stages, inundation extent or river flow velocities are investigated. These ~~methods~~ factors may have impacts on surface hydrology to different degrees for various regions. For instance, DEM correction and backwater effects are expected to have larger impacts on surface hydrology in regions with milder topography.

Subbasins are used as computation units in this study. Surface hydrologic simulations using subbasins as computation units are less scale-dependent than those using square grids as computation units (e.g., Getirana et al., 2010; Tesfa et al., 2014a, 2014b; Yamazaki et al., 2011). For instance, when computation units become coarser, using subbasin units can preserve the pathways of river flows better than using grid units (e.g., Getirana et al., 2010). In this study, the simulated hydrologic results are comparable to observations, although the subbasin units are relatively coarse (with an average area of 1091.7 $km^2$). For continental~~-~~ or global ~~–~~scale applications, using subbasin units could represent surface water transport more realistically than using grid units when the subbasin size is comparable to the grid size.

At the same time, some aspects of the model could be improved, such as the representation of water exchange between channels and floodplains. In this study, instantaneous channel–floodplain exchange is assumed, which could overestimate flooded area during the rising-flood period, and vice versa during the receding-flood period. The modeling of this exchange process could be improved by including a mechanistic representation of water flow over floodplains. For instance, Alsdorf et al. (~~–~~2005) demonstrated that the floodplain drainage could be simulated using a linear diffusion model and~~;~~ Miguez-Macho and Fan (2012) used diffusion wave method to simulate two dimensional flow over floodplains. Moreover, the mechanistic

representation of floodplain flow could be used to simulate water exchange over floodplains between neighboring subbasins, which was not accounted for in this study.

In addition, the modeling of surface water dynamics could benefit from integrating the surface-water transport model with land surface models or climate models by representing the interactions between surface hydrology and subsurface water fluxes as well as atmospheric processes. Such interactions could potentially have important effects on surface fluxes, with important implications to modeling of land – atmosphere interactions and tropical forest response to floods and droughts.

## Code availability

The MOSART code including the inundation parameterization described herein will be distributed through a git repository and made available upon request.

## Data availability

This study used the following datasets, which can be either accessed from the internet or acquired from the corresponding institution or person.

(1) The HydroSHEDS DEM datasets were developed by United States Geological Survey and are available on-line (-http://hydrosheds.cr.usgs.gov/ ).

(2) The dataset "Global 1km Forest Canopy Height (Simard et al., 2011)" is available on-line (http://webmap.ornl.gov/wcsdown/dataset.jsp?ds_id=10023) from the Oak Ridge National Laboratory Distributed Active Archive Center, Oak Ridge, Tennessee, USA.

(3) Hess, L.L., J.M. Melack, A.G. Affonso, C.C.F. Barbosa, M. Gastil-Buhl, and E.M.L.M. Novo. 2015. LBA-ECO LC-07 Wetland Extent, Vegetation, and Inundation: Lowland Amazon Basin. ORNL DAAC, Oak Ridge, Tennessee, USA. http://dx.doi.org/10.3334/ORNLDAAC/1284

(4) The surface and subsurface runoff inputs of 1-degree resolution were produced by Bertrand Decharme at CNRM/Météo-France (Getirana et al., 2014) and can be acquired by contacting Augusto Getirana (augusto.getirana@nasa.gov).

(5) The streamflow data of the stream gauges can be acquired by contacting the Brazilian Water Agency ANA (Agencia Nacional de Aguas).

(6) The river water levels are mainly based on altimetry data from the Envisat satellite and available from the HydroWeb data base (http://ctoh.legos.obs-mip.fr/products/hydroweb) maintained by CTOH (Center for Topographic studies of the Ocean and Hydrosphere) at LEGOS, France.

(7) The dataset GIEMS (Global Inundation Extent from Multi-Satellite) was developed by Catherine Prigent (Observatoire de Paris), Filipe Aires (Estellus and Observatoire de Paris) and Fabrice Papa (IRD, LEGOS), and can be acquired by contacting Fabrice Papa (fabrice.papa@ird.fr).

## Competing interests

The authors declare that they have no conflict of interest.

## Acknowledgements

This research was supported by the Office of Science of the U.S. Department of Energy as part of the Earth System Modeling program through the Accelerated Climate Modeling for Energy (ACME) project. The Pacific Northwest National Laboratory is operated by Battelle for the U.S. Department of Energy under Contract DE-AC05-76RLO1830. We would like to acknowledge the institutions/researchers those developed the datasets described in the section “Data availability”.

**References**


Alsdorf, D., Dunne, T., Melack, J., Smith, L. and Hess, L.: Diffusion modeling of recessional flow on central Amazonian floodplains, Geophys. Res. Lett., 32(21), L21405, doi:10.1029/2005GL024412, 2005.

Alsdorf, D. E., Rodríguez, E. and Lettenmaier, D. P.: Measuring surface water from space, Rev. Geophys., 45(2), RG2002, doi:10.1029/2006RG000197, 2007.

Arcement, G. J. and Schneider, V. R.: Guide for selecting Manning's roughness coefficients for natural channels and flood plains, United States Geological Survey., 1989.

Baugh, C. A., Bates, P. D., Schumann, G. and Trigg, M. A.: SRTM vegetation removal and hydrodynamic modeling accuracy, Water Resour. Res., 49(9), 5276–5289, doi:10.1002/wrcr.20412, 2013.

Beighley, R. E. and Gummadi, V.: Developing channel and floodplain dimensions with limited data: a case study in the Amazon Basin, Earth Surf. Process. Landf., 36(8), 1059–1071, doi:10.1002/esp.2132, 2011.

Beighley, R. E., Eggert, K. G., Dunne, T., He, Y., Gummadi, V. and Verdin, K. L.: Simulating hydrologic and hydraulic processes throughout the Amazon River Basin, Hydrol. Process., 23(8), 1221–1235, doi:10.1002/hyp.7252, 2009.

Bousquet, P., Ciais, P., Miller, J. B., Dlugokencky, E. J., Hauglustaine, D. A., Prigent, C., Van der Werf, G. R., Peylin, P., Brunke, E.-G., Carouge, C., Langenfelds, R. L., Lathière, J., Papa, F., Ramonet, M., Schmidt, M., Steele, L. P., Tyler, S. C. and White, J.: Contribution of anthropogenic and natural sources to atmospheric methane variability, Nature, 443(7110), 439–443, doi:10.1038/nature05132, 2006.

Chow, V. T., Maidment, D. R. and Mays, L. W.: Applied Hydrology, McGraw-Hill., 1988.

Coe, M. T., Costa, M. H. and Howard, E. A.: Simulating the surface waters of the Amazon River basin: impacts of new river geomorphic and flow parameterizations, Hydrol. Process., 22(14), 2542–2553, doi:10.1002/hyp.6850, 2008.

Cunge, J. A., Holly, F. M. and Verwey, A.: Practical aspects of computational river hydraulics, Pitman Publishing, Boston., 1980.

Dai, A. and Trenberth, K. E.: Estimates of Freshwater Discharge from Continents: Latitudinal and Seasonal Variations, J. Hydrometeorol., 3(6), 660–687, doi:10.1175/1525-7541(2002)003<0660:EOFDFC>2.0.CO;2, 2002.

Decharme, B., Douville, H., Prigent, C., Papa, F. and Aires, F.: A new river flooding scheme for global climate applications: Off-line evaluation over South America, J. Geophys. Res. Atmospheres, 113(D11), D11110, doi:10.1029/2007JD009376, 2008.

Decharme, B., Alkama, R., Douville, H., Becker, M. and Cazenave, A.: Global Evaluation of the ISBA-TRIP Continental Hydrological System. Part II: Uncertainties in River Routing Simulation Related to Flow Velocity and Groundwater Storage, J. Hydrometeorol., 11(3), 601–617, doi:10.1175/2010JHM1212.1, 2010.

Getirana, A. C. V., Bonnet, M.-P., Rotunno Filho, O. C., Collischonn, W., Guyot, J.-L., Seyler, F. and Mansur, W. J.: Hydrological modelling and water balance of the Negro River basin: evaluation based on in situ and spatial altimetry data, Hydrol. Process., 24(22), 3219–3236, doi:10.1002/hyp.7747, 2010.

Getirana, A. C. V., Boone, A., Yamazaki, D., Decharme, B., Papa, F. and Mognard, N.: The Hydrological Modeling and Analysis Platform (HyMAP): Evaluation in the Amazon Basin, J. Hydrometeorol., 13(6), 1641–1665, doi:10.1175/JHM-D-12-021.1, 2012.

Getirana, A. C. V., Boone, A., Yamazaki, D. and Mognard, N.: Automatic parameterization of a flow routing scheme driven by radar altimetry data: Evaluation in the Amazon basin, Water Resour. Res., 49(1), 614–629, doi:10.1002/wrcr.20077, 2013.

Getirana, A. C. V., Dutra, E., Guimberteau, M., Kam, J., Li, H.-Y., Decharme, B., Zhang, Z., Ducharne, A., Boone, A., Balsamo, G., Rodell, M., Toure, A. M., Xue, Y., Peters-Lidard, C. D., Kumar, S. V., Arsenault, K., Drapeau, G., Ruby Leung, L., Ronchail, J. and Sheffield, J.: Water Balance in the Amazon Basin from a Land Surface Model Ensemble, J. Hydrometeorol., 15(6), 2586–2614, doi:10.1175/JHM-D-14-0068.1, 2014.

Guimberteau, M., Drapeau, G., Ronchail, J., Sultan, B., Polcher, J., Martinez, J.-M., Prigent, C., Guyot, J.-L., Cochonneau, G., Espinoza, J. C., Filizola, N., Fraizy, P., Lavado, W., De Oliveira, E., Pombosa, R., Noriega, L. and Vauchel, P.: Discharge simulation in the sub-basins of the Amazon using ORCHIDEE forced by new datasets, Hydrol Earth Syst Sci, 16(3), 911–935, doi:10.5194/hess-16-911-2012, 2012.

Hess, L. L., Melack, J. M., Novo, E. M. L. M., Barbosa, C. C. F. and Gastil, M.: Dual-season mapping of wetland inundation and vegetation for the central Amazon basin, Remote Sens. Environ., 87(4), 404–428, doi:10.1016/j.rse.2003.04.001, 2003.

Hess, L. L., Melack, J. M., Affonso, A. G., Barbosa, C., Gastil-Buhl, M. and Novo, E. M. L. M.: Wetlands of the Lowland Amazon Basin: Extent, Vegetative Cover, and Dual-season Inundated Area as Mapped with JERS-1 Synthetic Aperture Radar, Wetlands, 35(4), 745–756, doi:10.1007/s13157-015-0666-y, 2015.

Junk, W. J., Piedade, M. T. F., Wittmann, F., Schöngart, J. and Parolin, P., Eds.: Amazonian Floodplain Forests, Springer Netherlands, Dordrecht. [online] Available from: http://link.springer.com/10.1007/978-90-481-8725-6 (Accessed 25 March 2016), 2011.

Li, H., Wigmosta, M. S., Wu, H., Huang, M., Ke, Y., Coleman, A. M. and Leung, L. R.: A Physically Based Runoff Routing Model for Land Surface and Earth System Models, J. Hydrometeorol., 14(3), 808–828, doi:10.1175/JHM-D-12-015.1, 2013.

Meade, R. H., Rayol, J. M., Conceicão, S. C. D. and Natividade, J. R. G.: Backwater effects in the Amazon River basin of Brazil, Environ. Geol. Water Sci., 18(2), 105–114, doi:10.1007/BF01704664, 1991.

Miguez-Macho, G. and Fan, Y.: The role of groundwater in the Amazon water cycle: 1. Influence on seasonal streamflow, flooding and wetlands, J. Geophys. Res., 117(D15), doi:10.1029/2012JD017539, 2012.

Neal, J. C., Odoni, N. A., Trigg, M. A., Freer, J. E., Garcia-Pintado, J., Mason, D. C., Wood, M. and Bates, P. D.: Efficient incorporation of channel cross-section geometry uncertainty into regional and global scale flood inundation models, J. Hydrol., 529, Part 1, 169–183, doi:10.1016/j.jhydrol.2015.07.026, 2015.

O'Loughlin, F. E., Paiva, R. C. D., Durand, M., Alsdorf, D. E. and Bates, P. D.: A multi-sensor approach towards a global vegetation corrected SRTM DEM product, Remote Sens. Environ., 182, 49–59, doi:10.1016/j.rse.2016.04.018, 2016.

Paiva, R. C. D., Collischonn, W. and Tucci, C. E. M.: Large scale hydrologic and hydrodynamic modeling using limited data and a GIS based approach, J. Hydrol., 406(3–4), 170–181, doi:10.1016/j.jhydrol.2011.06.007, 2011.

Paiva, R. C. D., Buarque, D. C., Collischonn, W., Bonnet, M.-P., Frappart, F., Calmant, S. and Bulhões Mendes, C. A.: Large-scale hydrologic and hydrodynamic modeling of the Amazon River basin, Water Resour. Res., 49(3), 1226–1243, doi:10.1002/wrcr.20067, 2013a.

Paiva, R. C. D., Collischonn, W. and Buarque, D. C.: Validation of a full hydrodynamic model for large-scale hydrologic modelling in the Amazon, Hydrol. Process., 27(3), 333–346, doi:10.1002/hyp.8425, 2013b.

Papa, F., Prigent, C., Aires, F., Jimenez, C., Rossow, W. B. and Matthews, E.: Interannual variability of surface water extent at the global scale, 1993–2004, J. Geophys. Res. Atmospheres, 115(D12), D12111, doi:10.1029/2009JD012674, 2010.

Prigent, C., Papa, F., Aires, F., Rossow, W. B. and Matthews, E.: Global inundation dynamics inferred from multiple satellite observations, 1993–2000, J. Geophys. Res. Atmospheres, 112(D12), D12107, doi:10.1029/2006JD007847, 2007.

Prigent, C., Papa, F., Aires, F., Jimenez, C., Rossow, W. B. and Matthews, E.: Changes in land surface water dynamics since the 1990s and relation to population pressure, Geophys. Res. Lett., 39(8), L08403, doi:10.1029/2012GL051276, 2012.

Richey, J. E., Melack, J. M., Aufdenkampe, A. K., Ballester, V. M. and Hess, L. L.: Outgassing from Amazonian rivers and wetlands as a large tropical source of atmospheric CO2, Nature, 416(6881), 617–620, doi:10.1038/416617a, 2002.

Sanders, B. F.: Evaluation of on-line DEMs for flood inundation modeling, Adv. Water Resour., 30(8), 1831–1843, doi:10.1016/j.advwatres.2007.02.005, 2007.

Simard, M., Pinto, N., Fisher, J. B. and Baccini, A.: Mapping forest canopy height globally with spaceborne lidar, J. Geophys. Res. Biogeosciences, 116(G4), G04021, doi:10.1029/2011JG001708, 2011.

Tesfa, T. K., Li, H.-Y., Leung, L. R., Huang, M., Ke, Y., Sun, Y. and Liu, Y.: A subbasin-based framework to represent land surface processes in an Earth system model, Geosci Model Dev, 7(3), 947–963, doi:10.5194/gmd-7-947-2014, 2014a.

Tesfa, T. K., Ruby Leung, L., Huang, M., Li, H.-Y., Voisin, N. and Wigmosta, M. S.: Scalability of grid- and subbasin-based land surface modeling approaches for hydrologic simulations, J. Geophys. Res. Atmospheres, 119(6), 2013JD020493, doi:10.1002/2013JD020493, 2014b.

Trigg, M. A., Wilson, M. D., Bates, P. D., Horritt, M. S., Alsdorf, D. E., Forsberg, B. R. and Vega, M. C.: Amazon flood wave hydraulics, J. Hydrol., 374(1–2), 92–105, doi:10.1016/j.jhydrol.2009.06.004, 2009.

Vörösmarty, C. J., Moore, B., Grace, A. L., Gildea, M. P., Melillo, J. M., Peterson, B. J., Rastetter, E. B. and Steudler, P. A.: Continental scale models of water balance and fluvial transport: An application to South America, Glob. Biogeochem. Cycles, 3(3), 241–265, doi:10.1029/GB003i003p00241, 1989.

Wilson, M., Bates, P., Alsdorf, D., Forsberg, B., Horritt, M., Melack, J., Frappart, F. and Famiglietti, J.: Modeling large-scale inundation of Amazonian seasonally flooded wetlands, Geophys. Res. Lett., 34(15), L15404, doi:10.1029/2007GL030156, 2007.

Yamazaki, D., Kanae, S., Kim, H. and Oki, T.: A physically based description of floodplain inundation dynamics in a global river routing model, Water Resour. Res., 47(4), W04501, doi:10.1029/2010WR009726, 2011.

Yamazaki, D., Lee, H., Alsdorf, D. E., Dutra, E., Kim, H., Kanae, S. and Oki, T.: Analysis of the water level dynamics simulated by a global river model: A case study in the Amazon River, Water Resour. Res., 48(9), W09508, doi:10.1029/2012WR011869, 2012.

**Table 1**

**Table 1. Coefficients in channel geometry formulae for the 10 subregions.**

| No. | Subregion name | Factor for adjusting channel width ($\alpha_w$) | Channel width coefficient | | Factor for adjusting channel depth ($\alpha_d$) | Channel depth coefficient | Factor for adjusting cross-sectional area ($\alpha_A = \alpha_w \cdot \alpha_d$) |
|---|---|---|---|---|---|---|---|
| | | | $A_u < 10000\,km^2$ | $A_u \geq 10000\,km^2$ | | | |
| 1 | Xingu | 1.0 | 1.956 | 0.403 | 1.0 | 0.245 | 1.00 |
| 2 | Tapajos | 1.6 | 3.130 | 0.645 | 0.7 | 0.172 | 1.12 |
| 3 | Madeira | 0.6 | 1.174 | 0.242 | 0.6 | 0.147 | 0.36 |
| 4 | Purus | 0.8 | 1.565 | 0.322 | 1.4 | 0.343 | 1.12 |
| 5 | Jurua | 0.7 | 1.369 | 0.282 | 1.5 | 0.368 | 1.05 |
| 6 | Upper-Solimoes tributaries | 1.0 | 1.956 | 0.403 | 1.0 | 0.245 | 1.00 |
| 7 | Japura | 1.8 | 3.521 | 0.725 | 0.7 | 0.172 | 1.26 |
| 8 | Negro | 1.7 | 3.325 | 0.685 | 0.5 | 0.123 | 0.85 |
| 9 | Northeast | 0.6 | 1.174 | 0.242 | 0.8 | 0.196 | 0.48 |
| 10 | Mainstem | 1.0 | 1.956 | 0.403 | 1.0 | 0.245 | 1.00 |

Note: $A_u$ is the upstream drainage area.

5

**Table 2**

**Table 2. Setup of seven simulations.**

| No. | Method for representing river flow | DEM | Manning roughness coefficients of channels | Channel cross-sectional geometry | Abbreviations |
|---|---|---|---|---|---|
| 1 | Diffusion wave method | Corrected | Varied | Adjusted | CTL |
| 2 | Diffusion wave method | Original | Varied | Adjusted | OriDEM |
| 3 | Diffusion wave method | Corrected | Varied | No adjusting | OriSec |
| 4 | Diffusion wave method | Corrected | 0.03 | Adjusted | n003 |
| 5 | Kinematic wave method | Corrected | Varied | Adjusted | KW |

| No. | Inundation scheme | DEM | Channel cross-sectional geometry | Manning roughness coefficients of channels | Method for representing river flow | Abbrevia-tions |
|---|---|---|---|---|---|---|
| 1 | On | Corrected | Refined | Sspatially varying | Diffusion wave method | CTL |
| 2 | Off | Corrected | Refined | Spatially varying | Diffusion wave method | NoInund |
| 3 | On | Original | Refined | Spatially varying | Diffusion wave method | OriDEM |
| 4 | On | Corrected | No refining | Spatially varying | Diffusion wave method | OriSec |
| 5 | On | Corrected | Refined | 0.03 | Diffusion wave method | n003 |
| 6 | On | Corrected | Refined | 0.04 | Diffusion wave method | n004 |
| 7 | On | Corrected | Refined | Spatially varying | Kinematic wave method | KW |

**Table 3**

**Table 3. ~~Adjusting~~ Refining the channel cross-sectional geometry affects inundated area in tributary subregions. [a]**

| Category | Cross-sectional area [b] | Inundated area over floodplains | Channel width [c] | Channel area | Total surface water area [d] | Subregions |
|---|---|---|---|---|---|---|
| A | – | + | + | + | + | h) Negro |
| B | – | + | – | – | + | c) Madeira; i) Northeast |
| C | + | – | + | + | + | b) Tapajos; g) Japura |
| D | + | – | – | – | – | d) Purus; e) Jurua |
| E | No ~~adjusting~~refining | No change | No ~~adjusting~~refining | No change | No change | a) Xingu; f) Upper-Solimoes tributaries |

Note: a. '+' means increase; '–' means decrease;

b. This variation depends on the factor $\alpha_A$ in Table 1: $\alpha_A$>1: '+'; $\alpha_A$<1: '–'; $\alpha_A$=1: 'No ~~adjusting~~ refining';

c. This variation depends on the factor $\alpha_w$ in Table 1: $\alpha_w$>1: '+'; $\alpha_w$<1: '–'; $\alpha_w$=1: 'No ~~adjusting~~ refining';

d. This change is shown by inundation results in Fig. 11.

**Table 4**

**Table 4. Nash–Sutcliffe efficiency coefficients (NSEs) of modeled daily streamflow of 12 years (1995 – 2006) at the 13 stream gauges for the simulations 'CTL', 'n004' and 'n003'.**

| Gauge index | Gauge name | NSE of Simulation 'CTL' | NSE of Simulation 'n004' | NSE of Simulation 'n003' | Subregion of the gauge |
|---|---|---|---|---|---|
| a | Altamira | - 0.677 | - 0.765 | - 0.889 | Xingu |
| b | Itaituba | - 0.310 | - 0.354 | - 0.420 | Tapajos |
| c | Fazenda vista alegre | 0.782 | 0.796 | 0.701 | Madeira |
| d | Canutama | 0.678 | 0.659 | 0.567 | Purus |
| e | Gaviao | 0.512 | 0.482 | 0.389 | Jurua |
| f | Acanaui | - 0.160 | - 0.312 | - 0.604 | Japura |
| g | Serrinha | 0.748 | 0.694 | 0.546 | Negro |
| h | Cach da porteira-con | 0.767 | 0.725 | 0.674 | Northeast |
| i | Santo antonio do ica | 0.428 | 0.413 | 0.297 | Mainstem |
| j | Itapeua | 0.570 | 0.593 | 0.140 | Mainstem |
| k | Manacapuru | 0.623 | 0.653 | 0.407 | Mainstem |
| l | Jatuarana+Careiro | 0.819 | 0.813 | 0.787 | Mainstem |
| m | Obidos | 0.911 | 0.907 | 0.931 | Mainstem |

**Fig. 1**

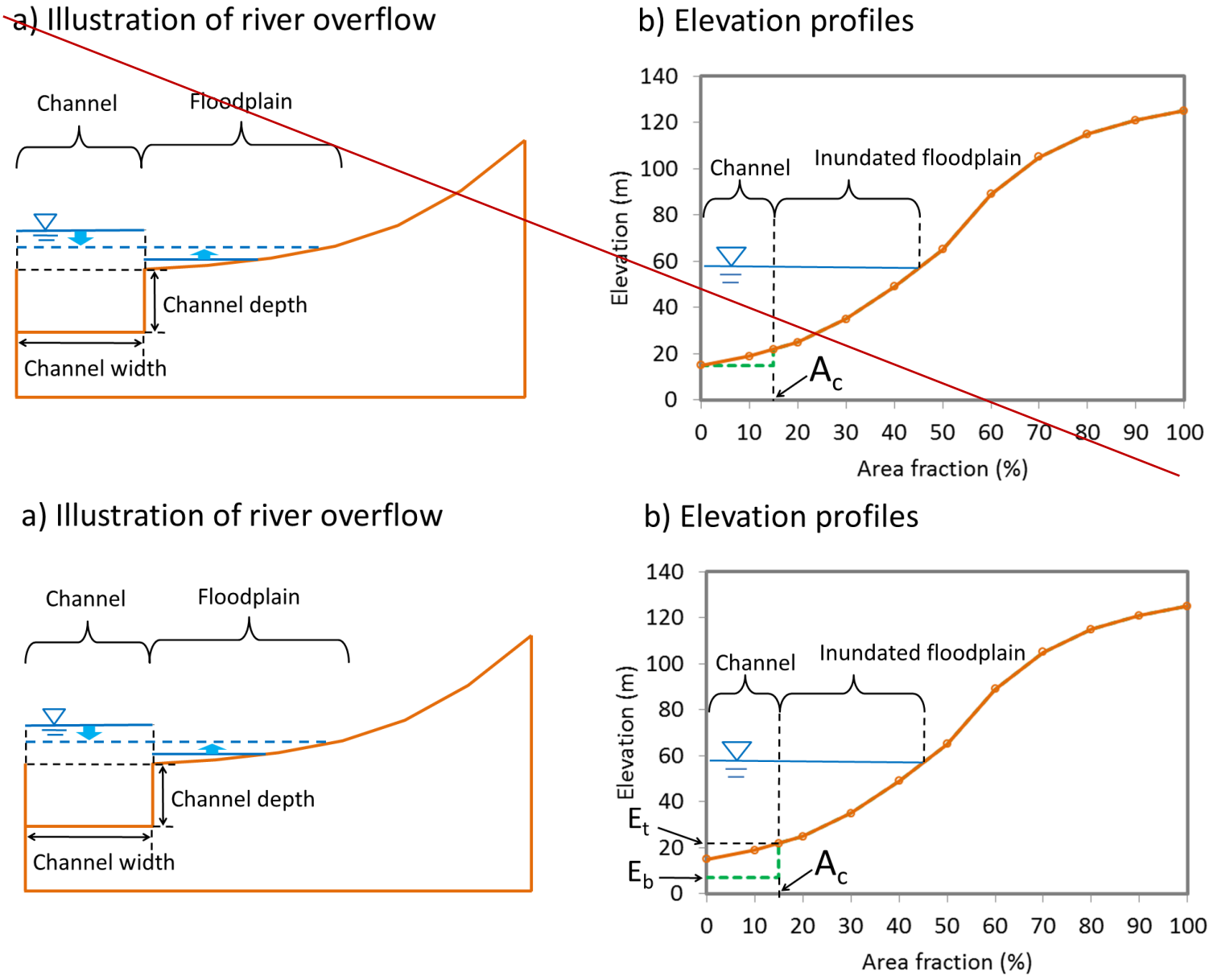


**Figure 1. Illustrations of the macro-scale inundation scheme: (a) Illustration of river overflow; (b) Elevation profiles of a computation unit (e.g., a grid cell or subbasin). The brown solid line is the original elevation profile. The green dash line is the amended elevation profile (its non-channel part overlaps with the original elevation profile). $A_c$ is the fraction of the channel area in the computation unit~~.~~; $E_t$ is the bank top elevation; and $E_b$ is the channel bed elevation.**

**Fig. 2**

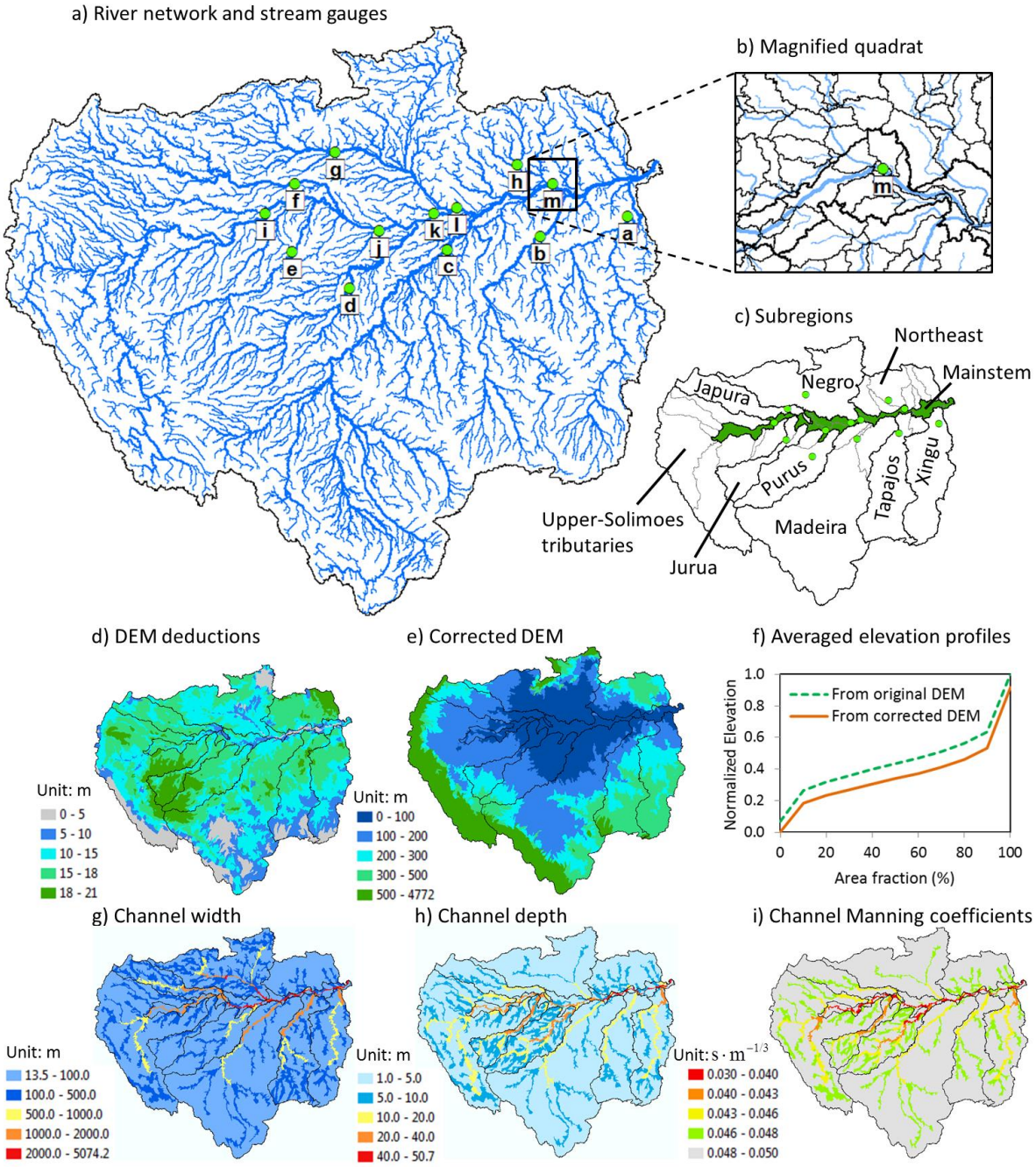


**Figure 2. Basin discretization and model inputs. (a) The river network extracted from the DEM overlaps with 13 stream gauges: a) Altamira; b) Itaituba; c) Fazenda vista alegre; d) Canutama; e) Gaviao; f) Acanaui; g) Serrinha; h) Cach da porteira-con; i) Santo antonio do ica; j) Itapeua; k) Manacapuru; l) Jatuarana+Careiro; m) Obidos. (b) Magnified quadrat. The thin (thick) black lines mark boundaries between subbasins (subregions). (c) Delineation of 10 subregions (including 9 tributary subregions and the mainstem subregion indicated by dark green color). (d) Average DEM deductions ~~for~~ at each subbasin ~~to~~ for alleviateing vegetation-caused biases. (e) The corrected DEM. (f) Averaged elevation profiles based on the original and corrected DEMs. (g) Channel widths. (h) Channel depths. (i) Manning roughness coefficients of channels.**

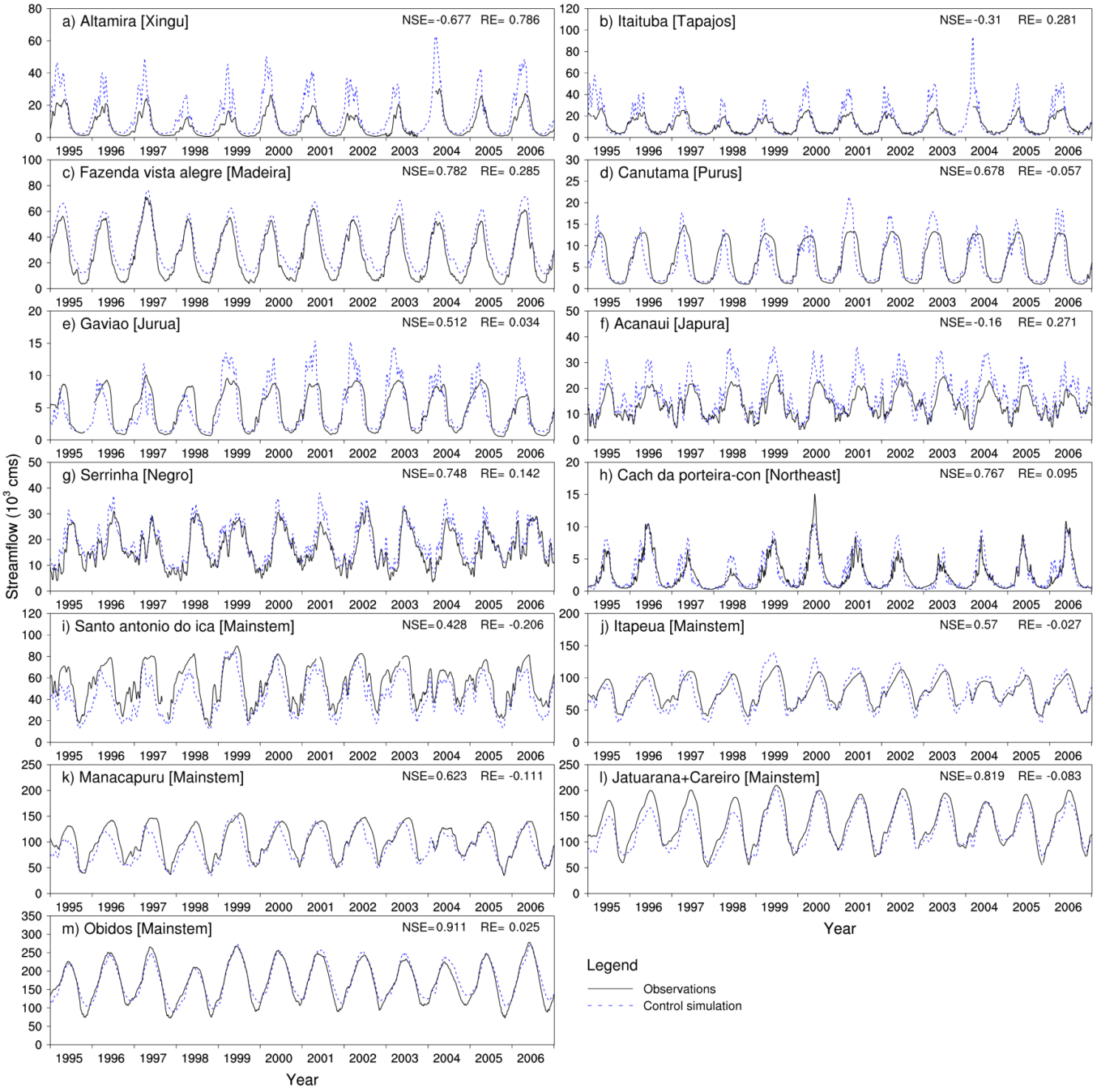


**Figure 3. Comparison between modeled and observed daily streamflow for a 12-year period (1995 – 2006) at 13 stream gauges (the corresponding subregion names are shown in the brackets): a) Altamira [Xingu]; b) Itaituba [Tapajos]; c) Fazenda vista alegre [Madeira]; d) Canutama [Purus]; e) Gaviao [Jurua]; f) Acanaui [Japura]; g) Serrinha [Negro]; h) Cach da porteira-con [Northeast]; i) Santo antonio do ica [Mainstem]; j) Itapeua [Mainstem]; k) Manacapuru [Mainstem]; l) Jatuarana+Careiro [Mainstem]; m) Obidos [Mainstem]. The Nash–Sutcliffe efficiency coefficient and the relative error of mean annual streamflow are indicated at the upper right corner of each panel. Figure 2a shows the stream- gauge locations.**

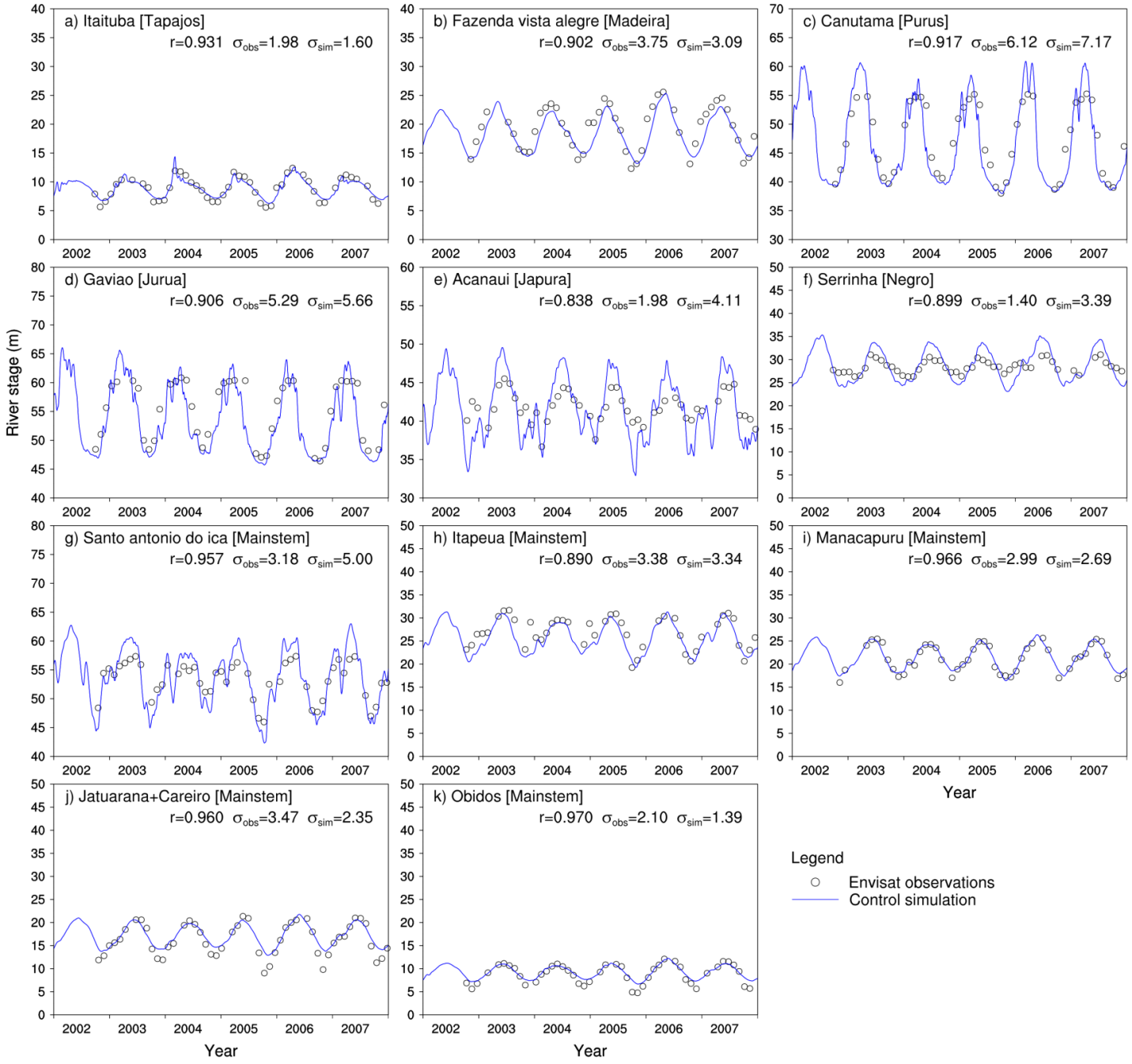


**Figure 4. Comparison of modeled daily river stages with the observations for a 6-year period (2002 – 2007) at the subbasins containing or close to 11 of the 13 stream gauges (the corresponding subregion names are shown in the brackets): a) Itaituba [Tapajos]; b) Fazenda vista alegre [Madeira]; c) Canutama [Purus]; d) Gaviao [Jurua]; e) Acanaui [Japura]; f) Serrinha [Negro]; g) Santo antonio do ica [Mainstem]; h) Itapeua [Mainstem]; i) Manacapuru [Mainstem]; j) Jatuarana+Careiro [Mainstem]; k) Obidos [Mainstem]. The Pearson correlation coefficient between modeled river stages and the observations, as well as standard deviation for modeled and observed river stages, are indicated in each panel. The simulated river stages are shifted to coincide with the observations for better visual comparison (please see the Sect. 3.2 for the detailed explanation).**

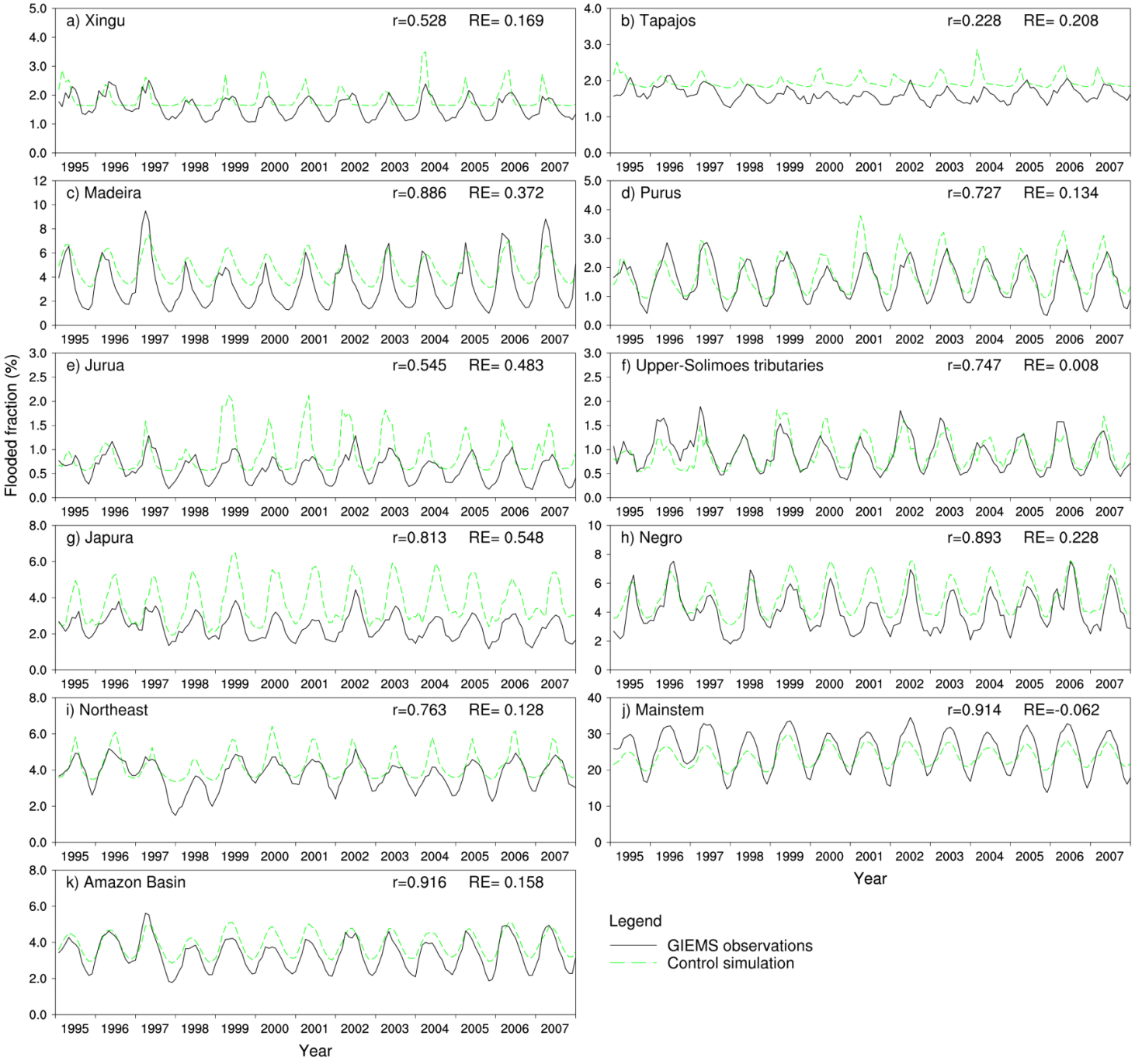


**Figure 5. Comparison of modeled monthly flood extent to the GIEMS satellite observations during a 13-year period (1995 – 2007) for 10 subregions and the entire Amazon Basin: a) Xingu; b) Tapajos; c) Madeira; d) Purus; e) Jurua; f) Upper-Solimoes tributaries; g) Japura; h) Negro; i) Northeast; j) Mainstem; k) Amazon Basin. The Pearson correlation coefficient between the modeled and observed monthly flood extent and the relative error of mean annual flood extent are indicated in each panel.**

**Fig. 6**

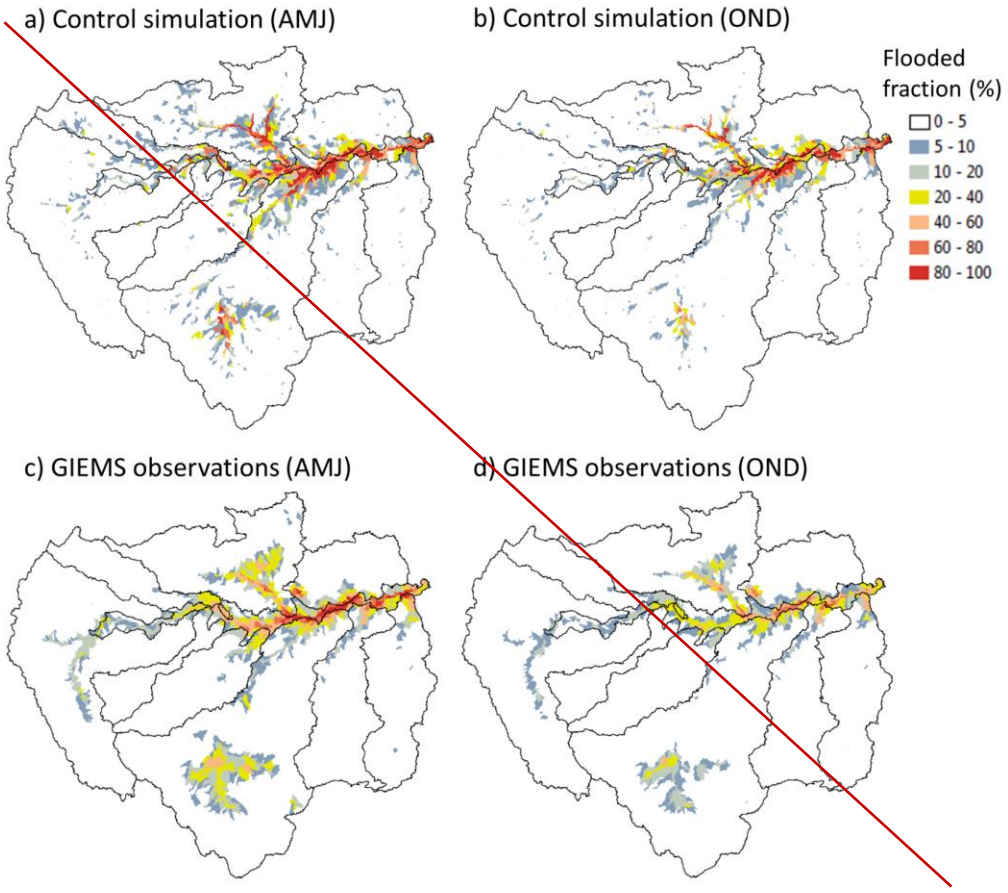
a) Control simulation (AMJ)
b) Control simulation (OND)
Flooded fraction (%)
0 - 5
5 - 10
10 - 20
20 - 40
40 - 60
60 - 80
80 - 100
c) GIEMS observations (AMJ)
d) GIEMS observations (OND)

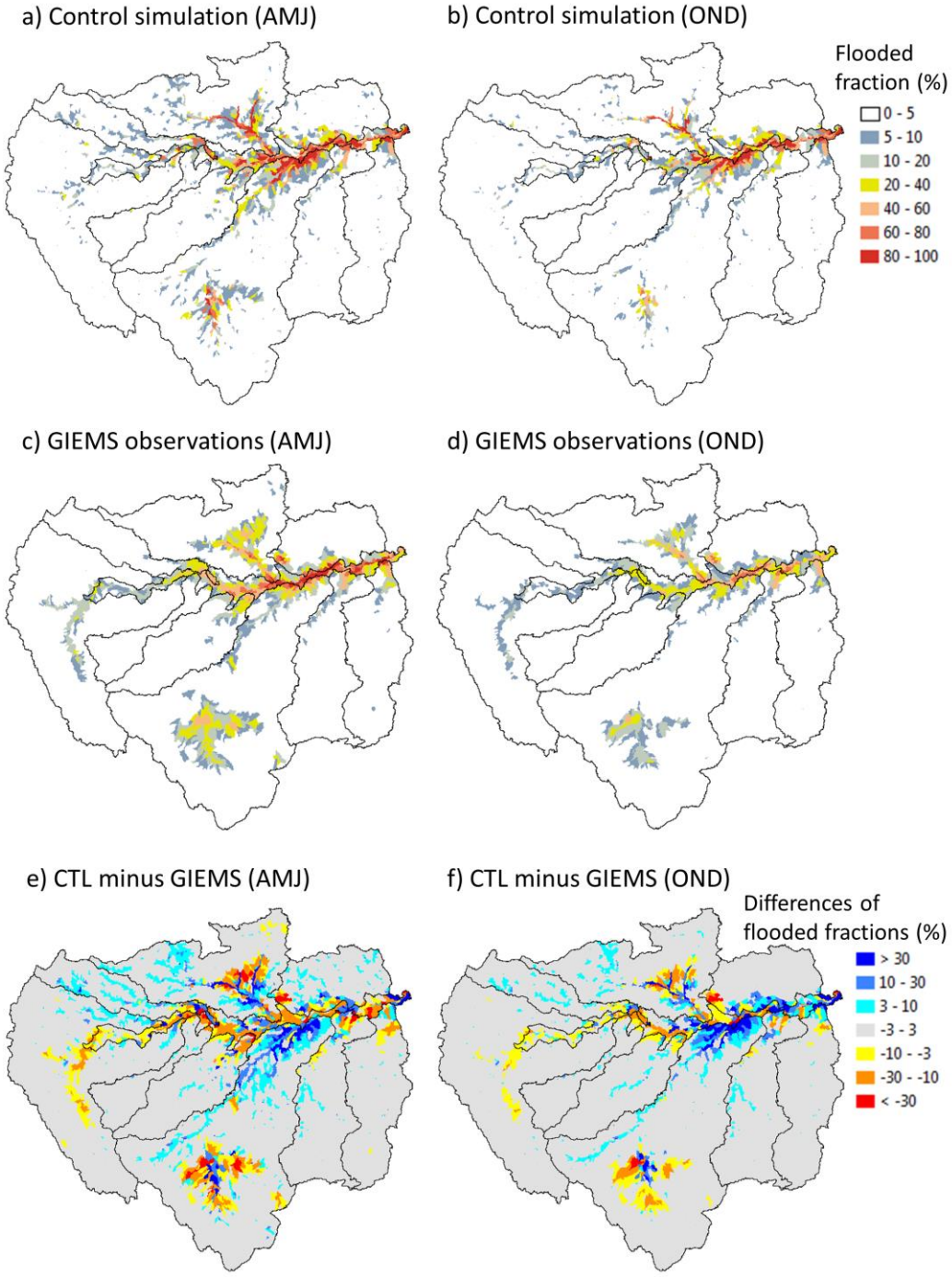


**Figure 6. Average spatial patterns of flooded fractions for all subbasins during 13 years (1995 – 2007): a) Results of the control simulation in the high-water season (AMJ – April, May and June); b) Results of the control simulation in the low-water season (OND – October, November and December); c) GIEMS observations in the high-water season; d) GIEMS observations in the low-water season; e) Differences between the control simulation and GIEMS observations in the high-water season; f) Differences between the control simulation and GIEMS observations in the low-water season.**

**Fig. 7**

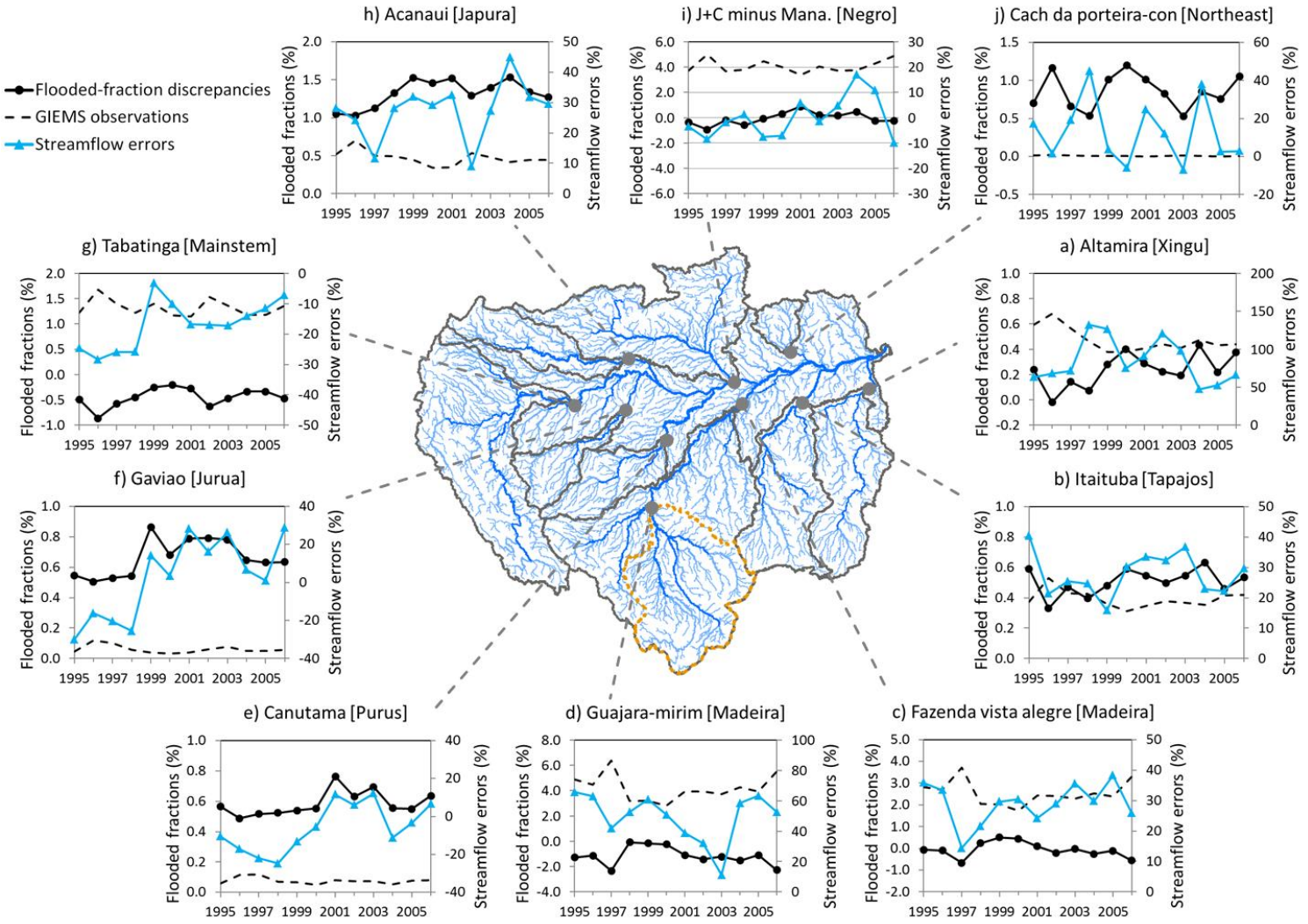


**Figure 7. Streamflow errors and the flood extent discrepancies (i.e., the differences between simulated flood extent and the GIEMS data) in the area upstream of the gauge for 10 gauges at the annual scale during 12 years (1995 – 2006). Streamflow of the Negro subregion (panel (i) ) is approximated by the streamflow difference between the Jatuarana+Careiro gauge and the Manacapuru gauge. The upstream area of each gauge is enclosed by the gray lines (or brown dotted lines for the Guajara-mirim gauge) in the basin map.**

**Fig. 8**

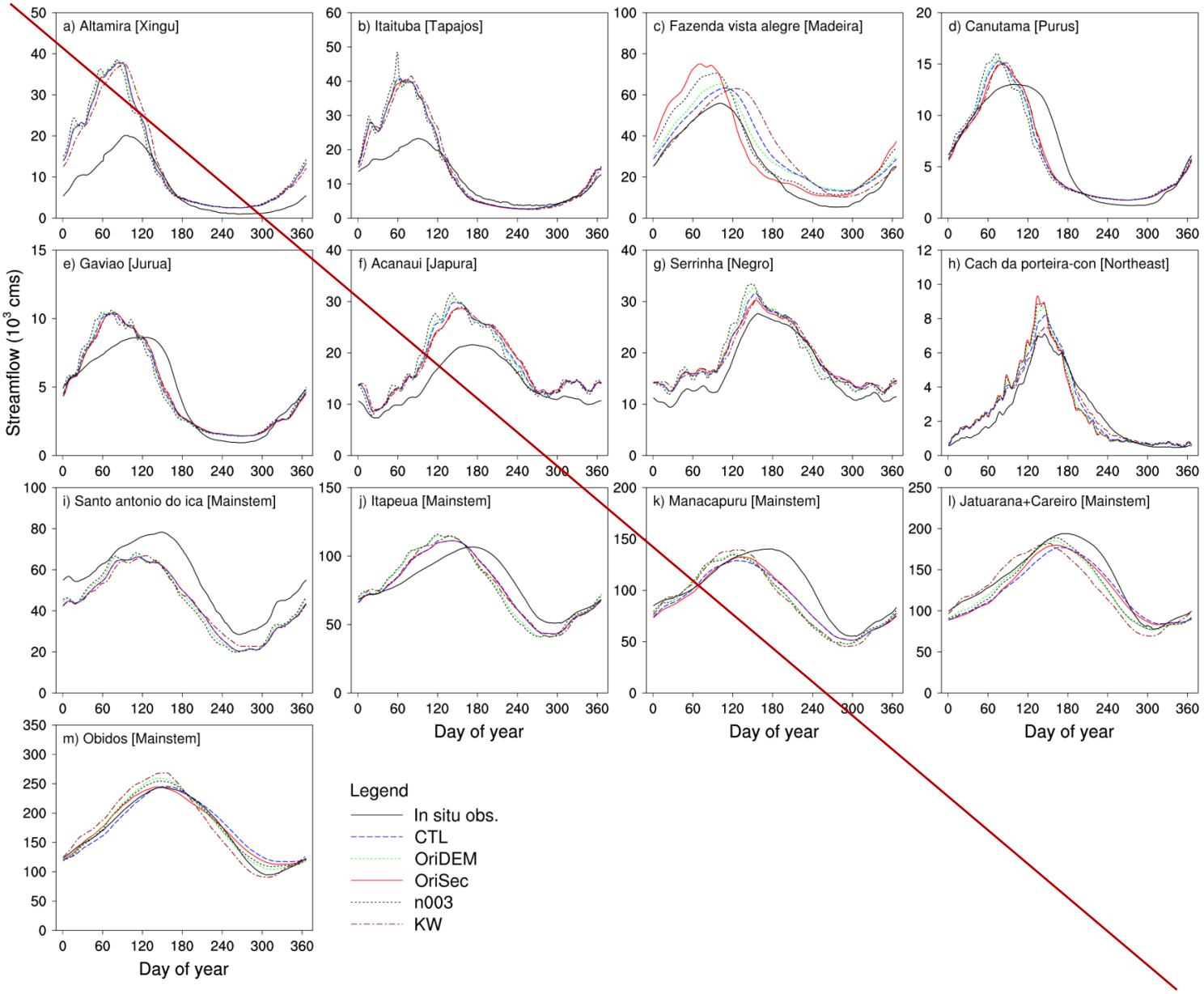
a) Altamira [Xingu]
b) Itaituba [Tapajos]
c) Fazenda vista alegre [Madeira]
d) Canutama [Purus]
e) Gaviao [Jurua]
f) Acanaui [Japura]
g) Serrinha [Negro]
h) Cach da porteira-con [Northeast]
i) Santo antonio do ica [Mainstem]
j) Itapeua [Mainstem]
k) Manacapuru [Mainstem]
l) Jatuarana+Careiro [Mainstem]
m) Obidos [Mainstem]
Streamflow ($10^3$ cms)
Day of year
Legend
In situ obs.
CTL
OriDEM
OriSec
n003
KW

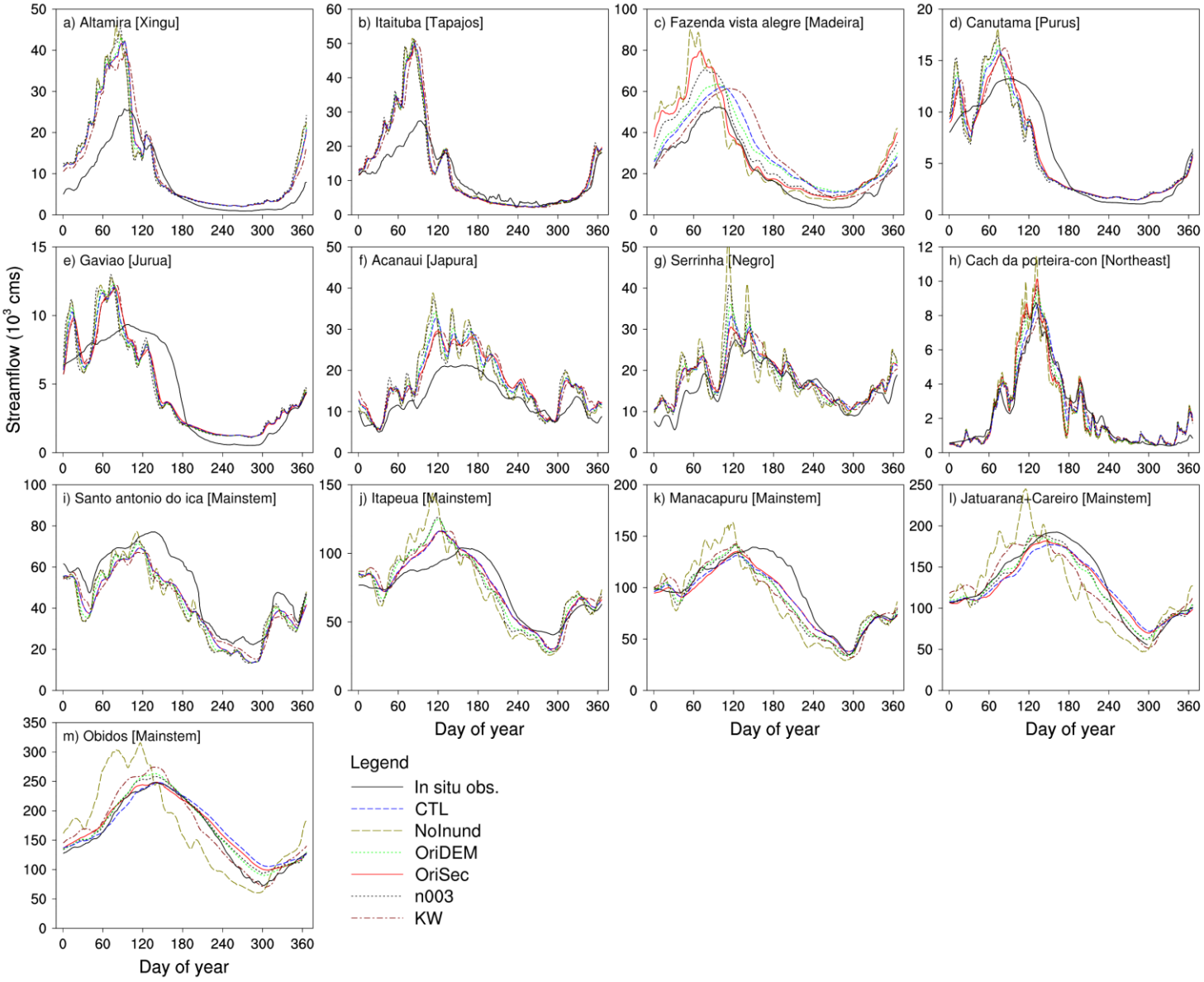


**Figure 8. Observed and modeled ~~average~~ daily streamflow of ~~12 years (1995 – 2006)~~year 2005 at 13 stream gauges. Setup of the ~~five~~ six simulations is described in Table 2: CTL – Control simulation; NoInund – Without inundation scheme; OriDEM – Using the original DEM (with vegetation-caused biases); OriSec – Using basin-wide channel geometry formulae; n003 – Using a uniform Manning roughness coefficient (i.e., 0.03) for all the channels; KW – Using kinematic wave method to represent river flow.**

**Fig. 9**

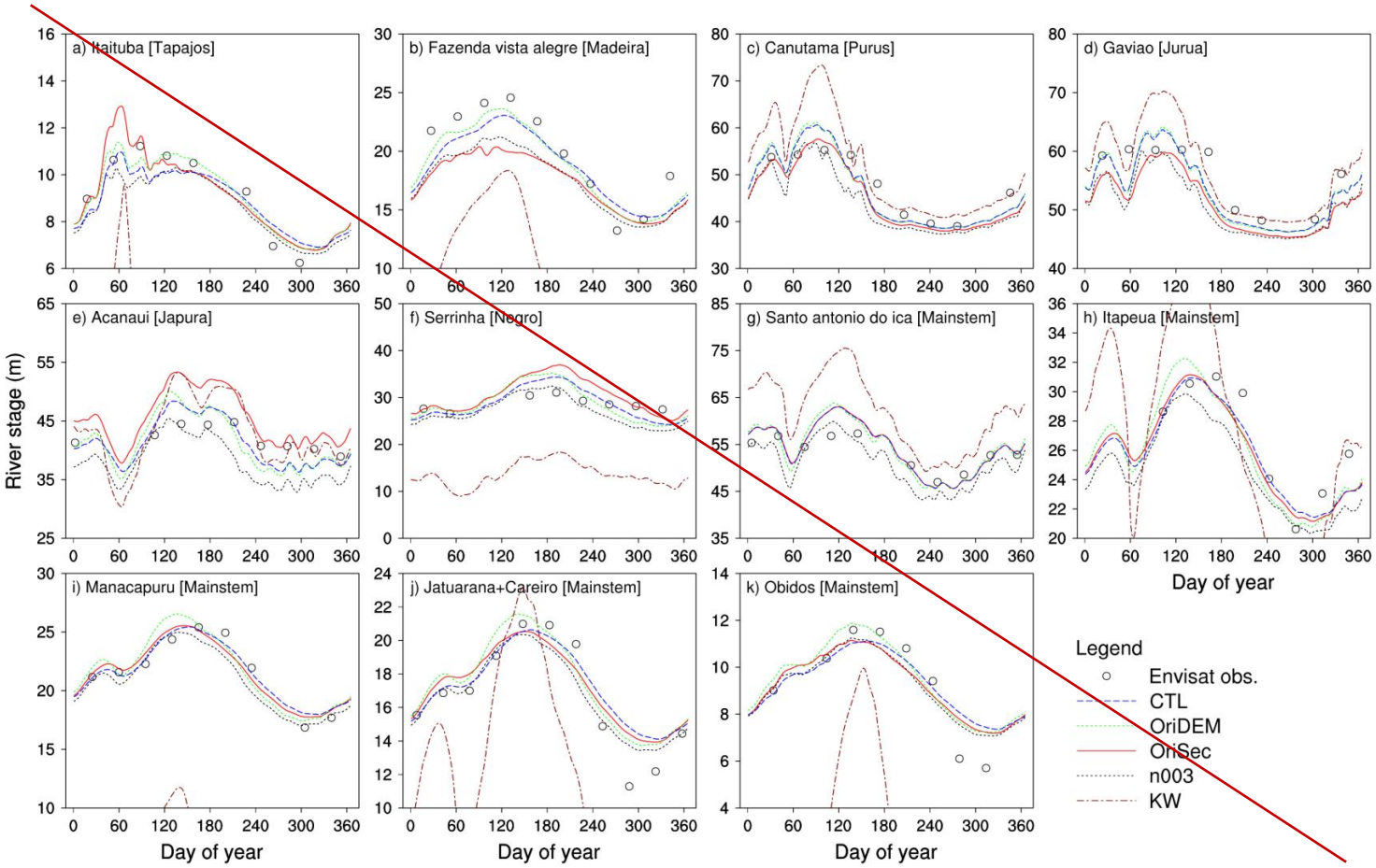
a) Itaituba [Tapajos]
b) Fazenda vista alegre [Madeira]
c) Canutama [Purus]
d) Gaviao [Jurua]
e) Acanaui [Japura]
f) Serrinha [Negro]
g) Santo antonio do ica [Mainstem]
h) Itapeua [Mainstem]
i) Manacapuru [Mainstem]
j) Jatuarana+Careiro [Mainstem]
k) Obidos [Mainstem]
River stage (m)
Day of year
Legend
Envisat obs.
CTL
OriDEM
OriSec
n003
KW

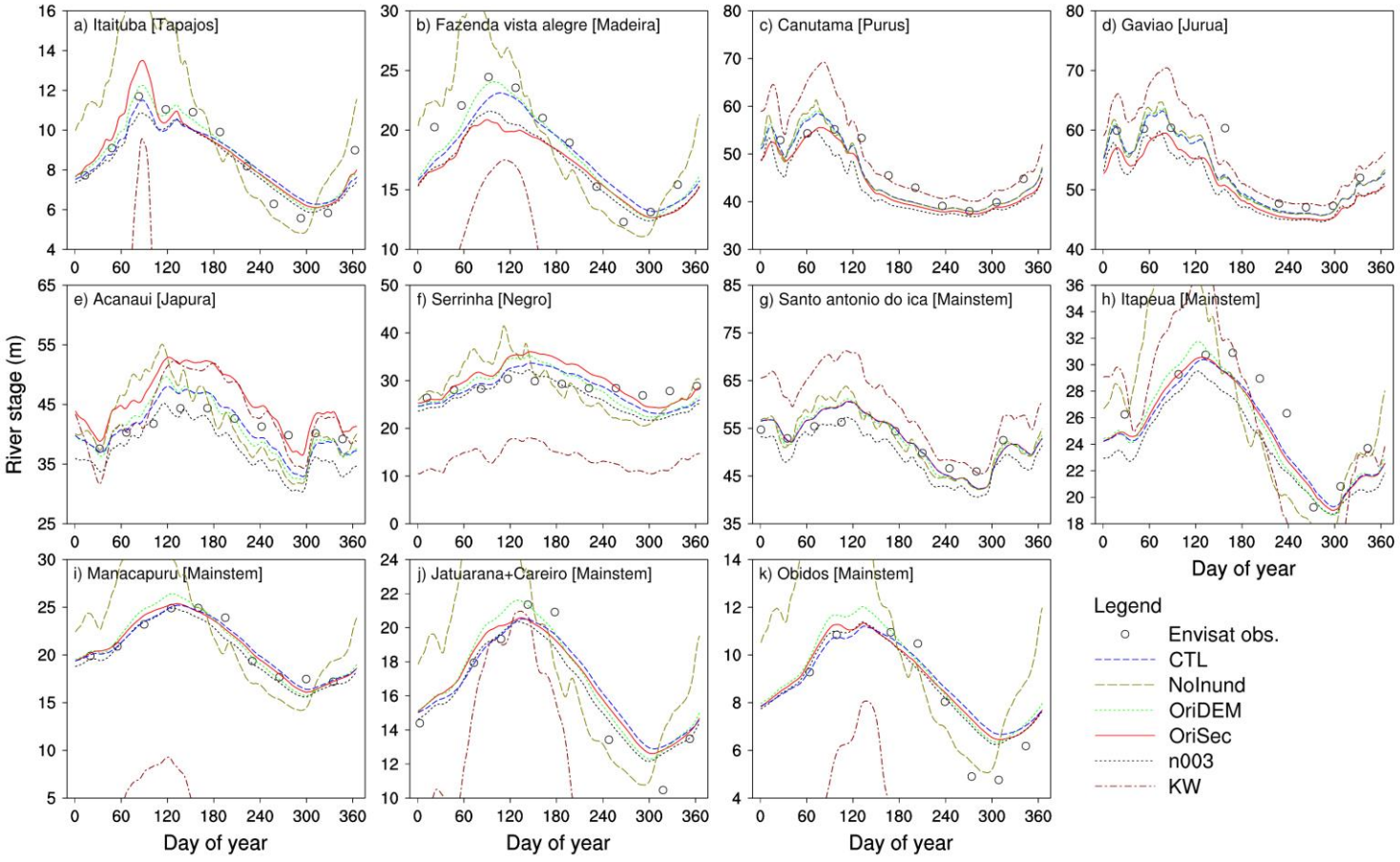


**Figure 9. Observed and modeled river stages at the daily scale in year ~~2007~~2005 for the subbasins containing or close to 11 of the 13 stream gauges. Setup of the ~~five~~ six simulations is described in Table 2: CTL – Control simulation; NoInund – Without inundation scheme; OriDEM – Using the original DEM (with vegetation-caused biases); OriSec – Using basin-wide channel geometry formulae; n003 – Using a uniform Manning roughness coefficient (i.e., 0.03) for all the channels; KW – Using kinematic wave method to represent river flow.**

**Fig. 10**

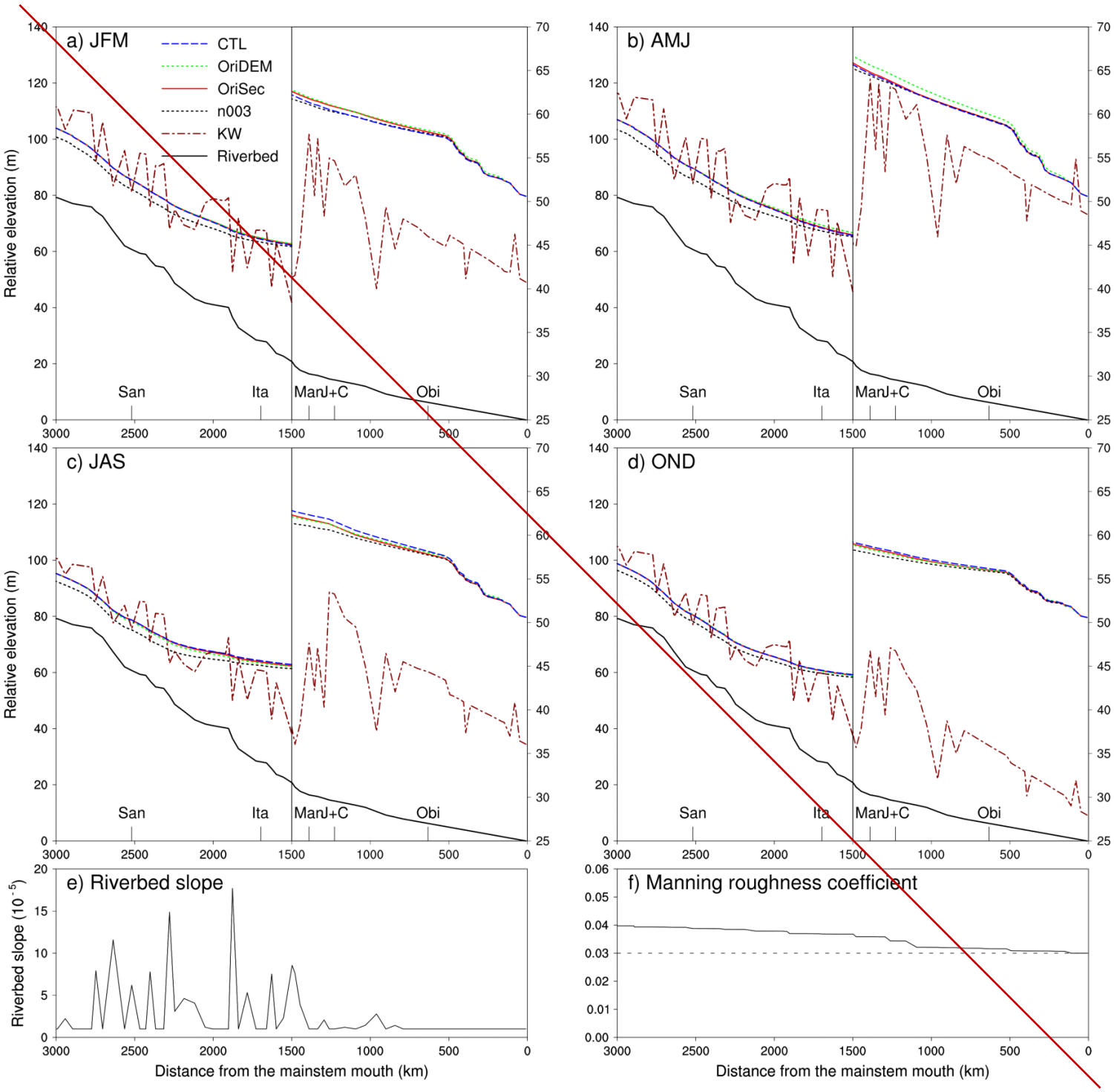
a) JFM
b) AMJ
c) JAS
d) OND
e) Riverbed slope
f) Manning roughness coefficient
CTL
OriDEM
OriSec
n003
KW
Riverbed
San
Ita
ManJ+C
Obi
Relative elevation (m)
Riverbed slope (10 -5)
Distance from the mainstem mouth (km)

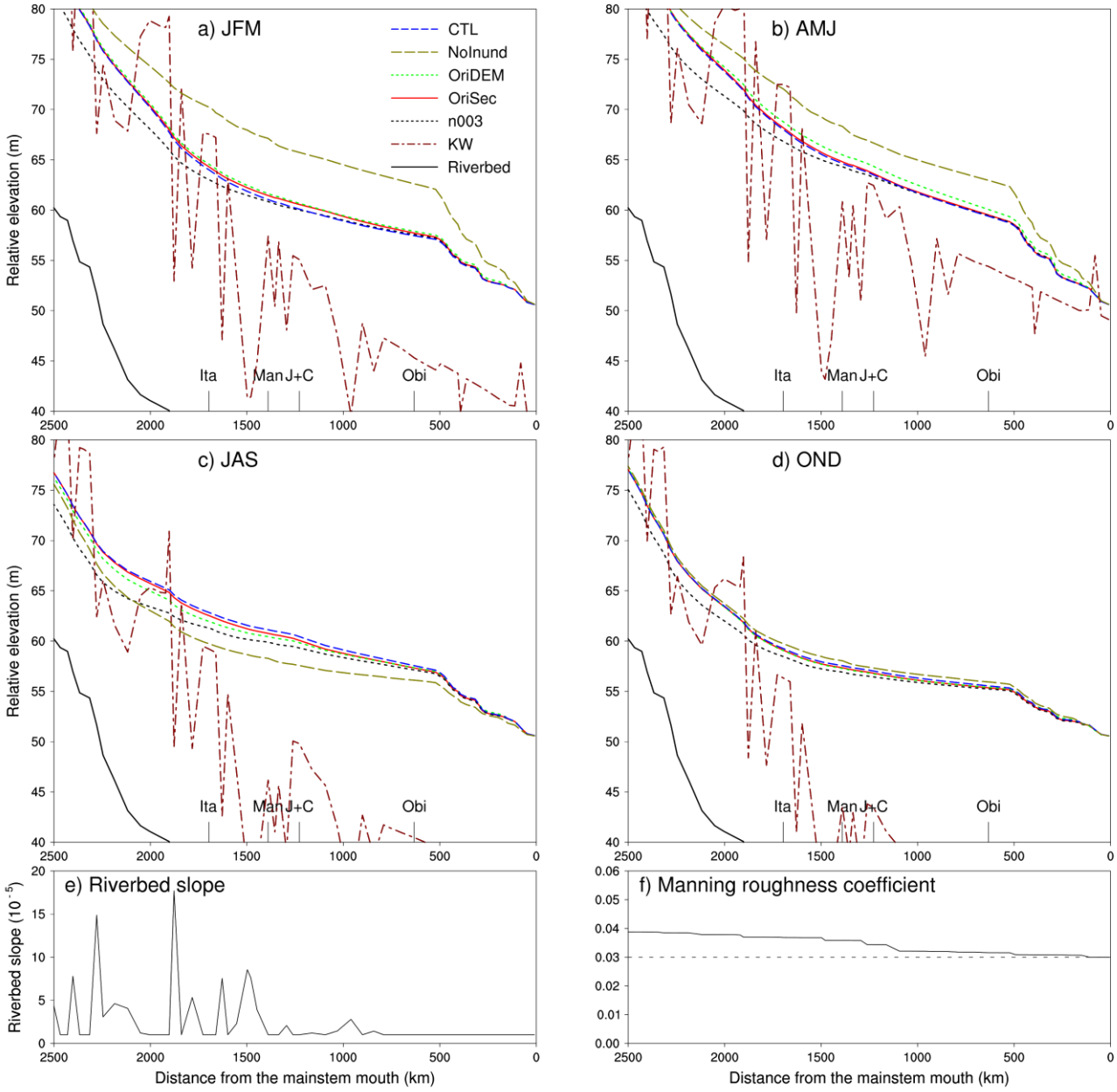


**Figure 10. Modeled average river surface profiles along the middle and lower mainstem in the four seasons of year ~~2007~~ 2005: (a) JFM (January, February and March; the period of rising flood); (b) AMJ (April, May and June; the period of high water); (c) JAS (July, August and September; the period of falling flood); and (d) OND (October, November and December; the period of low water). Results of ~~5~~six simulations are shown. ~~The curves in the right half panel (0 – 1500 km) use the right y-axis except the riverbed profile.~~ The ~~five~~ four stream-gauge locations are labeled on the x-axis: ~~San – Santo Antonio do ica;~~ Ita – Itapeua; Man – Manacapuru; J+C – Jatuarana+Careiro; Obi – Obidos. Riverbed slopes (e) and Manning roughness coefficients (f) along the mainstem are also shown. In the panel (f), the solid curve shows spatially ~~varied~~ varying Manning coefficients used in ~~four~~ five simulations; the dotted line shows the uniform Manning coefficient of 0.03 used in the simulation "n003".**

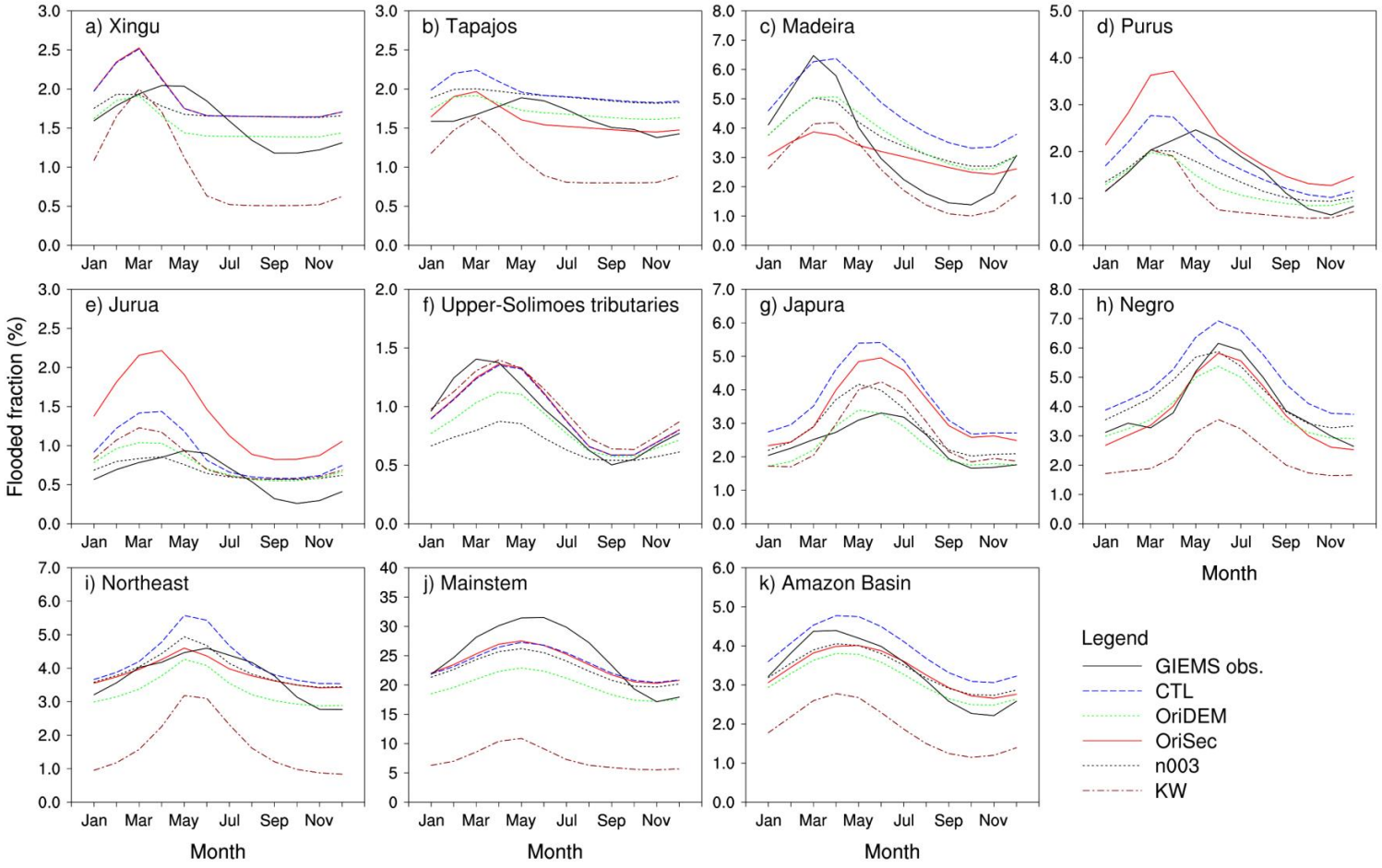


**Figure 11. Observed and modeled average monthly flood extent of 13 years (1995 – 2007) for the 10 subregions and the entire Amazon Basin. Setup of the five simulations is described in Table 2: CTL – Control simulation; OriDEM – Using the original DEM (with vegetation-caused biases); OriSec – Using basin-wide channel geometry formulae; n003 – Using a uniform Manning roughness coefficient (i.e., 0.03) for all the channels; KW – Using kinematic wave method to represent river flow.**

**Fig. 12**

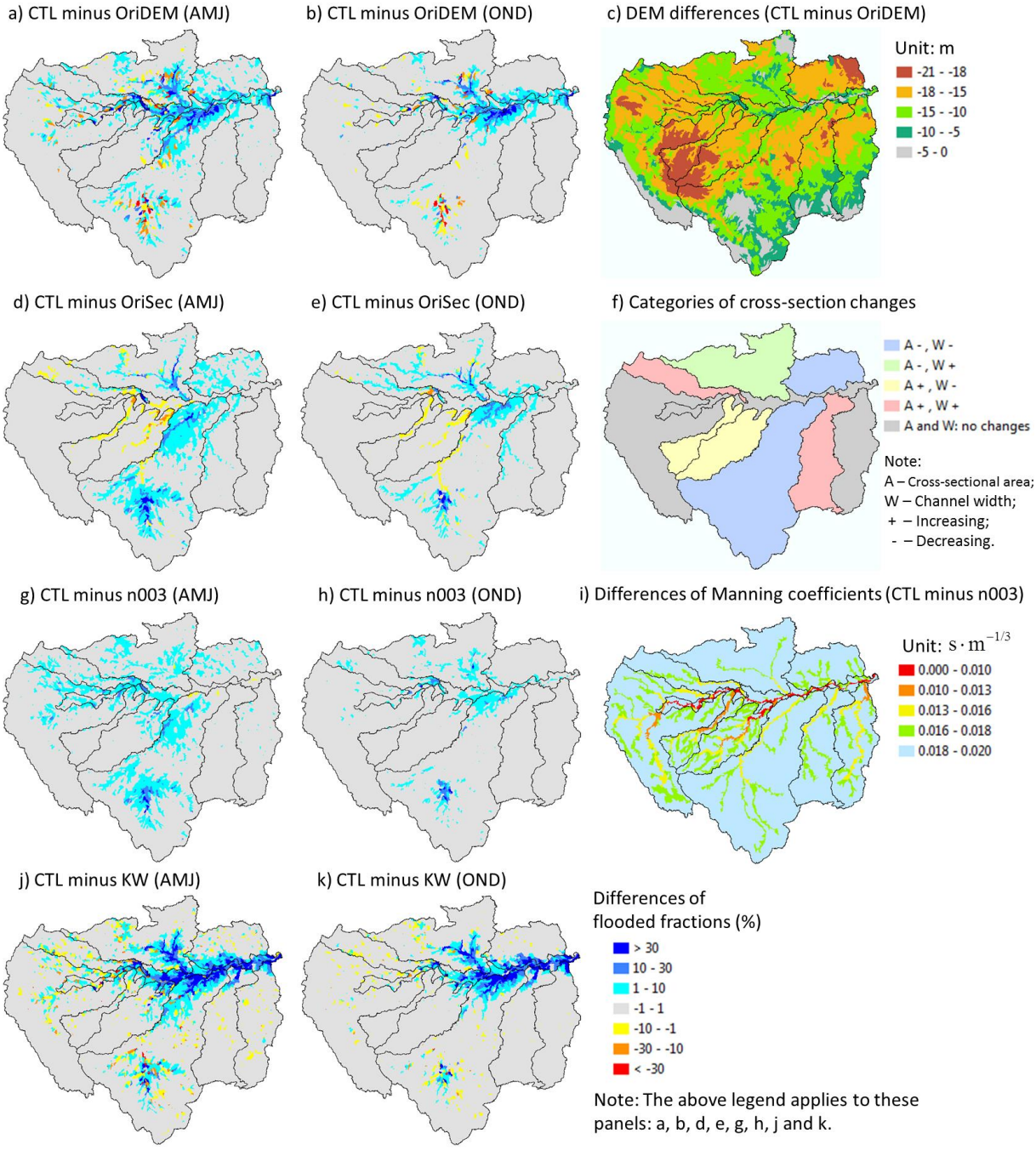


**Figure 12. Differences in subbasin flooded fractions averaged during 13 years (1995 – 2007) between the control simulation (CTL) and the four contrasting simulations (i.e., OriDEM, OriSec, n003 and KW) for the high-water season (AMJ – April, May and June) and low-water season (OND – October, November and December): (a) and (b): CTL minus OriDEM; (d) and (e): CTL minus OriSec; (g) and (h): CTL minus n003; (j) and (k): CTL minus KW. Panel (c) shows DEM differences (CTL minus OriDEM); Panel (f) shows categories of cross-section changes for the 10 subregions; Panel (i) shows Manning coefficient differences (CTL minus n003).**

**Fig. 13**

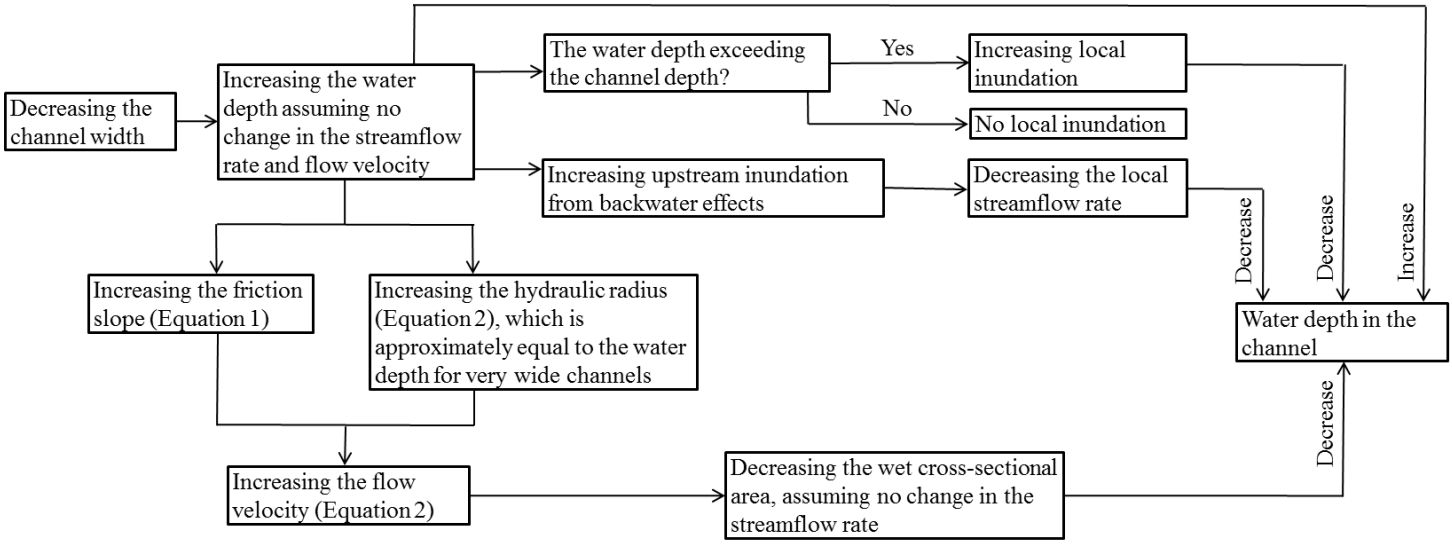


Figure 13. ~~An example of the effects of channel cross-sectional geometry on the water depth of the local channel.~~

**A diagram illustrating that decreasing the width of the local channel could bring about changes in the water depth of the local channel through various mechanisms. In general the phenomena before and after an arrow have the cause – effect relationship.**